International Journal of Analytical Chemistry

Fundamentals and Applications of Analytical Chemistry in Natural Products

Guest Editors: Norberto P. Lopes, Ernani Pinto, Michael Niehues, Paul J. Gates, and Ricardo Vessecchi

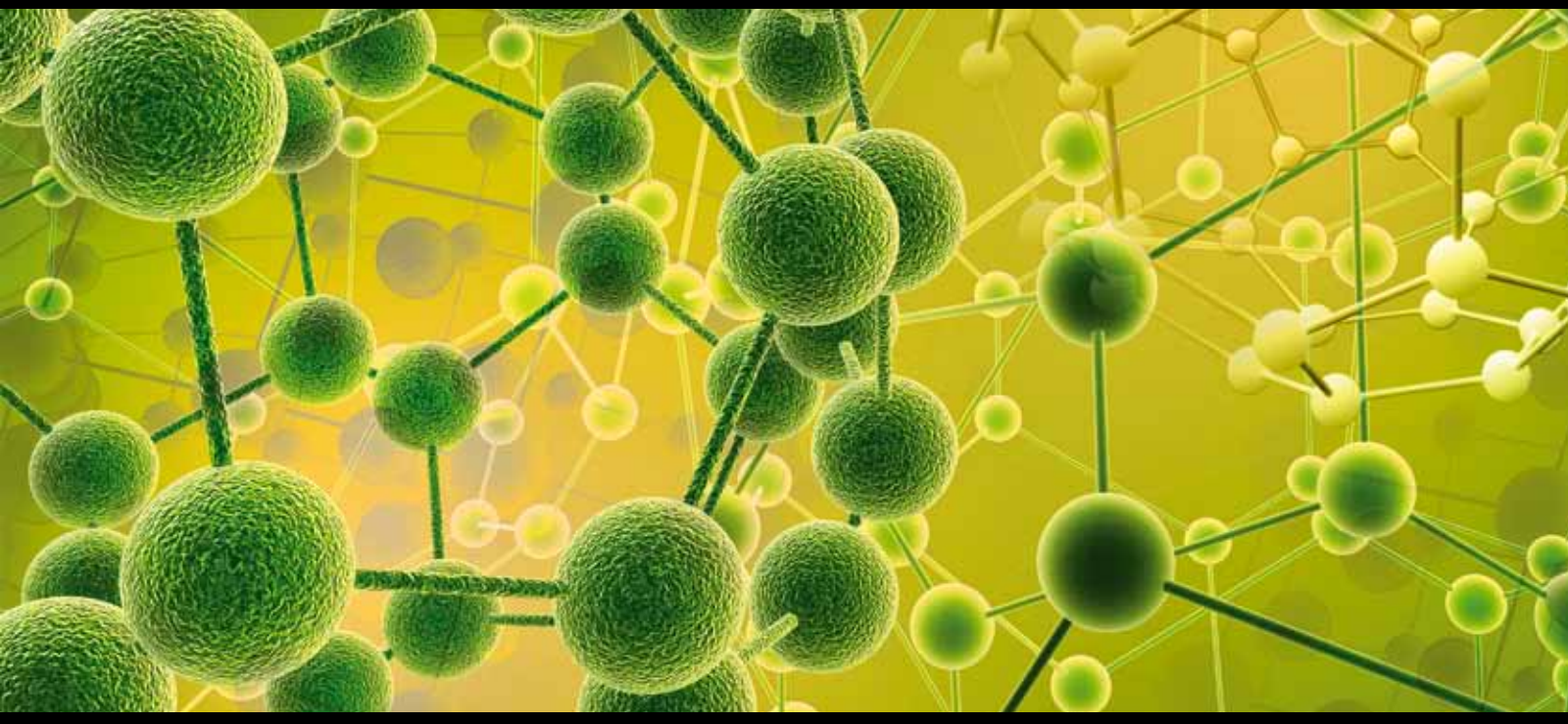

Fundamentals and Applications of Analytical Chemistry in Natural Products

International Journal of Analytical Chemistry

Fundamentals and Applications of Analytical Chemistry in Natural Products

Guest Editors: Norberto P. Lopes, Ernani Pinto, Michael Niehues, Paul J. Gates, and Ricardo Vessecchi

Editorial Board

Contents

Hindawi Publishing Corporation
International Journal of Analytical Chemistry
Volume 2012, Article ID 156201, 2 pages
doi:10.1155/2012/156201

Editorial

Fundamentals and Applications of Analytical Chemistry in Natural Products

Norberto P. Lopes,[1] Ernani Pinto,[2] Michael Niehues,[1] Paul J. Gates,[3] and Ricardo Vessecchi[1]

[1] *Núcleo de Pesquisa em Produtos Naturais e Sintético, Faculdade de Ciências Farmacêuticas de Ribeirão Preto, Universidade de São Paulo, 14040-901 Ribeirão Preto, SP, Brazil*
[2] *Departamento de Análises Clínicas e Toxicológicas, Faculdade de Ciências Farmacêuticas, Universidade de São Paulo, 05508-900 São Paulo, SP, Brazil*
[3] *School of Chemistry, University of Bristol, Cantock's Close, Bristol BS8 1TS, UK*

Correspondence should be addressed to Norberto P. Lopes, npelopes@fcfrp.usp.br

Received 15 March 2012; Accepted 15 March 2012

This special issue is aimed at collecting together recent developments in the field of natural product analysis. This issue covers methodologies and applications as diverse as secondary metabolite identification to the detection of metals in food stuffs. The chemistry of natural products has gained prominence not only due to the on-going search for new bioactive substances but also in related areas such as food chemistry and chemical ecology.

We feel that this special issue represents some of the wide ranging research currently performed in this diverse area and this is exemplified by the affiliations of the authors of the papers included which is made up of chemists, biochemists, biologists, physicists, toxicologists, physiologists, pharmaceutists, and geochemists. What all of these researchers have in common, despite their wide ranging backgrounds, is the need to make use of the powerful techniques of analytical chemistry to analyze natural compounds in complex matrices. Thus, this special issue is dedicated to all the readers that would like to apply analytical chemistry for natural products analysis.

This issue presents ten papers, which describe either a specific analytical method for specific types of natural products, the use of natural compounds to aid analytical developments, or modern techniques for the analysis of metals in food stuffs and food quality control (a growing area of interest).

The article by L. de S. Ferreira et al. describes the use of hyphenated techniques to determine fatty acids in a species of seaweed from the Fernando de Noronha archipelago. In addition, a second paper has used SRTXRF analysis as a technique to determine several inorganic species within the same archipelago. Both papers contribute to an increased understanding of adsorption and accumulation of such natural elements by algae in that specific area.

V. S. A. Devi and V. K. Reddy's paper presents a methodology for spectrophotometric determination of iron(II) and cobalt(II) using 2-hydroxi-1-naphthaldehyde-p-hydroxybenzoichydrazone which can then be applied for the analyses of biological and water samples that contain these metals.

The paper by G. C. Lopes et al. reports the preliminary estimation of the stability of the dried extract from the bark of *Guazuma ulmifolia Lam*. ("Mutamba"). Thermogravimetry analysis along with HPLC were used in the study. The results can be used as a chemical marker in the quality control of dried extracts of *G. ulmifolia*.

The study by M. F. Zampa et al. is the first report of the antimicrobial peptide from the skin of the *Phyllomedusa hypochondrialis* frog and its incorporation into nanostructured layered films in conjunction with nickel-tetrasulfonated phthalocyanines. The film was used as a biosensor to detect dopamine, a neurotransmitter associated with diseases such as Alzheimer's and Parkinson's.

S. B. A. Barros et al. demonstrate the exploitation of the polyelectrolytic behavior of natural cashew gum (*Anacardium occidentale L.*), found in northeast Brazil, as a

component of a nanocomposite electrode. The performance of the electrodes was evaluated by the determination of dopamine.

The paper by H. Tanaka et al. presents matrix-assisted laser desorption/ionization (MALDI) mass spectrometry for the confirmation of the hapten number in synthesized antigens. Two unique applications using MAb, Eastern blotting, and knockout extract have been introduced in this paper. The Eastern blotting method has great potential applications for the wide range of natural products.

The article of S. R. de Moraes et al. highlights the use of *Lippia sidoides Cham*. (also known as alecrim pimenta), native to northeastern Brazil and northern Minas Gerais, and their essential oils. The oxygenated monoterpene 1,8-cineole was the major constituent, followed by isoborneol and bornyl acetate. The chemical composition of essential oils described in this paper differs from that described in the literature for *L. sidoides* found in its native environment.

The paper of M. J. Kato et al. demonstrates the GC-MS monitoring of the major secondary metabolites and fatty acids occurring in the seeds of *Virola surinamensis*, during germination and seedling development. The authors conclude that the germination of *V. surinamensis* seeds and the seedling development are processes in which both fatty acids and secondary metabolites (lignans, isoflavonoids and juruenolides) are equally consumed in the seeds indicating their potential physiological role as energy and carbon sources.

The article of P. J. Gates and N. P. Lopes describes the application of negative ion chip-based nanospray tandem mass spectrometry for the analysis of flavonoid aglycones. The methodology is tested by the analysis of a crude green tea extract, where the expected flavonoids were readily identified.

Norberto P. Lopes
Ernani Pinto
Michael Niehues
Paul J. Gates
Ricardo Vessecchi

Hindawi Publishing Corporation
International Journal of Analytical Chemistry
Volume 2012, Article ID 721494, 5 pages
doi:10.1155/2012/721494

Research Article

Uptake of Seeds Secondary Metabolites by *Virola surinamensis* Seedlings

Massuo Jorge Kato,[1] Massayoshi Yoshida,[1] Norberto Peporine Lopes,[2] Denise Brentan da Silva,[3] and Alberto José Cavalheiro[4]

[1] *Instituto de Química, Universidade de São Paulo, CP 26077, 05599-970 São Paulo, SP, Brazil*
[2] *Núcleo de Pesquisa em Produtos Naturais e Sintéticos (NPPNS), Faculdade de Ciências Farmacêuticas de Ribeirão Preto, Universidade de São Paulo, 14040-903 Ribeirão Preto, SP, Brazil*
[3] *Lychnoflora Pesquisa e Desenvolvimento em Produtos Naturais LTDA, Incubadora Supera, Campus da USP, 14040-900 Ribeirão Preto, SP, Brazil*
[4] *Núcleo de Bioensaio, Biossíntese e Ecofisiologia de Produtos Naturais (NuBBE), Instituto de Química, Universidade Estadual Paulista, CP 355, 14800-900 Araraquara, SP, Brazil*

Correspondence should be addressed to Massuo Jorge Kato, majokato@iq.usp.br

Received 2 September 2011; Accepted 19 December 2011

Academic Editor: Ernani Pinto

The major secondary metabolites and fatty acids occurring in the seeds of *Virola surinamensis* were monitored by GC-MS during germination and seedling development. The role as carbon source for seedling development was indicated considering that both classes of compounds were similarly consumed in the seeds and that no selective consumption of compounds could be detected.

1. Introduction

Several neotropical trees produce fruits with large and heavy seeds [1]. *Virola surinamensis* is a myristicaceous tree growing in the Amazonian flooded plains and produces seeds during the rainy season [2, 3]. Seeds are viable shortly after ripening and are adapted to be dispersed by water or by large birds such as toucans and *araçaris*. The seedling formation can be divided in two distinct phases: seed germination and seedling development [4]. The cotyledons are hidden in the seed coat (cryptocotylar) and are storage organs of fatty material and polysaccharides that are recruited for the maintenance of seedling during its growth and development [5]. A study carried out on *V. venosa* revealed that the major lignans cubebin and dihydrokusunokinin accumulated in the seeds were not detected in its seedlings which accumulated a polyketide instead [6]. The major constituent identified in the seedling roots was shown to be the lignan sesamin, a minor constituent in the seeds. A different result were observed with *V. sebifera* in which a possible translocation of hydroxytetralone lignans and a preferential accumulation of a lignan hydroxy-otobain was observed in the whole seedlings [7].

In view of the lack of systematic investigation regarding this important event in the reproduction of tropical trees, the translocation of secondary metabolites occurring in large seeds to be used as a defensive compounds in the seedlings remains as a hypothesis [8, 9].

Virola surinamensis seeds contain 15.4% of soluble tannins as a dry mass and the highest concentration of compounds with a probable defensive function yet recorded [10]. Their cotyledons are rich in triacylglycerols and free fatty acids. Phytochemical analysis of *V. surinamensis* seeds collected at Combu Island demonstrated the occurrence of lignoids, propiophenone, and γ-lactones in these organs [11]. Analysis of seedling leaves of *V. surinamensis* growing in the field, in greenhouse conditions and in micropropagated plantlets revealed the absence of lignans and the exclusive occurrence of juruenolide C (**8a**) (Figure 1) [12]. Herein, we

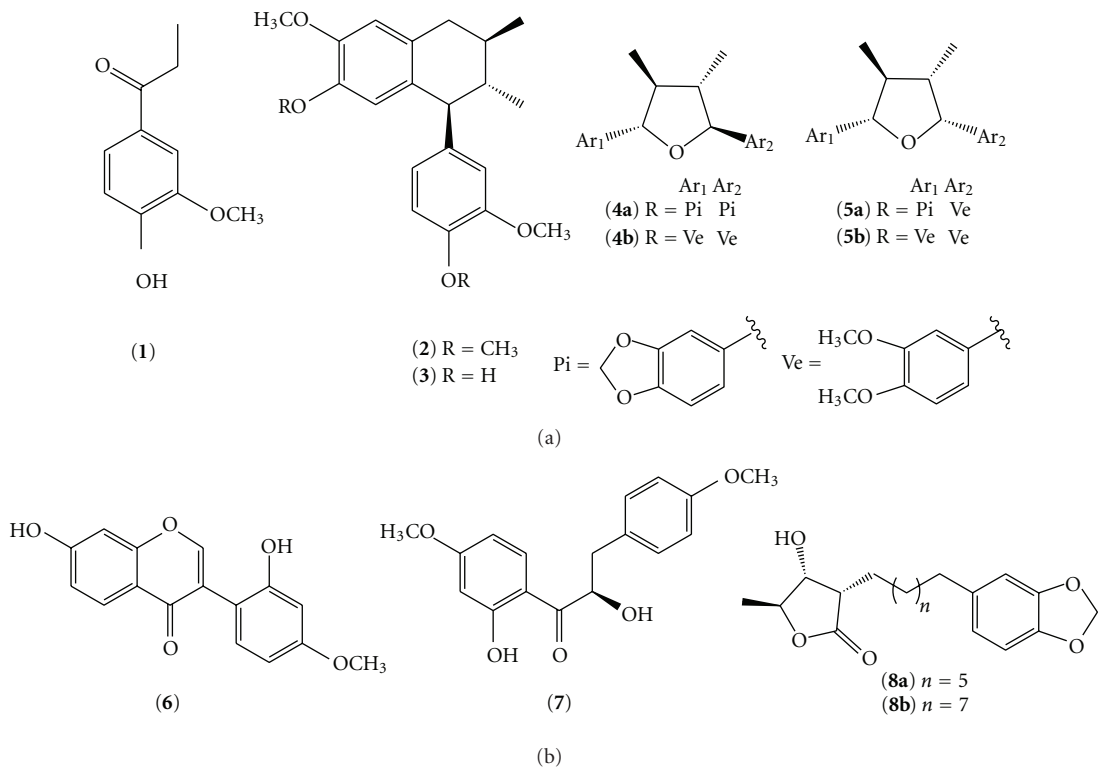

Figure 1: Chemical structures of the isolated substances: 4-hydroxy-3-methoxypropiophenone (**1**), galbulin (**2**), guaiacin (**3**), galbacin (**4a**), galbelgin (**4b**), calopeptin (**5a**), veraguensin (**5b**), 7,2′-dihydroxy-4′-methoxy-isoflavone (**6**), α,2′-dihydroxy-4,4′-dimethoxydihydrochalcone (**7**), juruenolide C (**8a**), and juruenolide D (**8b**).

wish to report the analyses of fatty acids and major secondary compounds in seeds of *V. surinamensis* in order to evaluate a selective consumption during the germination process.

2. Experimental Section

2.1. General Procedures. Preparative thin-layer chromatography (prep. TLC) was carried out on silica gel GF-254 (Merck) and column chromatography (CC) on silica gel 60H (0.005–0.045 mm) (Merck). The ^{1}H NMR (200 MHz) and ^{13}C NMR (50 MHz) spectra of samples were recorded on a Bruker-AC 200 in $CDCl_3$ with tetramethylsilane (TMS) as an internal standard. EIMS was obtained at 70 eV on HP 5988-A.

2.2. Plant Material. Seeds of *Virola surinamensis* (Rol.) Warb. were collected in February 1995 at Combu Island (01°30′10″S; 048°27′42″W), near Belém, Pará State, Brazil. A dry voucher sample (LOPES-037) has been deposited in the SPF-Herbário do Instituto de Biociências da Universidade de São Paulo. Mature seeds were frozen for analysis or germinated as previously reported [13] and maintained at greenhouse facilities of Instituto de Química-USP.

2.3. Standards Isolation. One dried seed (320 mg), after the germination process, was extracted with CH_3OH (3x 50 mL). The concentrated extract (70 mg) was suspended in CH_3OH/H_2O (6 : 4) and filtered through a Millipore membrane (0.45 μm). The filtered extract was submitted to preparative on HPLC (RP-8, 10 μm, 250 × 22 mm column; CH_3OH/H_2O 60 : 40 → CH_3OH 100% (50 min), 8 mL·min^{-1}, optimized conditions), followed by prep. TLC (silica gel; Hexane/EtOAc/*i*-PrOH or CH_2Cl_2/Me_2CO) to yield 4-hydroxy-3-methoxypropiophenone (**1**, 1.6 mg) [14], galbulin (**2**, 5.5 mg) [15], guaiacin **3** (1.4 mg) [15], galbacin (**4a**, 2.0 mg) [16], galbelgin (**4b**, 1.0 mg) [17], calopeptin (**5a**, 1.6 mg) [18], veraguensin (**5b**, 5.0 mg) [19], 7,2′-dihydroxy-4′-methoxy-isoflavone (**6**, 1.5 mg) [20], α,2′-dihydroxy-4,4′-dimethoxydihydrochalcone (**7**, 1.8 mg) [21], juruenolide C (**8a**, 1.2 mg) [12], and juruenolide D (**8b**, 1.3 mg) [11]. All these compounds were identified by comparison of spectroscopic data with that reported in the literature.

Table 1: Arithmetic mean of dry weight extracts and yields of *V. surinamensis* seeds.

Seeds*	Dry weight (mg)	Extract (mg)	Yield (%)
BG (*n*-hexane)	1030	310	30
AG (*n*-hexane)	290	81	28
BG (CH_3OH)	950	180	19
AG (CH_3OH)	270	46	17

BG: seeds before germination; AG: seeds after germination.
*Number of seeds used in each experiment = 7.

2.4. Fatty Acids Analyses. Individual seeds before and after germination process were extracted (3x) with 200 mL of

Table 2: Relative contents of secondary metabolites and fatty acids in *V. surinamensis* seeds.

	Seeds before germination			Seeds after germination			Statistical analysis
	S	SEM	CI	S	SEM	CI	*P*
1	2.01	0.461	0.729–3.291	0.64	0.319	0.0–1.528	0.041 (s)
2	14.25	1.800	9.179–19.321	13.37	1.766	8.974–18.766	0.884 (ns)
3	3.92	0.449	2.672–5.168	3.53	0.299	2.696–4.360	0.488 (ns)
4a	10.02	0.937	7.417–12.623	9.96	1.161	6.735–13.181	0.958 (ns)
4b	4.05	0.821	1.772–6.328	3.50	0.626	1.757–5.235	0.606 (ns)
5a	2.93	0.439	1.708–4.148	4.40	0.853	2.036–6.772	0.162 (ns)
5b	9.69	1.336	5.983–13.401	11.30	1.454	7.260–15.336	0.439 (ns)
6	3.58	0.562	2.015–5.141	2.28	0.2448	1.601–2.960	0.067 (ns)
7	2.28	0.292	1.471–3.197	2.06	0.264	1.333–2.799	0.595 (ns)
8a	3.71	0.361	2.707–4.709	4.08	0.219	3.472–4.962	0.402 (ns)
8b	1.98	0.157	1.552–2.424	2.00	0.365	0.995-0.021	0.961 (ns)
L	15.95	0.331	14.820–17.340	16.08	0.453	14.820–17.340	0.821 (ns)
M	71.04	1.230	67.630–74.450	69.78	0.491	68.420–71.130	0.356 (ns)
P	6.04	0.480	4.690–7.380	6.00	0.090	5.740–0.260	0.945 (ns)
S	7.92	0.040	7.820–8.020	7.92	0.248	7.230–0.610	0.438 (ns)

S: mean; SEM: standard error mean; CI: confidence interval (95%); $P < 0.05$; s: statistically significant; ns: not statistically significant; **L**: lauric acid; **M**: myristic acid; **P**: palmitic acid; **S**: stearic acid.

n-hexane. The transesterification of oils was carried out according to a procedure described by Maia and Rodrigues-Amaya, 1993 [22]. The methyl esters were dissolved with *n*-hexane ($2\,mg\cdot mL^{-1}$), and $1\,\mu L$ was injected in a Hewlett-Packard 5890 gas chromatograph coupled to a Hewlett-Packard 5988 mass spectrometer in the condition previously described [12, 23].

2.5. Analyses of Secondary Compounds. Individual seeds, before and after the germination process, were extracted (3x) with 20 mL of CH_3OH. The extract was concentrated to dryness and the residue dissolved with CH_2Cl_2 to obtain $2\,mg\cdot mL^{-1}$ as the final concentration, and $1\,\mu L$ was injected. All the analyses were performed with seven replicates in a Hewlett-Packard 5890 gas chromatograph coupled to a Hewlett-Packard 5988 mass spectrometer. The sample was injected (250°C) on a DB-5 column (30 m × 0.25 mm ID × 0.25 μm of film tickness). The column temperature was initially 120°C (2 min), then programmed to 230°C at $7°C\cdot min^{-1}$, kept at 230°C for 10 min, and then increased to 290°C in 15 min. The mass spectra were recorded at 70 eV. The identification of individual constituents was carried based on injection of isolated substances and comparison of their mass spectra.

2.6. Statistical Analysis. Statistical analyses were performed with the graphPad InStat software. All values were reported as means ± SEM, and were analyzed for statistical significance by two way analysis of variance followed by Student test. The minimum level of significance considered was $P < 0.05$.

3. Results and Discussion

Two groups of seeds of *V. surinamensis*, before germination (BG) and 6-7 months after germination (AG), were analyzed for fatty acids and major secondary metabolites. The second group (AG) showed a decrease of 30% in dry weight, but without significant changes in the extraction yield (Table 1). These results are in agreement with Durian's hypothesis, in which seeds are a nutrient storage organ to supply the seedling during the growth process [8]. The analyses of fatty acids content carried out in seeds of *V. surinamensis* before and after germination showed similar relative content of lauric acid (16%), myristic acid (70%), palmitic acid (6%), and stearic acid (8%). This result is similar to that previously reported [23], and since no preferential uptake of fatty acids could be detected, the major role of fatty material as carbon source is clearly supported (Table 2).

The secondary metabolites in both groups of seeds of *V. surinamensis* were analyzed by GC-MS. The chromatographic profile observed for both groups exhibited the predominance of galbulin (**2**), galbacin (**4a**), and veraguensin (**5b**) as the major compounds (Figure 2). After statistical analyses, no significant variation was observed in the relative content of monitored compounds, except to compound **1** ($P < 0.05$) (Table 2).

From *V. surinamensis*, new substances were isolated [24] and some neolignans showed allelopathic properties [25]. Recently, other neolignans showed antiinflammatory and antileishmanial activities [26, 27]. In addition, the increase of phenolic compounds was observed after elevated CO_2 submission in *V. surinamensis* [28] and a strong inhibition of CO_2 assimilation by sun exposure [29]. However, the analyses of the composition occurring in the seeds of this

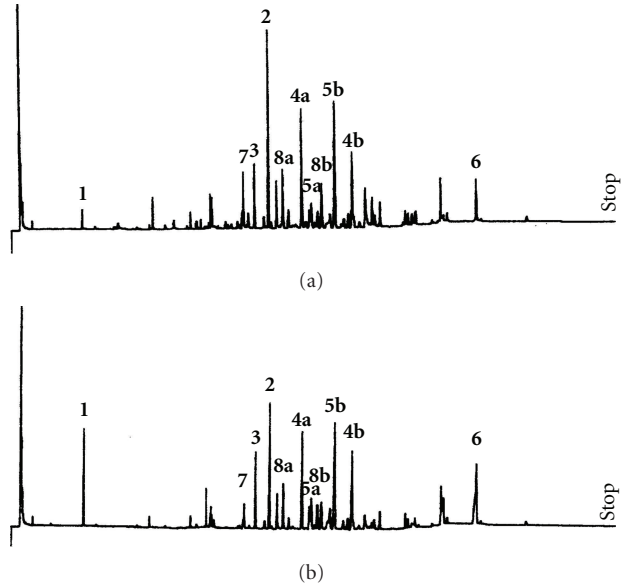

Figure 2: GC profile of secondary metabolites before (a) and after (b) germination of *V. surinamensis* seeds.

species during germination and seedling processes had not been studied yet.

In summary, the germination of *V. surinamensis* seeds and the seedling development are processes in which both fatty acids and secondary metabolites (lignans, isoflavonoids, and juruenolides) are equally consumed in the seeds indicating their physiological role as energy and carbon source, or by other physiological function. In spite of the large concentration of lignans in the seeds (8.5% as dry weight basis), no specific translocation to the seedlings and no consumption of a specific compound from the seeds could be detected. The lignans could have biological importance to the seeds, but after the lignans uptake to the seedling, our results, in addition to the previous phytochemical investigations [12], reinforce the use of these compounds as energy and carbon source by the seedlings.

Acknowledgments

This work was supported by financial aid provided by FAPESP and PADCT/CNPq. This work is dedicated to Professor Otto Richard Gottlieb.

References

[1] K. S. Bawa, P. S. Ashton, and S. M. Nor, "Reproductive ecology of tropical forest Plants: management issues," in *Reproductive Ecology of Tropical Forest Plants*, K. S. Bawa and M. Hadley, Eds., p. 3, UNESCO & Parthenon Publishing Group, Paris, France, 1990.

[2] J. M. Ayres, *As Matas de Várzea do Mamirauá*, MST-CNPq, Brasília, Brasil, 1993.

[3] W. A. Rodrigues, "Revisão taxonomica das espécies de *Virola* Aublet (Myristicaceae) do Brasil," *Acta Amazonica*, vol. 10, supplement, pp. 1–127, 1980.

[4] H. F. Howe, "Seed dispersal by birds and mammals implications for seedling demography," in *Reproductive Ecology of Tropical Forest Plants*, K. S. Bawa and M. Hadley, Eds., pp. 191–218, UNESCO & The Parthenon Publising Group, Paris, France, 1990.

[5] A. Hladik and S. Miquel, "Seedling types and plant establishment in an African rain forest," in *Reproductive Ecology of Tropical Forest Plants*, K. S. Bawa and M. Hadley, Eds., pp. 261–282, UNESCO & The Parthenon Publising Group, Paris, France, 1990.

[6] M. J. Kato, M. Yoshida, and O. R. Gottlieb, "Flavones and lignans in flowers, fruits and seedlings of *Virola venosa*," *Phytochemistry*, vol. 31, no. 1, pp. 283–287, 1991.

[7] A. P. Danelutte, A. J. Cavalheiro, and M. J. Kato, "Lignoids in seedlings of *Virola sebifera*," *Phytochemical Analysis*, vol. 11, no. 6, pp. 383–386, 2000.

[8] D. H. Janzen, "The ecology and evolutionary biology of seed chemistry as relates to seed predation," in *Biochemical Aspects of Plant and Animal Coevolution*, J. B. Harborne, Ed., pp. 163–206, Academic Press, London, UK, 1978.

[9] S. A. Foster, "On the adaptive value of large seeds for tropical moist forest trees: a review and synthesis," *The Botanical Review*, vol. 52, no. 3, pp. 260–299, 1986.

[10] H. F. Howe and G. A. V. Kerckhove, "Removal of wild nutmeg (*Virola surinamensis*) crops by birds," *Ecology*, vol. 62, no. 4, pp. 1093–1106, 1981.

[11] N. P. Lopes, E. E. De Almeida Blumenthal, A. J. Cavalheiro, M. J. Kato, and M. Yoshida, "Lignans, γ-Lactones and propiophenones of *Virola surinamensis*," *Phytochemistry*, vol. 43, no. 5, pp. 1089–1092, 1996.

[12] N. P. Lopes, S. C. Franca de, A. M. S. Pereira et al., "A butanolide from seedlings and micropropagated leaves of *Virola surinamensis*," *Phytochemistry*, vol. 35, no. 6, pp. 1469–1470, 1994.

[13] M. A. Cardoso, R. Cunha, and T. S. Pereira, "Germinação de sementes de *Virola surinamensis* (Rol.) Warb. (Myristicaceae) e *Guarea guidonea* (L.) Sleumer (Meliaceae)," *Revista Brasileira de Sementes*, vol. 16, no. 1, pp. 1–5, 1994.

[14] J. M. Bárbosa-Filho, M. S. D. Silva, M. Yoshida, and O. R. Gottlieb, "Neolignans from *Licaria aurea*," *Phytochemistry*, vol. 28, no. 8, pp. 2209–2211, 1989.

[15] M. M. M. Pinto, A. Kijjoa, I. O. Mondranondra, A. B. Gutiérrez, and W. Herz, "Lignans and other constituents of *knema furfuracea*," *Phytochemistry*, vol. 29, no. 6, pp. 1985–1988, 1990.

[16] L. E. S. Barata, P. M. Baker, O. R. Gottlieb, and E. A. Rùveda, "Neolignans of *Virola surinamensis*," *Phytochemistry*, vol. 17, no. 4, pp. 783–786, 1978.

[17] M. A. Sumathykutty and J. M. Rao, "8-Hentriacontanol and other constituents from *Piper attenuatum*," *Phytochemistry*, vol. 30, no. 6, pp. 2075–2076, 1991.

[18] R. W. Doskotch and M. S. Flom, "Acuminatin, a new *bis*-phenylpropide from *Magnolia acuminata*," *Tetrahedron*, vol. 28, no. 18, pp. 4711–4717, 1972.

[19] B. Talapatra, P. K. Chaudhuri, and S. K. Talapatra, "(-)-Maglifloenone, a novel spirocyclohexadienone neolignan and other constituents from *Magnolia liliflora*," *Phytochemistry*, vol. 21, no. 3, pp. 747–750, 1982.

[20] R. Braz Filho, O. R. Gottlieb, A. A. De Moraes et al., "The chemistry of Brazilian myristicaceae. IX. Isoflavonoids from amazonian species," *Lloydia*, vol. 40, no. 3, pp. 236–238, 1977.

[21] J. C. Martinez and L. E. Cuca, "Flavonoids from *Virola calophylloidea*," *Journal of Natural Products*, vol. 50, no. 6, pp. 1045–1047, 1987.

[22] E. L. Maia and D. B. Rodrigues-Amaya, "Avaliação de um método simples e econômico para a metilação de ácidos graxos com lipídios de diversas espécies de peixes," *Revista do Instituto Adolfo Lutz*, vol. 53, no. 1/2, pp. 27–35, 1993.

[23] D. H. S. Silva, N. P. Lopes, M. J. Kato, and M. Yoshida, "Fatty acids from Myristicaceous seeds of myristic acid-rich species," *Anais da Associação Brasileira de Química*, vol. 46, pp. 232–235, 1997.

[24] N. P. Lopes, P. A. Dos Santos, M. J. Kato, and M. Yoshida, "New butenolides in plantlets of *Virola surinamensis* (Myristicaceae)," *Chemical and Pharmaceutical Bulletin*, vol. 52, no. 10, pp. 1255–1257, 2004.

[25] F. C. Borges, L. S. Santos, M. J. C. Corrêa, M. N. Oliveira, and A. P. S. Souza Filho, "Allelopathy potential of two neolignans isolated from *Virola surinamensis* (Myristicaceae) leaves," *Planta Daninha*, vol. 25, no. 1, pp. 1045–1047, 2007.

[26] L. E. S. Barata, L. S. Santos, P. H. Ferri, J. D. Phillipson, A. Paine, and S. L. Croft, "Anti-leishmanial activity of neolignans from *Virola* species and synthetic analogues," *Phytochemistry*, vol. 55, no. 6, pp. 589–595, 2000.

[27] A. A. V. Carvalho, P. M. Galdino, M. V. M. Nascimento et al., "Antinociceptive and antiinflammatory activities of grandisin extracted from *Virola surinamensis*," *Phytotherapy Research*, vol. 24, no. 1, pp. 113–118, 2010.

[28] P. D. Coley, M. Massa, C. E. Lovelock, and K. Winter, "Effects of elevated CO_2 on foliar chemistry of saplings of nine species of tropical tree," *Oecologia*, vol. 133, no. 1, pp. 62–69, 2002.

[29] G. H. Krause, E. Grube, A. Virgo, and K. Winter, "Sudden exposure to solar UV-B radiation reduces net CO_2 uptake and photosystem I efficiency in shade-acclimated tropical tree seedlings," *Plant Physiology*, vol. 131, no. 2, pp. 745–752, 2003.

Hindawi Publishing Corporation
International Journal of Analytical Chemistry
Volume 2012, Article ID 923208, 10 pages
doi:10.1155/2012/923208

Research Article

Multilayer Films Electrodes Consisted of Cashew Gum and Polyaniline Assembled by the Layer-by-Layer Technique: Electrochemical Characterization and Its Use for Dopamine Determination

Sergio Bitencourt Araújo Barros,[1,2] Cleide Maria da Silva Leite,[1] Ana Cristina Facundo de Brito,[3] José Ribeiro Dos Santos Júnior,[1] Valtencir Zucolotto,[4] and Carla Eiras[5]

[1] *Departamento de Química, Centro de Ciências da Natureza (CCN), Universidade Federal do Piauí (UFPI), 64049550 Teresina, PI, Brazil*
[2] *DB, Universidade Federal do Piauí (UFPI), Campus Senador Helvídio Nunes de Barros (CSHNB), 64600000 Picos, PI, Brazil*
[3] *SEDIS, Universidade Federal do Rio Grande do Norte (UFRN), Caixa Postal 1524, Campus Universitário Lagoa Nova, 59072970 Natal, RN, Brazil*
[4] *Nanomedicine and Nanotoxicology Laboratory, IFSC, University of São Paulo, São Carlos, SP, Brazil*
[5] *Núcleo de Pesquisa em Biodiversidade e Biotecnologia, BIOTEC, Campus Ministro Reis Velloso, CMRV, Universidade Federal do Piauí, UFPI, 64202020 Parnaíba, PI, Brazil*

Correspondence should be addressed to Carla Eiras, carla.eiras.ufpi@gmail.com

Received 1 October 2011; Revised 10 December 2011; Accepted 3 January 2012

Academic Editor: Ricardo Vessecchi

We take advantage of polyelectrolyte feature exhibited by natural cashew gum (*Anacardium occidentale* L.) (CG), found in northeast Brazil, to employ it in the formation of electroactive nanocomposites prepared by layer-by-layer (LbL) technique. We used polyaniline unmodified (PANI) or modified with phosphonic acid (PA), PANI-PA as cationic polyelectrolyte. On the other hand, the CG or polyvinyl sulfonic (PVS) acids were used as anionic polyelectrolytes. The films were prepared with PANI or PANI-PA intercalated with CG or with PVS alternately resulting in four films with different sequences: PANI/CG PANI-PA/CG, PANI/PVS and PANI-PA/PVS, respectively. Analysis by cyclic voltammetry (CV) of the films showed that the presence of gum increases the stability of the films in acidic medium. The performance of the modified electrode of PANI-PA/CG was evaluated in electro analytical determination of dopamine (DA). The tests showed great sensitivity of the film for this analyte that was detected at 10^{-5} mol L^{-1}.

1. Introduction

The physicochemical properties of nanoscale composite are a result of molecular interaction between materials of interest, such as a conducting polymer, promoting greater structural control of the formed films [1–3]. Two of the most used methods to obtain nanostructured materials in the solid state are the Langmuir-Blodgett (LB) technique [4] and the process of layer-by-layer (LbL) assembly [5]. This last one emerges as a method of deposition of alternating layers formed through the electrostatic interaction between oppositely charged solutions, where the formation of the first monolayer on the substrate surface occurs initially through a process of adsorption. In addition to the possibility of controlling the structure formed at the supramolecular level, the LbL technique has the advantage of not requiring any sophisticated equipment or procedures such as the LB technique.

The technological interest of several research groups in composites, and more recently in nanocomposites, comes

mainly from the mechanical properties and biodegradability, which are both characteristic of natural polymers, allied to the conductive properties of some synthetic polymers, which provides a great versatility of applications in areas such as engineering, biotechnology, and medicine [6–8].

Natural gums are macromolecules formed from units of sugars, monosaccharides, linked by glycosidic bonds resulting in natural polymers with long chains and high molecular weight [9]. The gums may originate from plants exudates (e.g., Arabic gum and cashew gum), seaweed extract (e.g., agar), animal (e.g., chitosan), seeds (e.g., guar gum), and others [7]. The gum from exudates is produced in epithelial cells confined in the ducts of the trees that are released spontaneously or induced as a defense mechanism of the plant [10, 11]. The natural gums interact with water in two different ways: by retention of water molecules (thickness effect) or by building networks that enhance the connection areas (effect of gelation). Because of these behaviors, the gums are also known as hydrocolloids [12, 13].

The cashew gum (*Anacardium occidentale* L.) is particularly interesting because it is an exudate obtained from the cashew tree, very abundant in the northeast of Brazil. It belongs to the same family of Arabic gum, widely used in the food industry, and presents similarities in their composition and in their physicochemical properties [12–14]. Cashew gum (CG) is an acidic polysaccharide complex composed of a main chain of β-galactose ($1 \rightarrow 3$) with branches of β-galactose ($1 \rightarrow 6$), with the terminal residues glucuronic acid, arabinose, rhamnose, 4-O-methylglucuronic acid, xylose, glucose, and mannose [14]. Brazilian gum main constituents are galactose (73%), arabinose (5%), rhamnose (4%), glucose (11%), glucuronic acid (6.3%), and residues of other sugars (less than 2%) [12, 14] (Scheme 1(a)). Additionally, the terminal glucuronic acids in the structure of the gum are responsible for the anionic nature of the material when in aqueous solution. Cashew gum has antimicrobial properties for therapeutic treatment, as well as thickening and emulsifying properties [15, 16] used in foods and drugs industry. These characteristics are due to its heterogeneous structure and high molecular weight of the polysaccharide chain, which interacts strongly with water, creating an effect of thickening or gelling in solution [16].

The polyaniline (PANI) belongs to the class of conducting polymers with high technological interest due to their potential applications as electroluminescent devices, corrosion protection, sensors, and biosensors [17, 18]. The versatility of PANI is due to changes of its oxidation state, hence its electrical conductivity, which occurs rapidly and reversibly, and its chemical stability [19, 20]. The applications of polyaniline are limited by its poor solubility in aqueous media in its conductive form [17, 20]. A proposed solution for this limitation was given by Geng et al. [21] who prepared a water-soluble conductive polyaniline through the introduction of hydrophilic dopant such as phosphonic acid (PA) in the polymeric chain. The PA is a mixture of acids mono- and bihydroxyl phosphonate at 1 : 1 molar ratio (1). The PA organic properties derive from poly(ethylene glycol) monomethyl ether. Thus, the longer the hydrophilic chain of the conducting polymer, the higher its solubility in water [21], generating new applications:

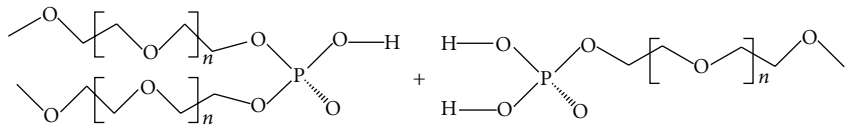

(1)

In this study, LbL films were produced with PANI or PANI-PA and the natural cashew gum (CG) in a bilayer fashion $(PANI/CG)_n$ or $(PANI\text{-}PA/CG)_n$ (where n is the number of bilayers). Films containing a conventional anionic polyelectrolyte, for example, poly(vinylsulfonic acid) PVS, were compared to cashew gum in the $(PANI/PVS)_n$ or $(PANI\text{-}PA/PVS)_n$ films. The films were studied through electrochemical experiments by cyclic voltammetry. We also investigated the ability of these nanocomposites to act as modified electrodes for dopamine sensing.

2. Experimental

Cashew gum, collected in the state of Ceará (northeast region of Brazil), was isolated and purified using sodium salt, as described by Costa et al. [22]. Afterwards 0.25 mL of ethanol was added to 5.0 g of cashew gum, which was immediately dissolved in 100 mL of Milli-Q water under stirring for 12 h, followed by filtration.

PANI was synthesized by the oxidative polymerization of aniline doubly distilled in 1.0 mol L^{-1} HCl solution containing a proper amount of ammonium persulfate ($(NH_4)_2S_2O_8$, Vetec). The solution temperature was kept between 0°C and 5°C, with continuous mechanical stirring. The product was maintained in ammonia hydroxide (Vetec) for 12 hours to obtain PANI in the form of emeraldine base (EB) [23]. The mixture of mono- and bihydroxyl acids designated as PA, with molecular average weight of 896 g mol^{-1}, was prepared as reported by Geng et al. [21].

For the processing of polyaniline solutions, 0.47 g PANI-EB powder (with or without PA dopant) was dissolved in 25 mL dimethylacetamide (DMAc, Vetec) under stirring for 12 h. The solutions were filtered and slowly added to 26 mL of HCl solution, and the pH was adjusted at 2.8. Poly(vinyl sulfonic acid) (PVS) was purchased from Aldrich Co. and used without previous purification in aqueous solutions at a concentration of 0.5 mg mL^{-1} and pH 2.8. Ultrapure water with a resistivity of 18.3 MΩ cm (Milli-Q, Millipore) was

used for preparation of all solutions. The chemical structures of the materials employed are depicted in Scheme 1(a).

Nanostructured layered films were assembled in a bilayer fashion using PANI or PANI-PA as polycationic solutions in conjunction with CG or PVS as polyanionic solutions. The deposition of each layer consisted in the immersion of the substrate in the dipping solution for 5 min, followed by rinsing in the washing solution (HCl, pH 2.8) and drying in N_2 flow. LbL films with four distinct architectures were investigated: $(PANI/PVS)_n$, $(PANI\text{-}PA/PVS)_n$, $(PANI/CG)_n$, and $(PANI\text{-}PA/CG)_n$ where n is the number of bilayers. Multilayer films with $n = 2, 4, 6$, and 8 were obtained onto glass covered with indium tin oxide (ITO), (Scheme 1(b)).

Electrochemical measurements were carried out using a potentiostat Autolab PGSTAT30 and a three-electrode electrochemical cell with 10 mL. A 1.0 cm^2 platinum foil and saturated calomel electrode (SCE) were used as auxiliary and reference electrodes, respectively. The LbL films onto ITO (0.4 cm^{-2}) were used as the working electrode. All the experiments were performed in inert N_2 atmosphere at 22°C in an electrolytic solution of 0.1 mol L^{-1} HCl. PANI-AP/GC LbL film containing 6 bilayers ($n = 6$) was subjected to dopamine (DA) detection using cyclic voltammetry in electrolytic solution containing 10 to 230 μmol L^{-1} of DA and sweep rate of 50 m Vs^{-1}. After the measurement the film tested was exhaustively washed with electrolytic solution and the reproducibility was investigated. Furthermore, the effects of the interfering ascorbic acid (AA) in the presence of DA were also studied using different proportions of AA and DA.

3. Results and Discussion

3.1. Electrochemical Characteristics of Nanostructured Films. Cyclic voltammograms of ITO unmodified and modified electrodes with LbL film produced with poly(allylamine-hydrochloride), PAH, and the natural cashew gum, $(PAH/CG)_6$, were obtained in HCl 0.1 mol L^{-1} and are shown in Figure 1. Under our experimental conditions, it is observed that the ITO substrate has no electrochemical response to the potential range studied. However, the modified substrate with $(PAH/CG)_6$ shows that the presence of the LbL film activates the electrode surface increasing the double electrical layer of this system and therefore catalyzes the processes of oxygen evolution observed in the forward sweep and hydrogen evolution observed in the reverse sweep. The increase in current values is observed in the potential in which these processes occur.

All films studied were prepared with six bilayers. A previous study about the influence of the size and nature of this anion in the supporting electrolyte for the systems studied here was carried out in HCl or H_2SO_4, both at 0.1 mol L^{-1}, with scan rate of 50 mV s^{-1}. The processes of oxidation and reduction, characteristic of conducting polymer, were shifted to more positive potentials in H_2SO_4 media when compared to the profile obtained in HCl solution (data not shown). The potential difference observed for this redox process was 0.05 V. According to Matveeva et al. [24], both the processes of oxidation and reduction (E_{RED} and E_{OX}) and the distance between the potential at which these transitions occur are dependent on the substrate used and the size and nature of the anion of the supporting electrolyte employed. The potential shift observed for the PANI in H_2SO_4 reflects a limitation in the processes of charge transfer across the interface between ITO and polymeric film and also in the interface polymeric film and the electrolyte. Probably this limitation of the charge transfer process could be related to differences in mobility and the steric hindrance originated from the anionic species present in both electrolytes studied, having HSO_4^- and SO_4^{2-} for sulfuric acid and Cl^- for hydrochloric acid, respectively. It was also noted that the degradation processes of PANI were more intense and were best defined in H_2SO_4 (data not shown). This observation is likely to be explained by the fact that H_2SO_4 is a more oxidant acid than HCl intensifying the processes observed. Thus, the whole study presented in this paper was performed in optimized conditions of HCl media.

Figure 2 shows the cyclic voltammograms obtained for the bilayers films containing the conductive polymer interspersed with cashew gum or PVS in HCl media. The electrochemical profile recorded for the LbL systems $(PANI/PVS)_6$ $(PANI\text{-}PA/PVS)_6$, $(PANI\text{-}GC)_6$, and $(PANI\text{-}PA/CG)_6$ (Figure 2) indicates the presence of two redox processes characteristic of PANI that correspond to interconversions in their states of oxidation [25]. During the direct scan there was the transition from leucoemeraldine state to emeraldine PANI, E_{pa1}, with the expulsion of the proton, and the transition from emeraldine to pernigraniline, E_{pa2}, was accompanied by the capture of the anion, Cl^-. During the inverse sweep two reduction processes were observed; pernigraniline to emeraldine, E_{pc2}, accompanied by the expulsion of the anion and emeraldine to leucoemeraldine, E_{pc1}, which was accompanied by proton uptake.

An intermediate process between the transitions related above is defined as acidic degradation of PANI with the formation of benzoquinone (oxidation) and hydroquinone (reduction) pair. The electrochemical behavior for the systems in Figure 2 shows that the interactions between the PANI or PANI-PA with PVS and CG do not suppress the electroactive and electrochemical properties observed and described for polyaniline. The films of PANI and PANI-PA interspersed with PVS showed the three well-known oxidation processes of PANI and a fourth oxidation process observed in the region of 0.86 V (Figures 2(a) and 2(b)). This fourth oxidation was not observed for films in which PVS was replaced by CG in the multilayer structure (Figures 2(c) and 2(d)). The oxidation process at 0.86 V can be explained as the result of an interaction between the cationic groups of PANI with anionic groups of PVS.

The phosphonic acid (PA) used in this study acts as both a modifying agent PANI, increasing its solubility, and a dopant acid promoting a further increase in current values observed in the redox processes of PANI-PA (Figures 2(a) and 2(c)). This increase in current values contributes to providing an enhancement in selectivity of the PANI-PA/PVS and PANI-PA/CG systems compared to PANI/PVS and PANI/CG, and thus the presence of PA becomes an

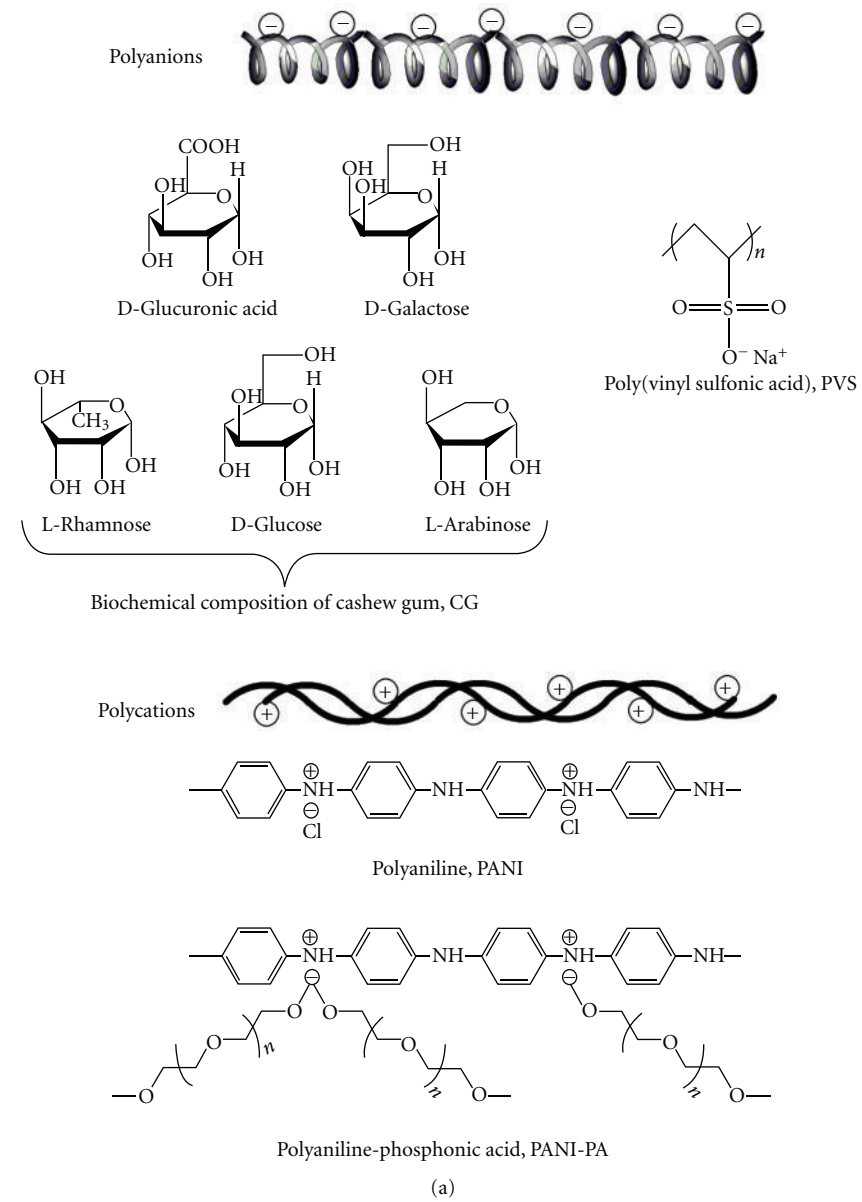

Scheme 1: (a) Chemical structures of material employed in the films and (b) schematic process of multilayer film formation.

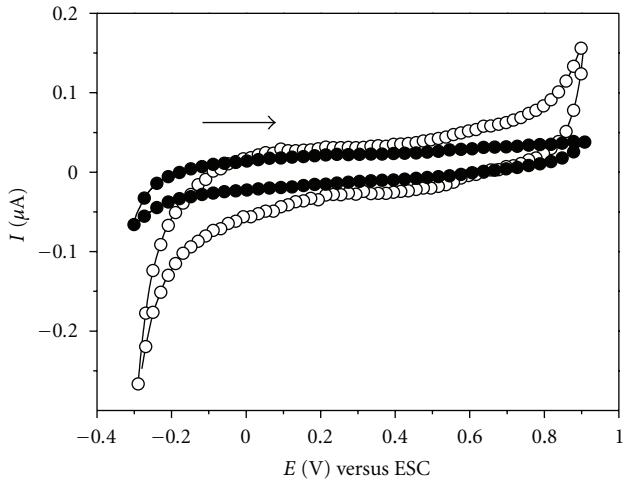

Figure 1: Cyclic voltammograms for bare ITO (—●—) and ITO modified with $(PAH/CG)_6$ LbL films (—○—) in HCl 0.1 mol/L at 50 mV s^{-1}.

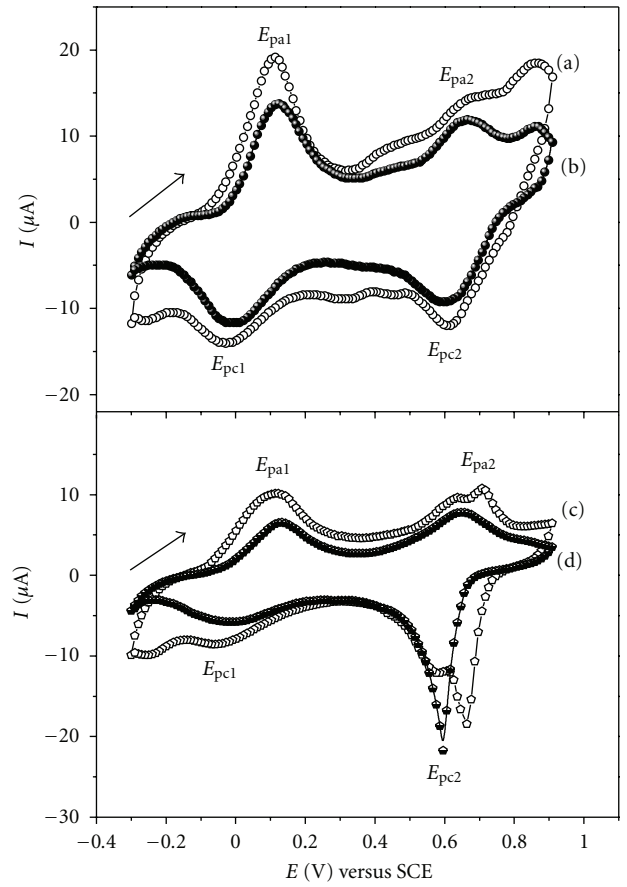

Figure 2: Cyclic voltammograms for LbL films: (a) $(PANI\text{-}PA/PVS)_6$, (b) $(PANI/PVS)_6$, (c) $(PANI\text{-}PA/CG)_6$, and (d) $(PANI/CG)_6$ in 0.1 mol L^{-1} HCl solution at 50 mV s^{-1}.

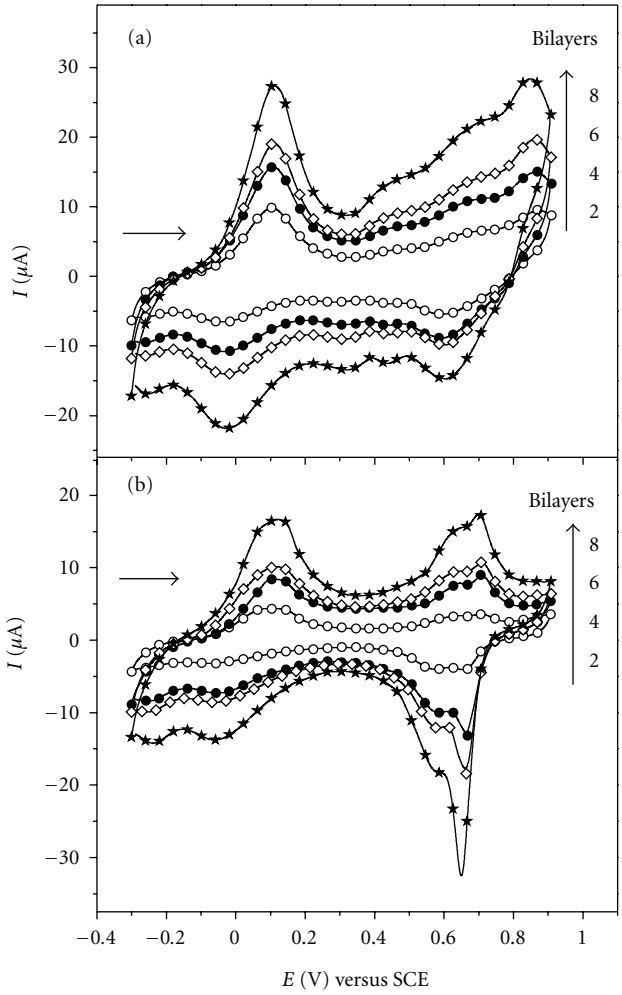

Figure 3: Cyclic voltammograms for LbL films from (a) $(PANI\text{-}PA/PVS)_n$ and (b) $(PANI\text{-}PA/CG)_n$, where $n = 2, 4, 6$, and 8 bilayers in 0.1 mol L^{-1} HCl solution at 50 mV s^{-1}.

important factor to be considered in analytical determinations using electrochemical techniques.

For the films PANI-PA/PVS (Figure 3(a)) and PANI-PA/CG (Figure 3(b)) with 2, 4, 6, and 8 bilayers, the cyclic voltammograms obtained at 50 mV s^{-1} reveal that the increase in the number of bilayers is reflected in the increase of current values. This result indicates an increment in the amount of material adsorbed on the substrate as the number of bilayers increases.

When PVS was replaced by cashew gum (Figure 3(b)) the fourth oxidation process disappeared because the interaction between PANI and PVS disappeared as well. The interaction between these PANI and PVS can occur by two distinct mechanisms, similarly as proposed by Raposo & Oliveira for LbL films of poly(*o*-methoxyaniline) (POMA) and PVS [26]. This process can occur through the establishment of links between PANI and PSV in the presence of electrical charge (Scheme 2(a)) and/or in the absence of electrical charge through the formation of networks of water molecules from the PANI present in solution with PVS (Scheme 2(b)).

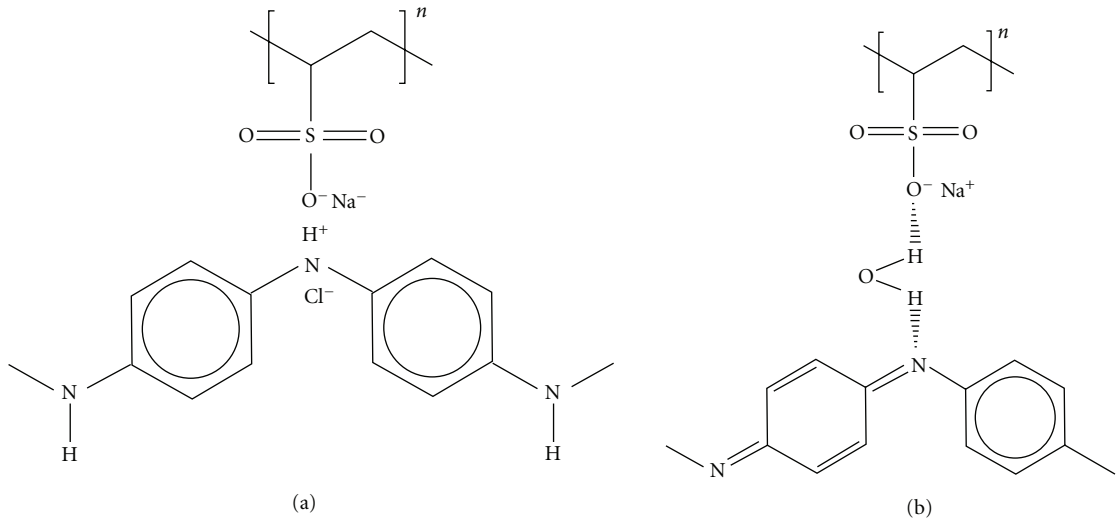

Scheme 2: Representation of the mechanisms of the adsorption process proposed for the PANI and PVS: (a) adsorption in the presence of electric charge and (b) adsorption in the absence of electric charge [26].

Probably the adsorption processes proposed for the PANI and PVS must be somehow related to the oxidation process observed in the region of 0.86 V in Figure 3(a). In our studies we observed that the presence of cashew gum significantly decreases the degradation of the polymer in acid media, which is observed in films PANI-PA/PVS around 0.43 V (shown in Figures 2(a) and 3(a)).

In Figure 4 the cyclic voltammograms of the films with 6 bilayers of PANI-PA/PVS (Figure 4(a)) and PANI-PA/CG (Figure 4(b)) the 5th and the 20th successive cycles of scanning potential at 50 mV s^{-1} are shown. The electrode polarization until 0.90 V led to a more visible degradation of the conducting polymer in system PANI-PA/PVS. Cyclic voltammograms for these films show the presence of intermediate redox process around 0.43 V, which is related to soluble products (radical benzoquinone/hydroquinone) formed during the acid degradation of polyaniline [25] accompanied by a decrease of the current values in all the processes observed. On the other hand, the process for proton expulsion and anion uptake seems more stable for the PANI-PA/CG film even after twenty successive cycles.

Therefore, the polyaniline suffers acid degradation, promoted by the high polarization potential and by electrolyte of HCl, and in the case in the PANI-PA/PVS system this process is enhanced by the presence of PA modifier. On the other hand, when PVS was replaced by CG the degradation process of PANI was reduced indicating that the cashew gum protects the film from the degradations processes mentioned above, presenting a greater stability during scanning in an acid medium and polarizations at 0.90 V compared to PANI-PA/PVS or PANI/PVS films studied. Therefore, the cashew gum acts as a kind of antioxidant for polyaniline. Previous works from our group [8] showed that LbL films of POMA and gums have greater stability during scanning potential in an acid medium than films POMA/PVS and that the

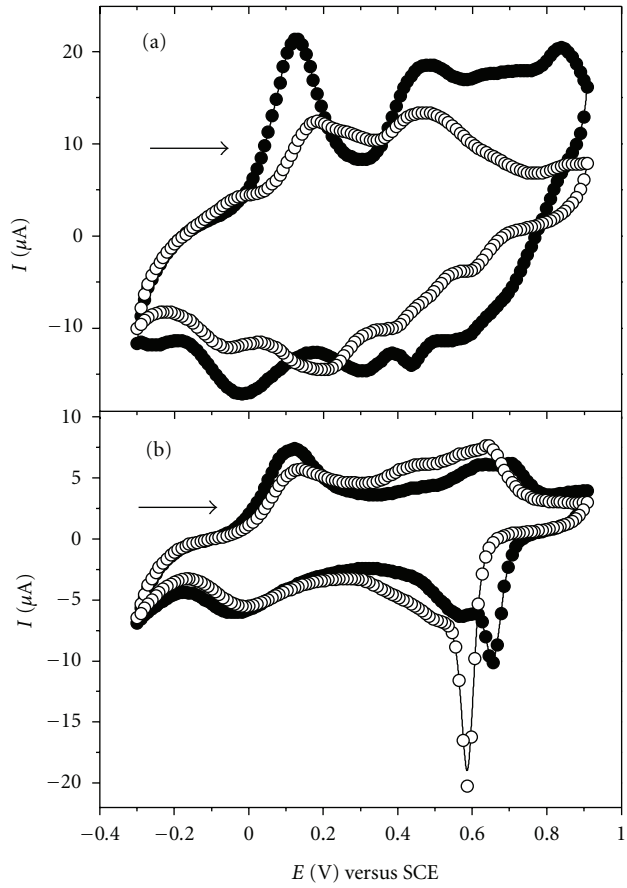

Figure 4: Cyclic voltammograms for LbL films from (a) $(PANI-PA/PVS)_6$ and (b) $(PANI-PA/CG)_6$ after five and twenty (5th cycle —●— and 20th cycle —○—) successive cycles in 0.1 mol L^{-1} HCl solution, at 50 mV s^{-1}.

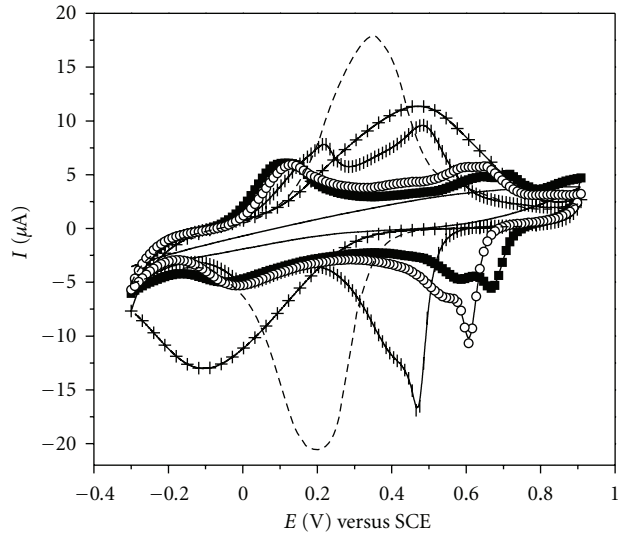

Figure 5: Cyclic voltammograms for LbL films from (PANI-PA/CG)$_6$ in HCl electrolyte at different pHs (—■— pH 1 initial; ——— pH 2; - - - pH 3; —+— pH 4; — pH 5; —○— pH 1 final). Scan rate: 50 mV s^{-1}.

gums as chichá (*Sterculia striata*) and angico (*Anadenanthera macrocarpa* B.) act protecting the polymer film from this degradation.

The process of charge transfer from the ITO-modified electrode with PANI-PA/CG film containing 6 bilayers was studied by varying the scan rate (v) in the range of 10 to 150 mV s^{-1} (data not shown). In these conditions it was observed that the values of the anodic peak current (I_{pa1}) increased linearly with scan rate for the film PANI-PA/CG, according to the equation $I_{pa1}(\mu A) = -1.92(\pm 0.76) + 0.30(\pm 0.010)\ v$ (mV s^{-1}), with a linear correlation, $r = 0.998$. This behavior indicates a redox process of electroactive species that are strongly adsorbed on the ITO surface, confirming that the electrochemical reaction is controlled by a kind of electron hopping mechanism of charge transfer on the electrode surface [33].

The dependence on pH solution of the electrochemical behavior of PANI-PA/CG film was studied and shown in Figure 5. When increasing the pH from 1 to 2 an approximation of PANI redox process occurs, and in pH 3.0 and 4.0 it is possible to observe the overlap of two redox processes at 0.30 V and 0.20 V for pH 3.0 and at 0.48 V and −0.10 V for pH 4. On the other hand at pH 5 the PANI-PA/CG film no longer presents any electrochemical activity. However, when the same film was scanned again at pH 1.0 it presented the characteristic processes of electroactive polyaniline with potential and current values similar to the first scan done at pH 1.0 before variations in pH described above. This reversibility in the electrochemical behavior in function of the pH media is not observed in films of PANI/PVS or PANI-PA/PVS. Thus, the results suggest that in the case of PANI-PA/CG films, the cashew gum acts as a stabilizing element of the polyaniline.

LbL films of cashew gum containing modified polyaniline with PA dopant are very interesting for applications in electrochemical sensors due to their high reproducibility and stability. Thus, the self-assembled film of PANI-PA/CG containing 6 bilayers was selected to be applied to detect dopamine (DA), an important neurotransmitter in the central nervous system of mammals [34, 35].

3.2. Study of Modified Electrode with PANI-PA/CG Nanocomposite as Biosensor. Figure 6(a) shows the cyclic voltammograms for the LbL film with 6-bilayers of PANI-PA/CG in different concentrations of dopamine (DA). In this figure a redox couple (E_{pa2}/E'_{pc}) appears associated with oxidation of dopamine in dopamine quinone at 0.63 V and its reduction at 0.29 V [34, 35].

The anodic current peak (I_{pa2}) increases linearly for concentrations of DA between 0.01 and 0.23 mmol L^{-1} for the modified electrode, as shown in the calibration curve in Figure 6(b). The calibration equation obtained by linear regression is $I_{pa2}(\mu A) = 0.15(\pm 0.043) + 23.10(\pm 0.37)$ [DA]/mmol L^{-1} with a correlation coefficient (r) equal to 0.998 (for $n = 10$) and sensibility of 23.10 μA mmol^{-1} L. The limit of detection (LD) of 1.5×10^{-8} mol L^{-1} was estimated using 3σ/slope ratio, where σ is the standard deviation calculated from 10 blank samples and slope refers to the slope of the calibration curve, according to the IUPAC recommendations [36]. The modified electrode presented reversibility after washing and a good repeatability for DA determinations with relative standard deviation, RSD = 6% in five determinations in the presence of 0.23 mmol L^{-1} DA.

Table 1 summarizes the analytical performance on different modified electrodes for DA detection by electrochemical process [27–32]. The lowest LD obtained was observed for film from (PANI-PA/CG)$_6$, revealing itself as a competitive electrode for this analysis when compared to other modified electrodes.

The relationship of peak current (I_{pa2}) for DA oxidation with the scan rate (v) has been investigated for 6 bilayers from PANI-PA/CG film in 0.1 mol L^{-1} HCl solution in the presence of 0.23 mmol L^{-1} DA (data not shown). Under these conditions a linear relationship between anodic current peak (I_{pa2}) and the square root of scan rate ($v^{1/2}$) for the PANI-PA/CG film was found according to the equation $I_{pa2}(\mu A) = -0.27(\pm 0.14) + 2.32(\pm 0.02)\ v^{1/2}$ (mV s^{-1})$^{1/2}$, $r = 0.999$. This behavior indicates that the electrocatalytic process of electron transfer is controlled by dopamine diffusion from the solution to the redox sites of PANI-PA/CG films [37].

In order to investigate the selectivity of the PANI-PA/CG modified electrode, we tested the simultaneous detection of 0.01 mmol L^{-1} DA in different ascorbic acid (AA) concentrations, the natural interfering of DA [34]. It is noted in Figure 7 that when we increase the concentration of AA a proportional increase in the current values at 0.45 V is accompanied. Moreover, in the oxidation potential of dopamine, 0.63 V, the increase of current with the addition of AA is minimal, showing that oxidation of dopamine at the surface of modified electrode is slightly affected by trace amounts of AA (Figure 7).

Table 1: Comparative performance of different electrodes for dopamine determination.

Electrode	Method	Dynamic range (mmol L^{-1})	LD (mol L^{-1})	Reference
ITO modified with LbL film from $(PANI\text{-}PA/CG)_6$	CV[a]	0.01–0.23	1.5×10^{-8}	This work
ITO modified with LbL film from (PAH/Chichá gum/PAH/NiTsPc[b])$_5$	CV	0.3–250	1.05×10^{-5}	[27]
ITO modified with LbL film from ([PAMAM-MWCNTs][c]/NiTsPc)$_3$	CV	2.5×10^{-3}–0.24	5.4×10^{-7}	[28]
GCE[d]/MWCNTs modified with LbL film from (Nafion/[PVI-dmeOs][e])$_3$	DPV[f]	1.0×10^{-4}–0.01	5.0×10^{-8}	[29]
GCE modified with poly(flavin adenine dinucleotide)	CV	2.5×10^{-6}–4.0×10^{-5}	5.0×10^{-9}	[30]
ITO modified with LB film of $(PANI/Rupy^{g})_{21}$	CV	0.04–1.2	4.0×10^{-5}	[31]
GCE modified with (LiTCNE/PLL)[h] membrane	DPV	1.0×10^{-5}–0.01	5.0×10^{-10}	[32]

[a]Cyclic voltammetry.
[b]Tetrasulfonated metallophthalocyanine of nickel.
[c]Polyamidoamine-multiwalled carbon nanotubes.
[d]Glassy carbon electrode.
[e]Poly(vinylimidazole)-Os(4,4′-dimethylbpy)$_2$Cl.
[f]Differential pulse voltammetry.
[g]Ruthenium complex *mer*-[$RuCl_3$(dppb)(py)] (dppb = $PPh_2(CH_2)_4PPh_2$; (py) = pyridine).
[h]Lithium tetracyanoethylenide/poly-L-lysine.

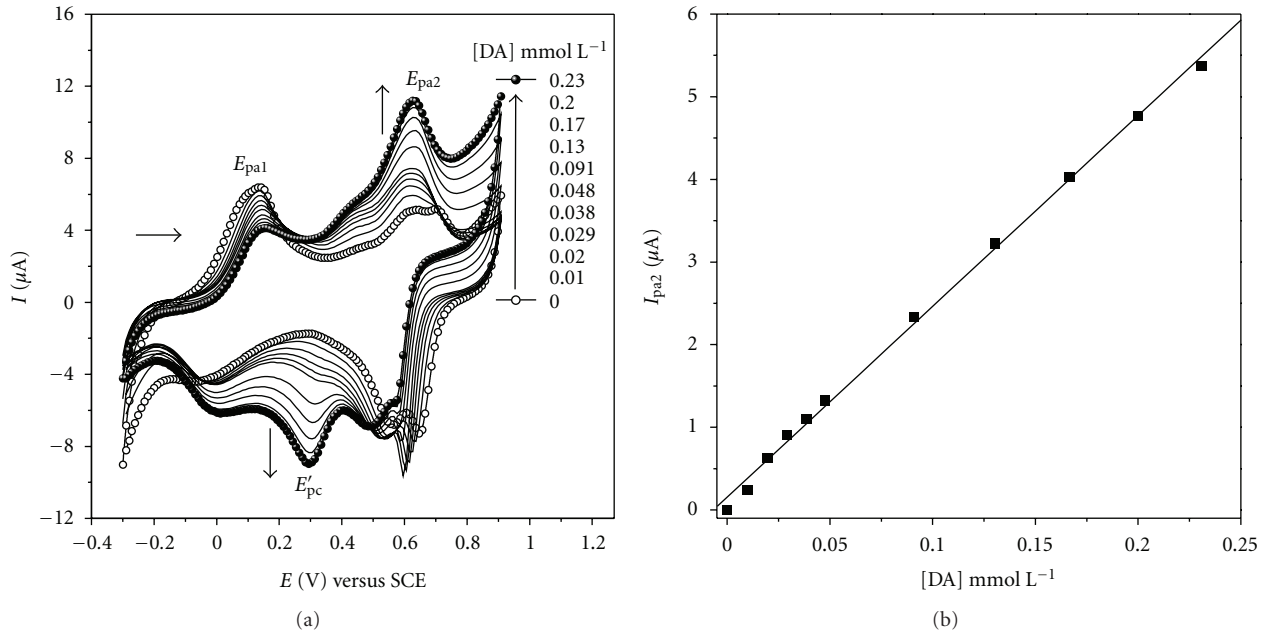

(a) (b)

Figure 6: (a) Cyclic voltammograms for LbL films from $(PANI\text{-}PA/CG)_6$ in 0.1 mol L^{-1} HCl solution in the presence of DA at concentrations ranging from 0.01 mmol L^{-1} to 0.23 mmol L^{-1} (from bottom to top). (b) The dependence of peak current (I_{ap2}) on the DA concentration. Scan rate: 50 mV s^{-1}.

Additionally it is important to observe that this new nanocomposite using cashew gum, which is a natural and biocompatible polymer, in the multilayer structure, gives rise to new applications as biosensor [38, 39]. Additionally, this film could be used in wound repair because it has been shown that very small exogenously applied electrical currents produce a beneficial therapeutic result for wounds [40]. In this work we propose a formation of electroactive nanocomposite, which can be a potential tool for wound repair when associated with the electrostimulation.

4. Conclusions

The electrochemical profiles observed for the films studied showed the redox intrinsic characteristic transitions of polyaniline. The presence of CG increases the electrochemical stability of the film, suggesting that it acts by protecting the conductive polymer from acid degradation. LbL films of PANI/PVS and PANI-PA/PVS show an oxidation process around 0.86 V, which can be related to interaction between PANI and PVS. Detailed studies showed that

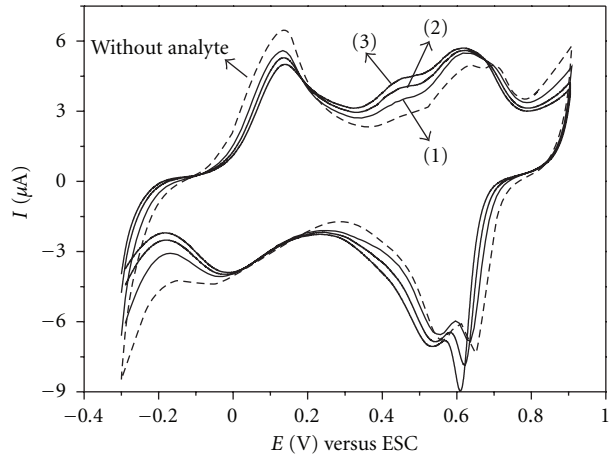

Figure 7: Cyclic voltammograms for LbL films from (PANI-AP/GC)$_6$ film in the absence and presence of 0.01 mmol L^{-1} DA containing ascorbic acid at a concentration of (1) 0.01 mmol L^{-1} (2) 0.02 mmol L^{-1} and (3) 0.03 mmol L^{-1} in 0.1 mol L^{-1} HCl solution, at 50 mV s^{-1}.

the electrochemical reaction in the PANI-PA/CG film is governed by a charge transfer mechanism at the surface electrode via electron hopping. The ITO-modified electrode with PANI-PA/CG film showed high reproducibility and stability, encouraging its use as a sensor of DA. This modified electrode was able to detect electroactive molecule of DA around 0.63 V in detection limits consistent with the pharmaceuticals formulations.

Acknowledgments

The S. B. A. Barros is indebted to CAPES for MSc fellowship. The authors thank the financial support from the Brazilian funding agencies FAPEPI, CAPES, and CNPq, as well as the technical support from LAPETRO-UFPI. The authors are grateful for the English revision done by our dear friend Mrs. Claudia Hissette.

References

[1] F. N. Crespilho, V. Zucolotto, O. N. Oliveira Jr., and F. C. Nart, "Electrochemistry of layer-by-layer films: a review," *International Journal of Electrochemical Science*, vol. 1, pp. 194–214, 2006.

[2] K. Fujimto, J. H. Kim, K. Ohmori, A. Ono, and S. Shiratori, "Flexible multilayer electrode films consisted of polyaniline and polyelectrolyte by layer-by-layer self-assembly," *Colloids and Surfaces A*, vol. 313-314, pp. 387–392, 2008.

[3] X. Zhang, H. Chen, and H. Zhang, "Layer-by-layer assembly: from conventional to unconventional methods," *Chemical Communications*, no. 14, pp. 1395–1405, 2007.

[4] K. B. Blodgett, "Monomolecular films of fatty acids on glass," *Journal of the American Chemical Society*, vol. 56, no. 2, p. 495, 1934.

[5] G. Decher, M. Eckle, J. Schmitt, and B. Struth, "Layer-by-layer assembled multicomposite films," *Current Opinion in Colloid and Interface Science*, vol. 3, no. 1, pp. 32–39, 1998.

[6] D. A. Silva, R. C. M. de Paula, J. P. A. Feitosa, A. C. F. De Brito, J. S. Maciel, and H. C. B. Paula, "Carboxymethylation of cashew tree exudate polysaccharide," *Carbohydrate Polymers*, vol. 58, no. 2, pp. 163–171, 2004.

[7] P. L. R. Da Cunha, R. C. M. de Paula, and J. P. A. Feitosa, "Polissacarídeos da biodiversidade brasileira: UMA oPortunidade de transformar conhecimento em valor econômico," *Química Nova*, vol. 32, no. 3, pp. 649–660, 2009.

[8] C. Eiras, I. N. G. Passos, A. C. F. De Brito et al., "Electroactive nanocomposites made of poly(o-methoxyaniline) and natural polysaccharides," *Química Nova*, vol. 30, no. 5, pp. 1158–1162, 2007.

[9] G. O. Aspinall, *The Polysaccharides*, Academic Press, New York, NY, USA, 1982.

[10] A. Nussinovitch, *Plant Gum Exudates of the World: Sources, Distribution, Properties, and Applications*, CRC Press, New York, NY, USA, 2010.

[11] C. G. Mothe and M. A. Rao, "Moths," *Thermochimica Acta*, vol. 9, pp. 357–358, 2000.

[12] R. C. M. de Paula and J. F. Rodrigues, "Composition and rheological properties of cashew tree gum, the exudate polysaccharide from *Anacardium occidentale* L," *Carbohydrate Polymers*, vol. 26, no. 3, pp. 177–181, 1995.

[13] C. G. Mothe and D. Z. Correia, *Revista Analytica*, no. 2, pp. 59–64, 2002.

[14] R. C. M. de Paula, F. Heatley, and P. M. Budd, "Characterization of *Anacardium occidentale* exudate polysaccharide," *Polymer International*, vol. 45, no. 1, pp. 27–35, 1998.

[15] G. V. Schirato, F. M. F. Monteiro, F. O. Silva, J. L. L. Filho, A. M. A. C. Carneiro Leão, and A. L. F. Porto, "The polysaccharide from *Anacardium occidentale* L. in the inflammatory phase of the cutaneous wound healing," *Ciencia Rural*, vol. 36, no. 1, pp. 149–154, 2006.

[16] J. Laska and J. Widlarz, "One-step polymerization leading to conducting polyaniline," *Synthetic Metals*, vol. 135, pp. 261–262, 2003.

[17] S. Bhadra, D. Khastgir, N. K. Singha, and J. H. Lee, "Progress in preparation, processing and applications of polyaniline," *Progress in Polymer Science*, vol. 34, no. 8, pp. 783–810, 2009.

[18] J. J. Langer, M. Filipiak, J. Kecinska, J. Jasnowska, J. Włodarczak, and B. Buładowski, "Polyaniline biosensor for choline determination," *Surface Science*, vol. 573, no. 1, pp. 140–145, 2004.

[19] A. Mirmohseni and A. Oladegaragoze, "Anti-corrosive properties of polyaniline coating on iron," *Synthetic Metals*, vol. 114, no. 2, pp. 105–108, 2000.

[20] S. A. Chen and G. W. Hwang, "Water-soluble self-acid-doped conducting polyaniline: structure and properties," *Journal of the American Chemical Society*, vol. 117, no. 40, pp. 10055–10062, 1995.

[21] Y. H. Geng, Z. C. Sun, J. Li, X. B. Jing, X. H. Wang, and F. S. Wang, "Water soluble polyaniline and its blend films prepared by aqueous solution casting," *Polymer*, vol. 40, no. 20, pp. 5723–5727, 1999.

[22] S. M. O. Costa, J. F. Rodrigues, and R. C. M. de Paula, "Monitoração do processo de purificação de gomas naturais: goma do cajueiro," *Polimeros: Ciencia e Tecnologia*, vol. 6, no. 2, pp. 49–55, 1996.

[23] L. H. C. Mattoso, A. G. MacDiarmind, and A. J. Epstein, "Controlled synthesis of high molecular weight polyaniline and poly(o-methoxyaniline)," *Synthetic Metals*, vol. 68, no. 1, pp. 1–11, 1994.

[24] E. S. Matveeva, C. F. Gimenez, and M. J. G. Tejera, "Charge transfer behaviour of the indium-tin oxide/polyaniline interface: dependence on pH and redox state of PANI," *Synthetic Metals*, vol. 123, no. 1, pp. 117–123, 2001.

[25] W. S. Huang, B. D. Humphrey, and A. G. Macdiarmid, "Polyaniline, a novel conducting polymer. Morphology and chemistry of its oxidation and reduction in aqueous electrolytes," *Journal of the Chemical Society, Faraday Transactions.1*, vol. 82, no. 8, pp. 2385–2400, 1986.

[26] M. Raposo and O. N. Oliveira Jr., "Energies of adsorption of poly(o-methoxyaniline) layer-by-layer films," *Langmuir*, vol. 16, no. 6, pp. 2839–2844, 2000.

[27] M. F. Zampa, A. C. F. de Brito, I. L. Kitagawa et al., "Natural gum-assisted phthalocyanine immobilization in electroactive nanocomposites: physicochemical characterization and sensing applications," *Biomacromolecules*, vol. 8, no. 11, pp. 3408–3413, 2007.

[28] J. R. Siqueira Jr., L. H. S. Gasparotto, O. N. Oliveira Jr., and V. Zucolotto, "Processing of electroactive nanostructured films incorporating carbon nanotubes and phthalocyanines for sensing," *Journal of Physical Chemistry C*, vol. 112, no. 24, pp. 9050–9055, 2008.

[29] H. F. Cui, Y. H. Cui, Y. L. Sun, K. Zang, and W. D. Zhang, "Enhancement of dopamine sensing by layer-by-layer assembly of PVI-dmeOs and nafion on carbon nanotubes," *Nanotechnology*, vol. 21, pp. 215–601, 2010.

[30] S. A. Kumar and S. M. Chen, "Electrochemical, microscopic, and EQCM studies of cathodic electrodeposition of ZnO/FAD and anodic polymerization of FAD films modified electrodes and their electrocatalytic properties," *Journal of Solid State Electrochemistry*, vol. 11, no. 7, pp. 993–1006, 2007.

[31] M. Ferreira, L. R. Dinelli, K. Wohnrath, A. A. Batista, and O. N. Oliveira Jr., "Langmuir-Blodgett films from polyaniline/ruthenium complexes as modified electrodes for detection of dopamine," *Thin Solid Films*, vol. 446, no. 2, pp. 301–306, 2004.

[32] R. C. S. Luz, F. S. Damos, A. B. de Oliveira, J. Beck, and L. T. Kubota, "Development of a sensor based on tetracyanoethylenide (LiTCNE)/poly-l- lysine (PLL) for dopamine determination," *Electrochimica Acta*, vol. 50, no. 12, pp. 2675–2683, 2005.

[33] W. S. Alencar, F. N. Crespilho, M. R. M. C. Santos, V. Zucolotto, O. N. Oliveira Jr., and W. C. J. Silva, "Influence of film architecture on the charge-transfer reactions of metallophthalocyanine layer-by-layer films," *The Journal of Physical Chemistry C*, vol. 111, pp. 12817–12821, 2007.

[34] T. Łuczak, "Preparation and characterization of the dopamine film electrochemically deposited on a gold template and its applications for dopamine sensing in aqueous solution," *Electrochimica Acta*, vol. 53, no. 19, pp. 5725–5731, 2008.

[35] X. Q. Lin and L. Zhang, "Simultaneous determination of dopamine and ascorbic acid at glutamic acid modified graphite electrode," *Analytical Letters*, vol. 34, no. 10, pp. 1585–1589, 2001.

[36] Analytical Methods Commitee, "Recommendations for the definition, estimation and use of the detection limit," *Analyst*, vol. 112, pp. 199–204, 1987.

[37] A. J. Bard and L. R. Faulkner, *Electrochemical Methods, Fundamentals and Applications*, John Wiley & Sons, New York, NY, USA, 2nd edition, 2001.

[38] R. A. A. Muzzarelli, "Chitins and chitosans for the repair of wounded skin, nerve, cartilage and bone," *Carbohydrate Polymers*, vol. 76, no. 2, pp. 167–182, 2009.

[39] T. Fujie, N. Matsutani, Y. Kinoshita, Y. Okamura, A. Saito, and S. Takeoka, "Adhesive, flexible, and robust polysaccharide nanosheets integrated for tissue-defect repair," *Advanced Functional Materials*, vol. 19, no. 16, pp. 2560–2568, 2009.

[40] S. C. Davis and L. G. Ovington, "Electrical stimulation and ultrasound in wound healing," *Dermatologic Clinics*, vol. 11, no. 4, pp. 775–781, 1993.

Hindawi Publishing Corporation
International Journal of Analytical Chemistry
Volume 2012, Article ID 981758, 12 pages
doi:10.1155/2012/981758

Research Article

Spectrophotometric Determination of Iron(II) and Cobalt(II) by Direct, Derivative, and Simultaneous Methods Using 2-Hydroxy-1-Naphthaldehyde-p-Hydroxybenzoichydrazone

V. S. Anusuya Devi[1] and V. Krishna Reddy[2]

[1] *Department of Chemistry, S.E.A. College of Engineering and Technology, Bangalore 560049, India*
[2] *Department of Chemistry, Sri Krishnadevaraya University, Anantapur 515003, India*

Correspondence should be addressed to V. S. Anusuya Devi, anukmp@gmail.com

Received 5 September 2011; Revised 24 October 2011; Accepted 3 November 2011

Academic Editor: Ricardo Vessecchi

Optimized and validated spectrophotometric methods have been proposed for the determination of iron and cobalt individually and simultaneously. 2-hydroxy-1-naphthaldehyde-p-hydroxybenzoichydrazone (HNAHBH) reacts with iron(II) and cobalt(II) to form reddish-brown and yellow-coloured [Fe(II)-HNAHBH] and [Co(II)-HNAHBH] complexes, respectively. The maximum absorbance of these complexes was found at 405 nm and 425 nm, respectively. For [Fe(II)-HNAHBH], Beer's law is obeyed over the concentration range of 0.055–1.373 μg mL^{-1} with a detection limit of 0.095 μg mL^{-1} and molar absorptivity ε, 5.6×10^4 L mol^{-1} cm^{-1}. [Co(II)-HNAHBH] complex obeys Beer's law in 0.118–3.534 μg mL^{-1} range with a detection limit of 0.04 μg mL^{-1} and molar absorptivity, ε of 2.3×10^4 L mol^{-1} cm^{-1}. Highly sensitive and selective first-, second- and third-order derivative methods are described for the determination of iron and cobalt. A simultaneous second-order derivative spectrophotometric method is proposed for the determination of these metals. All the proposed methods are successfully employed in the analysis of various biological, water, and alloy samples for the determination of iron and cobalt content.

1. Introduction

Iron and cobalt salts are widely used in industrial materials [1, 2], paint products [3], fertilizers, feeds, and disinfectants. They are important building components in biological systems [4]. Special cobalt-chromium-molybdenum alloys are used for prosthetic parts such as hip and knee replacements [5]. Iron-cobalt alloys are used for dental prosthetics [6]. There has been growing concern about the role of iron and cobalt in biochemical and environmental systems. Normally small amounts of iron and cobalt are essential for oxygen transport and enzymatic activation, respectively, in all mammals. But excessive intake of iron causes siderosis and damage to organs [7]. A high dosage of cobalt is very toxic to plants and moderately toxic to mammals when injected intravenously. Hence, quantification of various biological samples for iron and cobalt is very important to know their influence on these systems.

A good number of reviews have been made on the use of large number of chromogenic reagents for the spectrophotometric determination of iron and cobalt. Some of the recently proposed spectrophotometric methods for the determination of iron [8–15] and cobalt [16–22] are less sensitive and less selective. We are now proposing simple, sensitive and selective direct and derivative spectrophotometric methods for the determination of iron(II) and cobalt(II) in various complex materials using 2-hydroxy-1-naphthaldehyde-p-hydroxybenzoichydrazone as chromogenic agent. We are also reporting a highly selective second-order derivative method for the simultaneous determination of iron and cobalt in different samples.

2. Experimental

2.1. Preparation of Reagents. 0.01 M iron(II) and cobalt(II) solutions were prepared by dissolving appropriate amounts

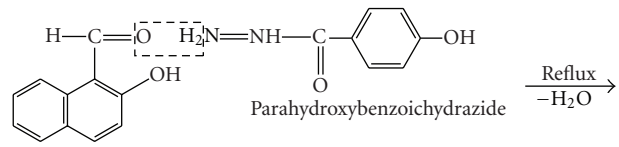

2-hydroxy-1-naphthaldehyde

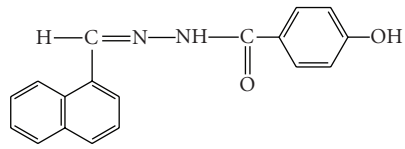

2-hydroxy-1-naphthaldehyde-p-hydroxybenzoichydrazone

Scheme 1

of ferrous ammonium sulphate (Sd. Fine) in 2 M sulphuric acid and cobaltous nitrate (Qualigens) in 100 mL distilled water. The stock solutions were diluted appropriately as required. Other metal ion solutions were prepared from their nitrates or chlorides in distilled water. 1% solution of cetyltrimethylammonium bromide (CTAB), a cationic surfactant in distilled water is used. Buffer solutions of pH 1–10 are prepared using appropriate mixtures of 1 M HCl–1 M CH_3COONa (pH 1–3.0), 0.2 M CH_3COOH, 0.2 M CH_3COONa (pH 3.5–7.0), and 1 M NH_4OH and 1 M NH_4Cl (pH 7.5–10.0). HNAHBH was prepared by mixing equal amounts of 2-hydroxy-1-naphthaldehyde in methanol and p-hydroxybenzoichydrazide in hot aqueous ethanol in equal amounts and refluxing for three hours on water bath. A reddish brown coloured solid was obtained on cooling. The product was filtered and dried. It was recrystallized from aqueous ethanol in the presence of norit. The product showed melting point 272–274°C.

The structure of the synthesized HNAHBH was determined from infrared and NMR spectral analysis. 1×10^{-2} M solution of the reagent was prepared by dissolving 0.306 g in 100 mL of dimethylformamide (DMF). Working solutions were prepared by diluting the stock solution with DMF (see Scheme 1).

2.2. Preparation of Sample Solutions

2.2.1. Soil Samples. The soil sample (5.0 g) was weighed into a 250 mL Teflon high-pressure microwave acid digestion bomb and 50 mL aquaregia were added. The bomb was sealed tightly and then positioned in the carousel of a microwave oven. The system was operated at full power for 30 minutes. The digested material was evaporated to incipient dryness. Then, 50 mL of 5% hydrochloric acid was added and heated close to boiling to leach the residue. After cooling, the residue was filtered and washed two times with a small volume of 5% hydrochloric acid. The filtrates were quantitatively collected in a 250 mL volumetric flask and diluted to the mark with distilled water.

2.2.2. Alloy Steel Sample Solution. A 0.1–0.5 g of the alloy sample was dissolved in a mixture of 2 mL HCl and 10 mL HNO_3. The resulting solution was evaporated to a small volume. To this, 5 mL of 1 : 1 H_2O and H_2SO_4 mixture was added and evaporated to dryness. The residue was dissolved in 15 mL of distilled water and filtered through Whatman filter paper no. 40. The filtrate was collected in a 100 mL volumetric flask and made upto the mark with distilled water. The solution was further diluted as required.

2.2.3. Food and Biological Samples. A wet ash method was employed in the preparation of the sample solution. 0.5 g of the sample was dissolved in a 1 : 1 mixture of nitric acid and perchloric acid. The solution was evaporated to dryness, and the residue was ashed at 300°C. The ash was dissolved in 2 mL of 1 M sulphuric acid and made up to the volume in a 25 mL standard flask with distilled water.

2.2.4. Blood and Urine Samples. Blood and urine samples of the normal adult and patient (male) were collected from Government General Hospital, Kurnool, India. 50 mL of sample was taken into 100 mL Kjeldal flask. 5 mL concentrated HNO_3 was added and gently heated. When the initial brief reaction was over, the solution was removed and cooled. 1 mL con. H_2SO_4 and 1 mL of 70% $HClO_4$ were added. The solution was again heated to dense white fumes, repeating HNO_3 addition. The heating was continued for 30 minutes and then cooled. The contents were filtered and neutralized with dil. NH_4OH in the presence of 1-2 mL of 0.01% tartrate solution. The solution was transferred into a 10 mL volumetric flask and diluted to the volume with distilled water.

2.2.5. Water Samples. Different water samples were collected from different parts of Anantapur district, A. P, India and filtered using Whatman filter paper.

2.2.6. Pharmaceutical Samples. A known quantity of the sample was taken in a beaker and dissolved in minimum volume of alcohol. Then added 3 mL of 0.01 M nitric acid and evaporated to dryness. The dried mass was again dissolved in alcohol. This was filtered through Whatman filter paper, and the filtrate was diluted to 100 mL with

Table 1: Tolerance limits of foreign ions, Amount of Fe(II) taken = 0.558 μg mL^{-1} pH = 5.0.

Foreign ion	Tolerance limit (μg mL^{-1})	Foreign ion	Tolerance limit (μg mL^{-1})	Foreign ion	Tolerance limit (μg mL^{-1})
Sulphate	1440	Na(I)	1565	La(III)	18
Iodide	1303	Mg(II)	1460	Ag(I)	15
Phosphate	1424	Ca(II)	1440	Hg(II)	16
Thiosulphate	1424	K(I)	1300	U(VI)	6,60[a]
Tartrate	1414	Ba(II)	1260	Mn(II)	4,55[a]
Thiourea	1140	Pd(II)	63	Th(IV)	3,50[a]
Bromide	1138	Cd(II)	45	In(III)	4,60[a]
Nitrate	930	Bi(III)	42	Sn(II)	<1,50[a]
Carbonate	900	W(VI)	37	Co(II)	<1,55[a]
Thiocyanate	870	Hf(IV)	36	Ni(II)	<1,60[b]
Chloride	531	Ce(IV)	28	Zn(II)	<1,80[b]
Fluoride	285	Cr(VI)	27	Al(III)	<1,45[a]
EDTA	124	Mo(VI)	22	Cu(II)	<1,50[a]
Citrate	115	Zr(IV)	19		
Oxalate	95	Sr(II)	18		

In the presence of a = 500 μg of tartrate, b = 400 μg of thiocyanate.

Table 2: Determination of iron in surface soil.

Sample	Source of the sample	Amount of iron (mg Kg^{-1}) ± SD*
S1	Groundnut cultivation soil Akuthotapalli, Anantapur	40.98 ± 0.45
S2	Cotton cultivation soil, Singanamala, Anantapur district,	27.48 ± 0.36
S3	Sweet lemon cultivation soil, Garladinne, Anantapur distrcct	44.88 ± 0.24
S4	Paddycultivation soil Garladinne, Anantapur district	20.86 ± 0.37

* Average of five determinations.

distilled water. The lower concentrations were prepared by the appropriate dilution of the stock solution.

2.3. Apparatus. A Perkin Elmer (LAMBDA25) spectrophotometer controlled by a computer and equipped with a 1 cm path length quartz cell was used for UV-Vis spectra acquisition. Spectra were acquired between 350–600 nm (1 nm resolution). ELICO model LI-120 pH-meter furnished with a combined glass electrode was used to measure pH of buffer solutions.

3. Results and Discussions

Iron(II) and cobalt(II) react with HNAHBH forming reddish brown and yellow coloured complexes. The colour of the complexes was stable for more than two days.

3.1. Direct Method of Determination of Iron(II). The absorption spectrum of [Fe(II)-HNAHBH] shows maximum absorbance at 405 nm. The preliminary investigations indicate that the absorbance of the complex is maximum and stable in pH range of 4.5–5.5. Hence pH 5.0 was chosen for further studies. A considerable increase in the colour intensity in the presence of 0.1% CTAB was observed. Studies on reagent (HNAHBH) concentration effect revealed that a maximum of 15-fold excess reagent is required to get maximum and stable absorbance for the complex. From the absorption spectra of [Fe(II)-HNAHBH] the molar absorptivity, coefficient ε is calculated as 5.6×10^4 L mol^{-1} cm^{-1}. Variable amounts of Fe(II) were treated with suitable amounts of reagent, surfactant, and buffer and the validity of Beer's law was tested by plotting the measured absorbance values of the prepared solutions against concentration of Fe(II). The calibration curve was linear over the range 0.055–1.373 μg mL^{-1}. The composition of the complex [Fe(II) : HNAHBH] was determined as 2 : 3 by Job's continuous variation method and the stability constant of the complex was calculated as 1.8×10^{18}. Other analytical results are presented in Table 5.

3.1.1. Effect of Diverse Ions in the Determination of Iron by Direct Method. Numerous cations and anions were added individually to the experimental solution containing 0.558 μg mL^{-1} of iron and the influence was examined (Table 1). All the anions and many cations were tolerable in more than 100 fold excess. The tolerance limits of some ions were in the range of 5–50 folds. Some of the metal ions, which strongly interfered, could be masked using appropriate masking agents.

3.1.2. Determination of Iron in Surface Soil and Alloy Steels by Direct Spectrophotometric Method. The applicability of the developed direct method was evaluated by applying the

Table 3: Determination of iron in alloy steels.

Alloy steel composition (%)	Amount of iron (%)		
	Certified value	Present method ± SD*	Relative error (%)
High tensile steel BY0110-1 (42.98 Zn, 19.89 Si, 0.351 Pb, 0.06 Sn, 0.04 Cd, 0.024 As, 0.14 Cu, and 4.13 Fe)	4.13	4.06 ± 0.021	0.17
YSBC19716 (34.26 Zn, 0.38 Si, 1.2 Cd, 48.57 Sb, 0.95 S, and 0.32 F)	34.26	4.18 ± 0.022	0.01
GSBD33001-94 (9.29 Al, 1.04 Ca, 9.53 Fe)	9.53	9.46 ± 0.039	0.08

* Average of five determinations.

Table 4: Tolerance limits of some cations in derivative methods.

Foreign ion	Tolerance limit (in folds)			
	Direct method	First derivative	Second derivative	Third derivative
Ag(I)	14	18	35	22
Hg(II)	11	20	40	30
U(VI)	11	12	25	18
Mn(II)	7	20	16	20
Th(IV)	5	10	16	20
In(III)	7	28	48	34
Au(III)	4	35	55	28
Sn(II)	<1	8	15	22
Co(II)	<1	interfere	7	15
Ni(II)	<1	interfere	5	10
Cu(II)	<1	5	12	10

method for the analysis of some surface soil and alloy steel samples for their iron content. Different aliquots of sample solutions containing suitable amounts of iron were treated with known and required volume of HNAHBH at pH 5.0 and 0.1% CTAB and diluted to 10 mL with distilled water. The absorbance of the resultant solutions was measured at 405 nm, and the amount of iron present was computed from the predetermined calibration plot. The results were compared with the certified values and presented in Tables 2 and 3.

3.2. Determination of Iron(II) by Derivative Method. Different amounts of Fe(II) (0.027–1.375 μg mL^{-1}) were treated with suitable amounts of HNAHBH in buffer solutions of pH 5.0 along with 0.1% CTAB and made upto 10 mL with distilled water. 1st, 2nd, and 3rd order derivative spectra were recorded in the wavelength region 350–600 nm. The first-order derivative spectra showed maximum derivative amplitude at 427 nm (Figure 1). The second-order derivative spectra gave one large trough at 421 nm and a large crust at 435 nm with zero cross at 428 nm (Figure 2). A large crust at 415 nm and a large trough at 426 nm with zero cross at 421 nm were observed for the third-derivative spectra (Figure 3). Hence Fe(II) was determined by measuring the derivative amplitudes at 427 nm for 1st order, at 421 nm and 435 nm for 2nd order, and at 415 nm and 426 nm for 3rd order spectra.

3.2.1. Determination of Iron(II). The derivative amplitudes measured at the analytical wavelengths as mentioned above for different derivative spectra were plotted against the amount of Fe(II). The calibration plots are linear in the range 0.027–1.375 μg mL^{-1}. All the derivative methods are found to be more sensitive with a wider Beer's law range than the zero order method (Table 5)

3.2.2. Effect of Foreign Ions in Derivative Method of Determination of Iron. The influence of some of the cations, which showed serious interference in zero order method, on the derivative amplitudes was studied by the reported methods and the results obtained are shown in Table 4. It can be observed from the table that large number of ions showed significantly high-tolerance limits in some of the derivative methods.

3.2.3. Determination of Iron in Food and Biological Samples by First Order Derivative Method. Known aliquots of the prepared food and biological sample solutions were treated with suitable volumes of HNAHBH, buffer solution, and CTAB surfactant and diluted to the volume in 10 mL volumetric flasks. The first-order derivative spectra were recorded, and the derivative amplitudes were measured at analytical wave lengths. The amounts of Fe(II) in the samples were computed from predetermined calibration plots and presented in Table 6. The food and biological samples were further analyzed by Atomic Absorbance Spectrophotometric method, and the results obtained were compared with those of the present method.

3.3. Direct Method of Determination of Cobalt(II). [Co(II)-HNAHBH] complex shows maximum absorbance at 425 nm. Maximum and stable absorbance of the complex is achieved in the pH range of 5.0–7.0. Hence pH 6.0 was chosen for further studies. A marginal increase in the absorbance was observed in presence of 0.15% of

Table 5: Analytical characteristics of [Fe(II)-HNAHBH].

Parameter	Direct method	First derivative	Second derivative		Third derivative	
	405 nm	427 nm	421 nm	435 nm	415 nm	426 nm
Beer's law range (μg mL^{-1})	0.055–1.373	0.027–1.376	0.027–1.376	0.027–1.376	0.027–1.376	0.027–1.376
Molar absorptivity, (L mol^{-1} cm^{-1})	5.6×10^4			—	—	—
Sandell's sensitivity, (μg cm^{-2})	0.0012			—	—	—
Angular coefficient (m)	0.974	0.072	0.006	0.093	0.002	0.085
Y-intercept (b)	0.0047	−0.0045	-0.1×10^{-3}	-0.1×10^{-3}	0.2×10^{-4}	0.9×10^{-3}
Correlation coefficient	0.9997	0.9999	0.9999	0.9999	0.9999	0.9999
RSD (%)	2.19	0.85	0.76	0.89	1.31	1
Detection limit (μg mL^{-1})	0.065	0.1	0.022	0.0268	0.036	0.304
Determination limit, (μg mL^{-1})	0.197	0.3	0.068	0.8	0.11	0.914
Composition (M : L)	2 : 3	—	—		—	
Stability constant	1.8×10^{18}	—	—		—	

Table 6: Determination of iron in food and biological samples.

Samples	Amount of iron(μg mL^{-1}) ± SD ($n = 4$)					
	Found		Recovered			
	present	AAS	Added	present	AAS	recovery
Wheat	6.68 ± 0.18	6.40 ± 0.09	5	11.40 ± 1.15	11.28 ± 0.10	97.6
Rice	14.10 ± 40.25	16.46 ± 0.18	5	19.7 ± 40.27	21.04 ± 0.48	102
Tomato	11.96 ± 1.20	12.68 ± 0.14	5	17.68 ± 0.25	17.44 ± 0.95	104
Orange	18.12 ± 0.73	16.94 ± 0.66	5	22.20 ± 0.75	22.26 ± 0.68	96
Banana	10.12 ± 1.46	11.4 ± 0.12	5	14.86 ± 1.45	15.86 ± 1.46	98.3
Prostate gland	3.26 ± 0.28	2.98 ± 0.08	6.5	10.04 ± 1.68	9.54 ± 0.94	103
Benign (enlarged prostate gland	12.38 ± 3.18	13.15 ± 1.18	6.5	17.96 ± 1.56	20.18 ± 1.66	95.12

Table 7: Tolerance limits of foreign ions, amount of Co(II) taken = 1.767 μg mL^{-1}, pH = 6.0.

Foreign ion	Tolerance limit (μg mL^{-1})	Foreign ion	Tole limit (μg mL^{-1})	Foreign ion	Toler limit (μg mL^{-1})
Tartrate	1707	Na(I)	1666	Au(III)	20
Phosphate	1425	Mg(II)	1530	Sr(II)	18
Sulphate	1440	Ca(II)	1426	Mo(VI)	15
Oxalate	1320	K(I)	1200	Tl(IV)	13
Bromide	1198	Ba(II)	1162	Pd(II)	11,100[c]
Thiourea	1140	Hf(IV)	72	Th(IV)	6,60[a]
Thiosulphate	1120	Se(IV)	64	U(VI)	5,60[a]
Nitrate	930	Cd(II)	56	Mn(II)	5,50[a]
Chloride	525	W(VI)	55	Cu(II)	2,50[a]
Carbonate	300	Zr(IV)	46	Ni(II)	<1,80[b]
Fluoride	285	Pb(II)	42	Zn(II)	<1
EDTA	144	Hg(II)	40	Sn(II)	<1
Citrate	115	Cr(VI)	26	In(III)	<1,60[a]
		Bi(III)	21	Ga(III)	<1,50[a]
		Ru(III)	21	V(V)	<1,50[b]

In the presence of $a = 700\,\mu$g of tartrate, $b = 400\,\mu$g of oxalate and $c = 500\,\mu$g of thiourea.

Table 8: Determination of cobalt in surface soil samples.

	Sample and source	Cobalt (μg mL^{-1})	
		Present method*	Reference method [23]
S1	Agricultural land (red soil Anantapur.)	16.48 ± 0.030	17.20 ± 0.024
S2	Agricultural land (black soil, Tadipatri.)	24.15 ± 0.026	23.68 ± 0.022
S3	Riverbed soil (Tungabhadra river, Kurnool)	14.68 ± 0.034	15.26 ± 0.018
S4	Industrial soil (electroplating industry, Anantapur)	118.40±0.042	122.12 ± 0.029

* Average of four determinations.

Table 9: Analysis of blood and urine samples for cobalt content.

Sample source	Sample	Cobalt (μg mL^{-1})	
		Present method ± SD ($n = 5$)	AAS method ± SD ($n = 5$)
Normal adult (male)	Blood	2.44 ± 0.020	2.48 ± 0.014
	Urine	0.38 ± 0.010	0.35 ± 0.022
Anemia patient (female)	Blood	0.86 ± 0.020	0.92 ± 0.020
	Urine	0.24 ± 0.030	0.23 ± 0.014
Paralysis patient	Blood	8.46 ± 0.030	8.65 ± 0.032
	Urine	2.65 ± 0.020	2.43 ± 0.025
Pulmonary patient	Blood	4.32 ± 0.015	4.26 ± 0.010
	Urine	1.96 ± 0.022	2.04 ± 0.018

Table 10: Tolerance limit of foreign ions (μg mL^{-1}).

Diverse ion	Zero order	Second derivative	Third derivative
Th(IV)	6	55	35
U(VI)	5	40	45
Mn(II)	5	60	20
Cu(II)	2	80	45
Ni(II)	<1	30	50
Zn(II)	<1	45	20
Sn(II)	<1	25	18
In(III)	<1	15	28
Ga(III)	<1	20	35
V(V)	<1	15	20

CTAB. 10-folds excess of HNAHBH is sufficient to get maximum absorbance. Molar absorptivity of the complex was calculated as 2.3×10^4 L mol^{-1} cm^{-1}. Beer's law is tested taking the different amounts of Co(II) in presence of suitable buffer, surfactant, and HNAHBH, linearity of the calibration curve is found between 0.118–3.534 μg mL^{-1} with a detection limit of 0.04 μg mL^{-1} and determination limit 0.124 μg mL^{-1} (Table 11), which shows the sensitivity of the present method. The stoichiometry of the complex

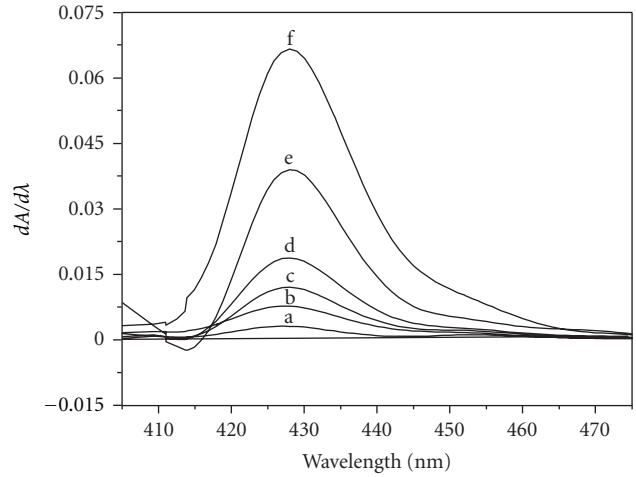

Figure 1: First-order derivative spectra of [Fe(II)-HNAHBH]. Amount of Fe(II) μg mL^{-1}: a = 0.027; b = 0.055; c = 0.11; d = 0.22; e = 0.33; f = 0.88.

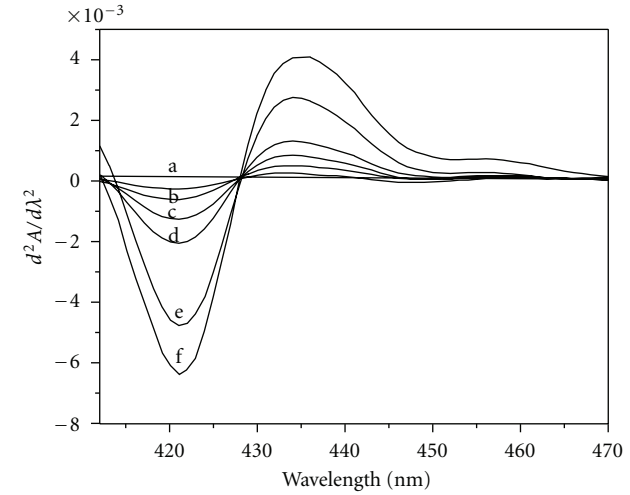

Figure 2: Second-order derivative spectra of [Fe(II)-HNAHBH]. Amount of Fe(II) μg mL^{-1}: a = 0.027; b = 0.055; c = 0.11; d = 0.22; e = 0.33; f = 0.88.

was found to be 2 : 3 (Metal : Ligand) by Job's method. The stability constant is calculated as 7.7×10^{19}.

3.3.1. Effect of Foreign Ions in the Determination of Cobalt by Direct Method. The effect of various anions and cations normally associated with Co(II) on the absorbance of the experimental solution was studied. The tolerance limits of the tested foreign ions, which bring about a change in the absorbance by ±2% were calculated and presented in Table 7.

Among anions, except EDTA and citrate, all other tested ions were tolerable in more than 200-fold excess. EDTA and citrate were tolerable in 144- and 150-fold excess, respectively. Of the tested cations, some of them did not interfere even when present in more than 500 fold excess, many cations were tolerable between 10–80-folds. Cations which interfere seriously are masked with suitable anions.

Table 11: Analytical characteristics of [Co(II)-HNAHBH].

Parameter	Direct method	Second derivative		Third derivative	
	425 nm	431 nm	443 nm	437 nm	449 nm
Beer's law range (μg mL^{-1})	0.118–3.534	0.059–4.712	0.059–4.712	0.059–1.380	0.056–1.380
Molar absorptivity, (L mol^{-1} cm^{-1})	2.3×10^4	—	—	—	—
Sandell's sensitivity, μg cm^{-2}	0.003	—	—	—	—
Angular coefficient (m)	0.375	0.0003	0.093	0.0002	0.009
Y-intercept (b)	0.0197	3.2×10^{-5}	-0.9×10^{-4}	-0.2×10^{-4}	-0.9×10^{-4}
Correlation coefficient	0.9999	0.999	0.9999	0.9999	0.9999
RSD (%)	1.37	1.84	4.3	1.15	7.6
Detection limit (μg mL^{-1})	0.04	0.06	0.13	0.04	0.21
Determination limit, (μg mL^{-1})	0.124	0.18	0.39	0.114	0.65
Composition (M : L)	2 : 3	—	—		—
Stability constant	7.7×10^{19}	—	—		—

Table 12: Determination of cobalt in environmental water samples.

Sample	cobalt (μg mL^{-1})			
	Added	Found	Recovery (%)	RSD (%)
Tap water (municipality water supply, Anantapur)	0.0	0.32	—	2.5
	1.5	1.80	98.90	1.8
	3.0	3.35	100.90	3.0
	4.5	4.83	100.20	2.2
River water (Penna, Tadipatri.)	0.0	1.52	—	3.0
	1.5	3.00	99.34	1.6
	3.0	4.55	100.66	2.8
	4.5	5.95	98.84	4.0
Drain water (vanaspati industry, Tadipatri.	0.0	3.60	—	1.7
	1.5	5.31	104.12	3.2
	3.0	6.48	98.18	2.5
	4.5	8.07	99.63	3.6

Table 13: Determination of cobalt in pharmaceutical tablets.

Sample (mg/tablet)	Amount of cobalt (μg mL^{-1})		
	Reported	Found*	Relative error (%)
Neurobion forte (cyanocobalamine-15 mg)	7.45	7.4	−0.67
Basiton forte (cyanocobalamine-15 mg)	7.42	7.24	−2.42

* Average of four determinations.

3.3.2. Determination of Cobalt in Surface Soil, Blood and Urine Samples by Direct Method. Suitable aliquots of the soil, blood, and urine sample solutions were taken and analyzed for cobalt content by the proposed method, and the results are presented in Tables 8 and 9. The soil solutions were further analyzed by a reference method [23], and biological samples were analyzed by flame atomic absorption spectrophotometer, and the results obtained were compared with those of present method, which indicate the acceptability of the present method.

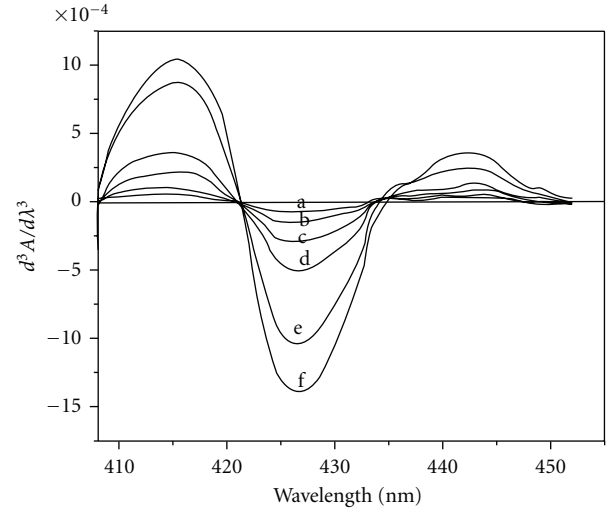

Figure 3: Third-order derivative spectra of [Fe(II)-HNAHBH]. Amount of Fe(II) μg mL-1: a = 0.027; b = 0.055; c = 0.11; d = 0.22; e = 0.33; f = 0.88.

3.4. Determination of Cobalt by Derivative Method. Variable amounts (0.059–4.712 μg mL^{-1}) of Co(II), taken in different 10 mL volumetric flasks, were treated with optimal amounts of reagent HNAHBH at pH 6.0 in presence of 0.15% CTAB, and the derivative spectra were recorded in the wavelength region 350–600 nm against reagent blank. The second-derivative curves (Figure 4) gave a trough at 431 nm and a crust at 443 nm with a zero cross at 437 nm. In the third-derivative spectra (Figure 5), maximum amplitude was observed at 424 nm, 437 nm, 449 nm, and at 462 nm with zero crossings at 431 nm, 443 nm, and 456 nm.

Table 14: Linear regression analysis of the determination of Fe(II) and Co(II) in mixture by second derivative spectrophotometry.

Metal ion determined	Wave length (nm)	Other metal present (μg mL^{-1})		Slope	Intercept	Correlation coefficient
		Fe(II)	Co(II)			
Fe(II)	436			3.9×10^{-3}	2.4×10^{-4}	0.9994
			0.589	3.2×10^{-3}	1.9×10^{-4}	0.9995
Co(II)	426			1.4×10^{-4}	2.3×10^{-6}	0.9999
		0.33		1.4×10^{-4}	2.0×10^{-6}	0.9998

Table 15: Simultaneous second-order derivative spectrophotometric determination of Fe(II) and Co(II).

Amount taken (μg mL^{-1})		Amount found* (μg mL^{-1})		Relative error (%)	
Fe(II)	Co(II)	Fe(II)	Co(II)	Fe(II)	Co(II)
0.06	0.59	0.053 (96.3)	0.572 (98.8)	−3.6	−2.8
0.12	0.59	0.120 (103.4)	0.592 (100.5)	3.44	0.5
0.23	0.59	0.230 (99.1)	0.586 (99.4)	−0.86	−0.5
0.33	0.59	0.334 (101.2)	0.572 (98.8)	1.21	−2.8
0.44	0.59	0.441 (100.2)	0.590 (100.1)	0.22	0.2
0.55	0.59	0.542 (98.5)	0.586 (99.3)	−1.45	−0.5
0.33	0.59	0.328 (99.3)	1.120 (94.9)	−0.60	−0.7
0.33	1.18	0.326 (89.6)	2.280 (96.6)	−1.21	−5.0
0.33	2.36	0.324 (98.1)	3.600 (101.7)	−1.81	−3.3
0.33	3.54	0.336 (101.8)	4.670 (98.9)	1.81	1.6
0.33	4.72	0.332 (100.6)	4.670 (98.9)	0.60	−1.0

* Average of four determinations.

3.4.1. Determination of Cobalt. The derivative amplitudes measured for different concentrations of Co(II) at appropriate wavelengths for 2nd and 3rd order derivative spectra were plotted against the amount of Co(II) which gave linear plots in the specified concentration regions. All the parameters like detection limit, correlation coefficient, and relative standard deviation values are presented in Table 11.

3.4.2. Effect of Foreign Ions. The selectivity of the derivative methods was evaluated by studying the effect of metal ions closely associated with cobalt on its derivative amplitudes under experimental conditions. The results are presented in Table 10. The results show that the tolerance limits of Th(IV), U(VI), Mn(II), Cu(II), Ni(II), Zn(II), Sn(II), In(II), Ga(III) and V(V) which interfere seriously in zero order method were greatly enhanced in the derivative methods indicating the greater selectivity of derivative methods over the direct method.

3.4.3. Determination of Cobalt in Water and Pharmaceutical Samples by Second-Order Derivative Method. Suitable aliquots of water and pharmaceutical samples were taken and analysed for cobalt by second-order derivative method. The results obtained in the analysis of water samples by the proposed method are presented in Table 12 and the validity of the results was evaluated by adding known amounts of Co(II) and calculating their recovery percentage. The results obtained with pharmaceutical samples were compared with those obtained by AAS method and presented in Table 13.

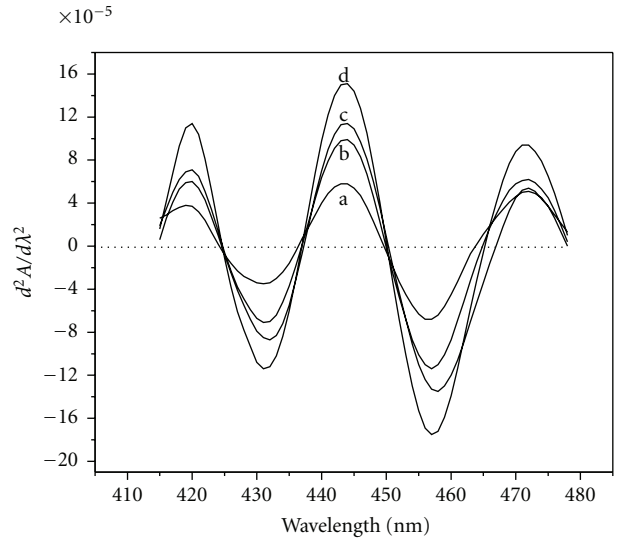

Figure 4: Second-order derivative spectra of [Co(II)-HNAHBH]. Amount of Co(II) μg mL^{-1}: a = 0.059, b = 0.118, c = 0.236, and d = 0.354.

3.5. Simultaneous Second-Order Derivative Spectrophotometric Determination of Iron(II) and Cobalt(II). Iron and

Table 16: Determination of iron and cobalt in alloy samples.

Sample (composition)	Amount (%)				Relative error (%)	
	Certified		Found ($n = 3$) ± SD			
	Fe(II)	Co(II)	Fe(II)	Co(II)	Fe(II)	Co(II)
Elgiloy-M (20 Cr; 15 Ni; 0.15 C; 2 Mn; 7 Mo;.05 Be)	15	40	14.82 ± 0.15	39.39 ± 0.20	1.33	1.52
Rim alloy (17 Mo; 3Mn)	68	12	69.28 ± 0.86	12.08 ± 0.38	1.88	0.66
Sofcomag 25 (Fe and Co)	75	25	73.89 ± 1.38	25.98 ± 0.86	1.48	3.92
Sofcomag 49 (Fe and Co)	51	49	52.12 ± 0.35	49.18 ± 0.06	2.18	0.36

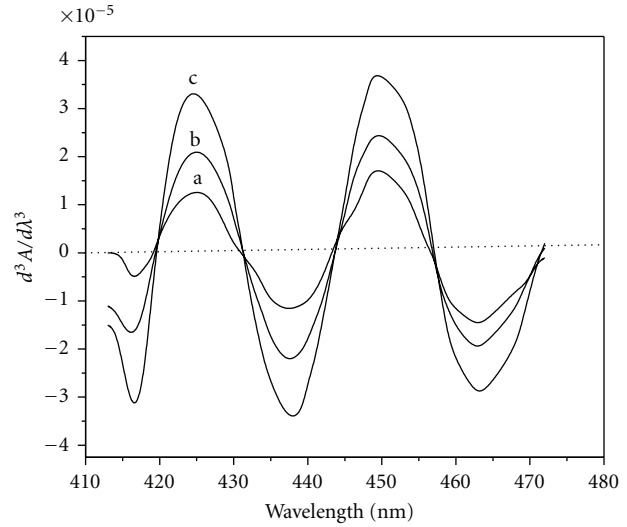

Figure 5: Third-order derivative spectra of [Co(II)-HNAHBH]. Amount of Co(II) μg mL^{-1}: a = 0.059, b = 0.118, c = 0.236, and d = 0.354.

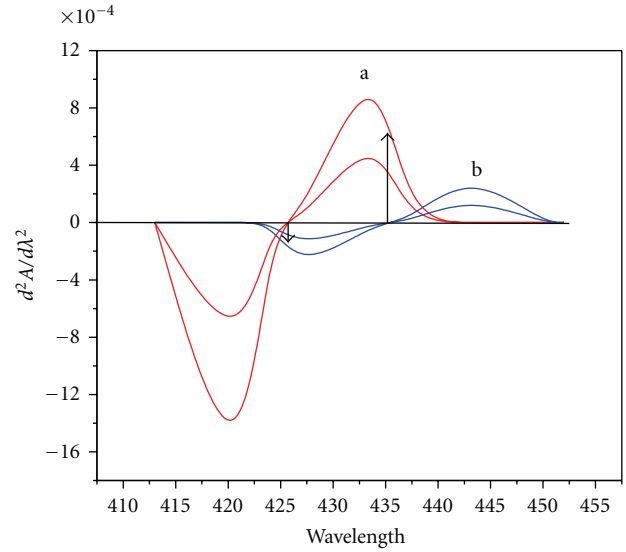

Figure 6: Second-order derivative spectra of (a) [Fe(II)-HNAHBH] and (b) [Co(II)-NAHBH]. Amount of Fe(II) (μg mL^{-1}): 0.055, 0.11; Co(II) (μg mL^{-1}): 3.53; 4.719.

cobalt occur together in many real samples like alloy steels, biological fluids, and environmental samples. In most cases, the characterizations of these samples include the determination of their metal ion content. The need for the determination of iron and cobalt in environmental and biochemical materials has increased after reports on different roles of these metals in human health and diseases. We are now reporting a simple, sensitive, and selective second-order derivative spectrophotometric method for the simultaneous determination of Fe(II) and Co(II) using HNAHBH without the need to solve the simultaneous equations.

3.5.1. Derivative Spectra . The 2nd order derivative spectra recorded for [Fe(II)-HNAHBH] and [Co(II)-HNAHBH] at pH 5.5 showed sufficiently large derivative amplitude for cobalt at 426 nm while the Fe(II) species exhibit zero amplitude (Figure 6). At 436 nm, maximum derivative amplitude was noticed for Fe(II) where there was no amplitude for Co(II). This facilitates the determination of Fe(II) and Co(II) simultaneously by measuring the second-derivative amplitudes of binary mixtures containing Fe(II) and Co(II)at 436 nm and 426 nm, respectively.

3.5.2. Determination of Fe(II) and Co(II). Aliquots of solutions containing 0.055–1.650 μg mL^{-1} of Fe(II) or 0.117–4.719 μg mL^{-1} of Co(II) were transferred into a series of 10 mL calibrated volumetric flasks. HNAHBH (1×10^{-2} M, 0.3 mL), CTAB (1%, 1.5 mL), and buffer solution (pH 5.5, 4 mL) were added to each of these flasks and diluted to the mark with distilled water. The zero-crossing points of [Fe(II)-HNAHBH] and [Co(II)-HNAHBH] species were determined by recording the second-order derivative spectra of both the systems with reference to the reagent blank. Calibration plots for the determination of Fe(II) and Co(II) were constructed by measuring the second-derivative amplitudes at zero crossing points of [Co(II)-HNAHBH] (436 nm) and [Fe(II)-HNAHBH] (426 nm), respectively, and plotting

Table 17: Comparision of the results with already reported methods.

Metal ion	Reagent	λ_{max} (nm)	pH/medium	Aqueous/extraction	Beer's law $\mu g\,mL^{-1}$	$\varepsilon \times 10^4 L\,mol^{-1}\,cm^{-1}$	Interference	Reference
Fe(II)	Thiocyanate-phenanthroline	520	—	Aqueous	0–24	1.87	—	[10]
Fe(II)	2-[2-(3,5-Dibromopyridyl-azo]-5-dimethyl amino-benzoic acid	615	2.0–7.0	Extraction	0–5.5	9.36	Tl(I), Zn(II), Cr(III), W(VI), Co(II), Cu(II), Ni(II), and Pd(II)	[24]
Fe(II)	1,10-Phenanthroline and picrate	510	2.0–9.0	Extraction	0.1–3.6	13	EDTA, CN^-	[25]
Fe(II)	4-(2-Pyridylazo)resorcinol	505	6.0–7.5	Extraction	0–2.0	6	Ni(II), Co(II), Pb(II), and EDTA	[26]
Fe(II)	1,10-Phenanthroline-tetraphenylborate	515	4.25	Aqueous	2.24–37.29	1.2	—	[27]
Fe(II)	1,3-Diphenyl-4-carboethoxy pyrazole-5-one	525	3.5–4.0	Aqueous	0.5–10	1.156	Cu(II), Co(II), Zn(II), Mo(VI), EDTA	[28]
Fe(II)	Dyformyl hydrazine	470	7.3–9.3	Aqueous	0.25–13	0.3258	—	[29]
Fe(II)	4,7-Diphenyl-1,10-phenanthroline and tetraphenylborate	534	—	Extraction	0–20.0	2	—	[30]
Fe(II)	Thiocyanate-acetone	480	$HClO_4$	Aqueous	—	2.1	Cu(II), NO_2^-, $S_2O_3^{-2}$, $H_2PO_4^{-2}$, and $C_2O_4^{-2}$	[31]
Fe(II)	2-Hydroxy-1-naphthaldehyde-p-hydroxybenzoic hydrazone	405	5	Aqueous	0.05–1.37	5.6	Sn(II), Co(II) Ni(II) Zn(II) Al(III) Cu(II)	Present method
Co(II)	Sodium isoamyl xanthate	400	4.5–9.0	Aqueous	3.0–35	1.92		[16]
Co(II)	2-Pyridine carboxalde hydeisonicotinyl-hydrazine	346	9	Aqueous	0.01–2.7	7.1	Au(III), Ag(I), Pt(III)	[18]
Co(II)	2-Hydroxy-1-naphthalidene salicyloyl hydrazone	430	8.0–9.0	Extraction	0–10	0.16		[22]
Co(II)	Pyridine-2-acetaldehyde salicyloyl hydrazone	415	1.0–6.0	Extraction	0.5–7.0	1.04	—	[32]
Co(II)	Bis-4-phenyl-3-thiosemicarbazone	400	4	—	0.6–6.0	2.2	—	[33]
Co(II)	2-Hydroxy-l-naphthalidene-salicyloylhydrazone	430	8.0–9.0	Extraction	0–10	1.6×10^3	—	[22]
Co(II)	2-(2-Quinolynylazo)-5-dimethylamino aniline	625	5.5	Extraction	0.01–0.6	4.3	Many cations and anions	[34]
Co(II)	2-Hydroxy-3-methoxy benzaldehyde thiosemicarbazone	390	6	Aqueous	0.06–2.35	2.74	—	[35]
Co(II)	2-Hydroxy-1-naphthaldehyde-p-hydroxybenzoic hydrazone	425	5	Aqueous	0.12–3.54	2.3	Ni(II), Zn(II), Sn(II), In(III), and Ga(IIII)	Present method

against the respective analyte concentrations. Fe(II) and Co(II) obeyed Beer's law in the range 0.055–1.650 μg mL^{-1} and 0.117–4.719 μg mL^{-1} at 436 nm and 426 nm, respectively. Calibration plots were constructed for the standard solutions containing Fe(II) alone and in the presence of 0.589 μg mL^{-1} of Co(II). Similarly, the calibration graphs were constructed for standards containing Co(II) alone and in the presence of 0.330 μg mL^{-1} of Fe(II). The slopes, intercepts, and correlation coefficients of the prepared calibration plots were calculated and given in Table 14. The derivative amplitudes measured at 436 nm and 426 nm were found to be independent of the concentration of Co(II) and Fe(II), respectively. This allows the determination of Fe(II) and Co(II) in their mixtures without any significant error and without the need for their prior separation.

3.5.3. Simultaneous Determination of Co(II) and Fe(II) in Binary Mixtures. Fe(II) and Co(II) were mixed in different proportions and then treated with required amount of HNAHBH in the presence of buffer solution (pH 5.5) and 0.15% of CTAB and diluted to the volume in 10 mL volumetric flasks. The second-order derivative spectra for these solutions were recorded (350–600 nm) and the derivative amplitudes were measured at 436 nm and 426 nm. The amounts of Fe(II) and Co(II) in the mixtures taken were calculated from the measured derivative amplitudes using the respective predetermined calibration plots. The results obtained along with the recovery percentage and relative errors are presented in Table 15, which indicate the usefulness of the proposed method for the simultaneous determination of Fe(II) and Co(II) in admixtures.

3.5.4. Simultaneous Determination of Iron and Cobalt in Alloy Samples. The developed second-order derivative spectrophotometric method was employed for the simultaneous determination of iron and cobalt in some alloy samples. Appropriate volumes of the alloy samples were treated with required amount of HNAHBH at pH 5.5 in the presence of 0.15% CTAB and diluted to 10 mL in standard flasks. The second-derivative curves for the resultant solutions were recorded, and the derivative amplitudes were measured at 426 nm and 436 nm. The amounts of iron and cobalt in the samples were evaluated with the help of predetermined calibration plots and presented in Table 16.

4. Conclusions

A comparison of the analytical results of the proposed methods was made with those of some of the recently reported spectrophotometric methods and presented in Table 17. The data in the above table reveals that the proposed method of determination of iron is more sensitive than those reported by Malik and Rao [27], Patil and Dhuley [28], Nagabhushana et al. [29], Wang et al. [30], Zhang et al. [31], and Martins et al. [36]. The methods proposed by Katmal and Hoyakava [24], Morales and Toral [25], and Reddy et al. [26] are more sensitive than the present method. However they are less selective than the proposed method as they suffer interference from W(VI), Pd(II), Cr(III), Tl(I), Pb(II), Bi(III), Hg(II), Mo(VI), EDTA, CN^-. Regarding the determination of cobalt, the present method is more sensitive than those reported by Malik et al [16], Patil and Sawant [32], Adinarayana Reddy et al. [33], and Prabhulkar et al. [22]. However, the preset method is less sensitive than the methods reported by Guzor and Jin [21] and Qiufen et al. [34], but these methods are less selective due to the interference of many cations and anions. The results obtained in the simultaneous determination of Fe(II) and Co(II) are well comparable with the reported methods. Above all most of the reported methods involve extraction into spurious organic solvents where as the present methods are simple, nonextractive, and reasonably accurate.

References

[1] E. Wildermuth, H. Stark, G. Friedrich et al., "Iron compounds," in *Ullmann's Encyclopedia of Industrial Chemistry*, Wiley-VCH, 2000.

[2] F. C. Campbell, "Cobalt and cobalt alloys," in *Elements of Metallurgy and Engineering Alloys*, pp. 557–558, ASM International, 2008.

[3] M. L. C. Adolfsson, A. K. Saloranta, and M. K. Silander, "Colourant composition for paint products," US Patent, Patent number: 5985987, 1999.

[4] M. W. Hentze and L. C. Kühn, "Molecular control of vertebrate iron metabolism: mRNA-based regulatory circuits operated by iron, nitric oxide, and oxidative stress," *Proceedings of the National Academy of Sciences of the United States of America*, vol. 93, no. 16, pp. 8175–8182, 1996.

[5] R. Michel, M. Nolte, M. Reich, and F. Loer, "Systemic effects of implanted prostheses made of cobalt-chromium alloys," *Archives of Orthopaedic and Trauma Surgery*, vol. 110, no. 2, pp. 61–74, 1991.

[6] J. A. Disegi, R. L. Kennedy, and R. Pillia, *Cobalt-Base Alloys for Biomedical Applications*, ASTM International Standards, 1999.

[7] J. T. Ellis, I. Schulman, and C. H. Smith, "Generalized siderosis with fibrosis of liver AND pancreas in cooley's (Mediterranean) anemia with observations on the pathogenesis of the siderosis AND fibrosis," *American Journal of Pathology*, vol. 30, no. 2, pp. 287–309, 1954.

[8] Wu, Li-Xiang, Guo, and J. Cun, *Metallurgical Analysis*, vol. 24, no. 3, pp. 66–68, 2004.

[9] L. Zaijun, F. You, L. Zhongyun, and T. Jian, "Spectrophotometric determination of iron(III)-dimethyldithiocarbamate (ferbam) using 9-(4-carboxyphenyl)-2,3,7-trihydroxyl-6-fluorone," *Talanta*, vol. 63, no. 3, pp. 647–651, 2004.

[10] Qi-Kai Zhang, Ling-Zhao Kong, and Li Wang, "Spectrophotometric determination of micro amount of iron in oils with thiocyanate-phenanthroline-OP," *Fenxi Shiyanshi (Analytical Laboratory)*, vol. 24, no. 1, pp. 77–79, 2005.

[11] P. K. Tarafder and R. Thakur, "Surfactant-mediated extraction of iron and its spectrophotometric determination in rocks, minerals, soils, stream sediments and water samples," *Microchemical Journal*, vol. 80, no. 1, pp. 39–43, 2005.

[12] F. G. Martins, J. F. Andrade, A. C. Pimenta, L. M. Lourenco, J. R. M. Casto, and V. R. Balbo, "Spectrophotometric study of iron oxidation in the iron(II)/thiocyanate/acetone system and some analytical applications," *Eclética Química*, vol. 30, no. 3, pp. 63–71, 2005.

[13] A. K. Sharma and I. Singh, "Spectrophotometric trace determination of iron in food, milk, and tea samples using a new bis-azo dye as analytical reagent," *Food Analytical Methods*, vol. 2, no. 3, pp. 221–225, 2009.

[14] L. I. Cheng-hong, G. E. Chang-hua, L. Hua-ding, and P. Fu-you, "Spectrophotometric determination of iron with 2-(5-carboxy-1,3,4-triazolylazo)-5-diethylamino aniline ," *Science Technology and Engineering*, vol. 21, pp. 5780–5782, 2008.

[15] Q. Z. Zhai, "Catalytic kinetic spectrophotometric determination of trace copper with copper(II)-p-acetylchlorophosphonazo-hydrogen peroxide system," *Bulletin of the Chemical Society of Ethiopia*, vol. 23, no. 3, pp. 327–335, 2009.

[16] A. K. Malik, K. N. Kaul, B. S. Lark, W. Faubel, and A. L. J. Rao, "Spectrophotometric determination of cobalt, nickel palladium, copper, ruthenium and molybdenum using sodium isoamylxanthate in presence of surfactants," *Turkish Journal of Chemistry*, vol. 25, no. 1, pp. 99–105, 2001.

[17] B. R. Reddy, P. Radhika, J. R. Kumar, D. N. Priya, and K. Rajgopal, "Extractive spectrophotometric determination of cobalt(II) in synthetic and pharmaceutical samples using cyanex 923," *Analytical Sciences*, vol. 20, no. 2, pp. 345–349, 2004.

[18] G. A. Shar and G. A. Soomro, "Spectrophotometric determination of cobalt(II), nickel(II) and copper (II) with 1-(2 pyridylazo)-2-naphthol in micellar medium," *The Nucleus*, vol. 41, pp. 77–82, 2004.

[19] N. Veerachalee, P. Taweema, and A. Songsasen, "Complexation and spectrophotometric determination of cobalt(II) ion with 3-(2′-thiazolylazo)-2,6-diaminopyridine," *Kasetsart Journal—Natural Science*, vol. 41, no. 4, pp. 675–680, 2007.

[20] Y. Haoyi, Z. Guoxiu, and Y. Gaohua, "Determination of cobalt in terephthalic acid by picramazochrom spectrophotometry," *Chemical Analysis and Meterage*, vol. 1, 2009.

[21] S. H. Guzar and Q. H. Jin, "Simple, selective, and sensitive spectrophotometric method for determination of trace amounts of nickel(II), copper (II), cobalt (II), and iron (III) with a novel reagent 2-pyridine carboxaldehyde isonicotinyl hydrazone," *Chemical Research in Chinese Universities*, vol. 24, no. 2, pp. 143–147, 2008.

[22] S. G. Prabhulkar and R. M. Patil, "2-Hydroxy-1-naphthalidine salicylohydrazone as an analytical reagent for extractive spectrophotometric determination of a biologically and industrially important metal Cobalt(II)," *International Journal of Chemical Sciences*, vol. 6, no. 3, pp. 1480–1485, 2008.

[23] J. E. Huheey, E. A. Keiter, and R. L. Keiter, *Inorganic Chemistry*, Harper Collins, New York, NY, USA, 4th edition, 1993.

[24] T. Katami, T. Hayakawa, M. Furukawa, and S. Shibata, "Extraction—spectrophotometric determination of iron with 2-[2-(3,5-Dibromopyridyl)azo]-5-dimethylaminobenzoic acid," *The Analyst*, vol. 109, no. 2, pp. 159–162, 1984.

[25] A. Morales and M. I. Toral, "Extraction—spectrophotometric determination of iron as the ternary tris(1,10-phenanthroline)-iron(II)-picrate complex," *The Analyst*, vol. 110, no. 12, pp. 1445–1449, 1985.

[26] M. R. P. Reddy, P. V. S. Kumar, J. P. Shyamsundar, and J. S. Anjaneyulu, "Extractive spectrophotometric method for the determination of iron in titanium base alloys using 4-(2-Pyridylazo) resorcinol and a long chain quaternary ammonium salt," *Journal of the Indian Chemical Society*, vol. 66, pp. 437–439, 1989.

[27] A. K. Malik and A. L. J. Rao, "Spectrophotometric determination of iron(III) dimethyldithiocarbamate (ferbam)," *Talanta*, vol. 44, no. 2, pp. 177–183, 1997.

[28] R. K. Patil and D. G. Dhuley, "Solvent extraction and spectrophotometric determination of Fe(II) with 1,3-diphenyl-4-carboethoxy pyrazole-5-one," *Indian Journal of Chemistry*, vol. 39, no. 10, pp. 1105–1106, 2000.

[29] B. M. Nagabhushana, G. T. Chandrappa, B. Nagappa, and N. H. Nagaraj, "Diformylhydrazine as analytical reagent for spectrophotometric determination of iron(II) and iron(III)," *Analytical and Bioanalytical Chemistry*, vol. 373, no. 4-5, pp. 299–303, 2002.

[30] L. M. Wang, C. Song, and J. Jin, "Spectrophotometric determination of iron by extraction of its ternary complex with 4,7-diphenyl-1,10-phenanthroline and tetraphenylborate into molten naphthalene," *Fenxi Shiyanshi (Analytical Laboratory)*, vol. 23, no. 9, pp. 48–50, 2004.

[31] F. G. Martins, J. F. Andrade, A. C. Pimenta, L. M. Lourenco, J. R. M. Casto, and V. R. Balbo, "Spectrophotometric study of iron oxidation in the iron(II) thiocyanateacetone system and some analytical application," *Electica Quimica*, vol. 30, no. 3, pp. 63–71, 2005.

[32] S. S. Patil and A. D. Sawant, "Pyridine-2-acetaldehyde salicyloylhydrazone as reagent for extractive and spectrophotometric determination of cobalt(II) at trace level," *Indian Journal of Chemical Technology*, vol. 8, no. 2, pp. 88–91, 2001.

[33] S. Adinarayana Reddy, K. Janardhan Reddy, S. Lakshmi Narayana, Y. Sarala, and A. Varada Reddy, "Synthesis of new reagent 2,6-diacetylpyridine bis-4-phenyl-3- thiosemicarbazone (2,6-DAPBPTSC): Selective, sensitive and extractive spectrophotometric determination of Co(II) in vegetable, soil, pharmaceutical and alloy samples," *Journal of the Chinese Chemical Society*, vol. 55, no. 2, pp. 326–334, 2008.

[34] Q. Qiufen, G. Yang, X. Dong, and J. Yin, "Study on the solid phase extraction and spectrophotometric determination of cobalt with 2-(2-quinolylazo)-5-diethylaminoaniline," *Turkish Journal of Chemistry*, vol. 28, no. 5, pp. 611–619, 2004.

[35] A. P. Kumar, P. R. Reddy, and V. K. Reddy, "Direct and derivative spectrophotometric determination of cobalt (II) in microgram quantities with 2-hydroxy-3-methoxy benzaldehyde thiosemicarbazone," *Journal of the Korean Chemical Society*, vol. 51, no. 4, pp. 331–338, 2007.

[36] F. G. Martins, J. F. Andrade, A. C. Pimenta, L. M. Lourenço, J. R. M. Castro, and V. R. Balbo, "Spectrophotometric study of iron oxidation in the iron(II)/thiocyanate/ acetone system and some analytical applications," *Ecletica Quimica*, vol. 30, no. 3, pp. 63–71, 2005.

Hindawi Publishing Corporation
International Journal of Analytical Chemistry
Volume 2012, Article ID 363919, 4 pages
doi:10.1155/2012/363919

Research Article

Chemical Constituents of Essential Oil from *Lippia sidoides* Cham. (Verbenaceae) Leaves Cultivated in Hidrolândia, Goiás, Brazil

Sandra Ribeiro de Morais,[1,2] Thiago Levi Silva Oliveira,[2,3] Maria Teresa Freitas Bara,[4] Edemilson Cardoso da Conceição,[4] Maria Helena Rezende,[5] Pedro Henrique Ferri,[6] and José Realino de Paula[4]

[1] *Programa de Pós-Graduação em Biologia, Instituto de Ciências Biológicas, Universidade Federal de Goiás, 74001 970 Goiânia, GO, Brazil*
[2] *Instituto de Ciências da Saúde, Universidade Paulista, Campus Flamboyant, 74845 090 Goiânia, GO, Brazil*
[3] *Programa de Pós-Graduação em Ciências Farmacêuticas, Laboratório de Pesquisa de Produtos Naturais, Faculdade de Farmácia, Universidade Federal de Goiás, 74605 220 Goiânia, GO, Brazil*
[4] *Faculdade de Farmácia, Universidade Federal de Goiás, 74605 220 Goiânia, GO, Brazil*
[5] *Instituto de Ciências Biológicas, Universidade Federal de Goiás, Campus Samambaia, 74001 970 Goiânia, GO, Brazil*
[6] *Instituto de Química, Laboratório de Bioatividade Molecular, Universidade Federal de Goiás, Campus Samambaia, 74001 970 Goiânia, GO, Brazil*

Correspondence should be addressed to Sandra Ribeiro de Morais, sandrarmorais@hotmail.com

Received 1 September 2011; Revised 24 November 2011; Accepted 8 December 2011

Academic Editor: Norberto Peporine Lopes

Several studies involving the family Verbenaceae, occurring in the Brazilian Cerrado, have emphasized the popular use of many aromatic species. We highlight the use of *Lippia sidoides* Cham., known as "alecrim pimenta," native to northeastern Brazil and northern Minas Gerais. Leaves of this species were collected in antropized Brazilian Cerrado area, in Hidrolândia, Goiás, and their essential oils were extracted by hydrodistillation in a Clevenger-type apparatus and thereafter analyzed GC/MS. Among the compounds identified in this study were the most abundant oxygenated monoterpenes, followed by sesquiterpenes hydrocarbons. The oxygenated monoterpene 1,8-cineole was the major constituent followed by isoborneol and bornyl acetate. The chemical composition of essential oil described in this paper differs from that described in the literature for *L. sidoides* found in its native environment, where the major constituents are thymol and carvacrol.

1. Introduction

The knowledge of chemical constituents of essential oils is of fundamental importance to the pharmaceutical, food, and perfumery industries. As the use of aromatic compounds requires detailed chemical characterization and evaluation of possible modifications within their compositions, which are due to the different geographical origins and/or climatic conditions and various population genetics that can lead to the formation of different chemotypes [1, 2].

Various studies involving the Verbenaceae family have highlighted the importance of many species used within popular medicine by the presence of principle aromas [3–9]. It is worth noting that in this family, the species *Lippia sidoides*, popularly known as "alecrim-pimenta," native to the northeastern region of Brazil and north of the state of Minas Gerais, is an aromatic species commonly used in the form of infusions and inhalations, allergic rhinitis, and in the treatment of vaginal, mouth, and throat infections [10].

Within the chemical components described of this species, thymol and carvacrol are major constituents of the essential oil [11–13], with a remarkable inhibitory activity regarding the development of microorganisms [14–17]. Moreover, the studies show variations in the concentration

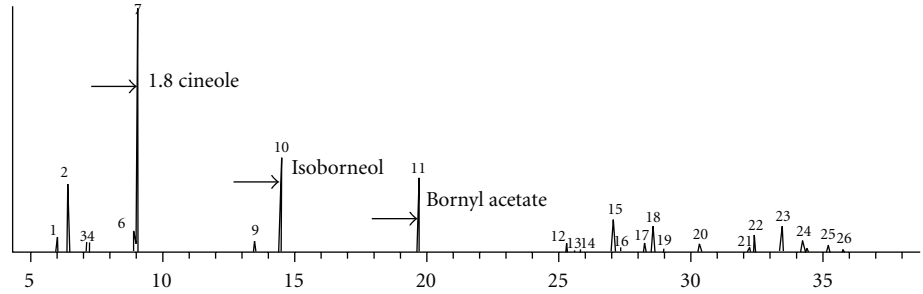

Figure 1: Total ion chromatogram (TIC) of chemical constituents of essential oil from *Lippia sidoides* Cham., (Verbenaceae) leaves, cultivated in Hidrolândia, Goiás, Brazil. (arrow: major constituents).

of thymol in different stages of the plant's development [18]. This work aims to determine the chemical composition of the essential oil of *L. sidoides* cultivated in an area of antropized cerrado in Hidrolândia, Goiás, Brazil.

2. Experimental

The leaves of *Lippia sidoides* Cham. were collected from three plants grown in the municipality of Hidrolândia, Goiás, Brazil (altitude 835 m, 16° 54′ 1.3″ south, 49° 15′ 35.2″ west) in august/2010, both northwest Minas Gerais, Brazil origin. Botanic material was identified by Dr. Marcos José da Silva, of Departamento de Biologia Geral do Instituto de Ciências Biológicas/UFG, and vouchers were deposited in the Herbarium of Universidade Federal de Goiás (UFG) under code number 45121.

Leaves were dried at room temperature and then pulverized by blade mill. Essential oil was extracted by hydrodistillation in a Clevenger-type apparatus for 2 hours from 50 g of powered leaves in 1000 mL of water. At the end of each distillation, the oils were measured in Clevenger trap, collected, dried with anhydrous Na_2SO_4, stored in hermetically sealed glass containers with rubber lids, covered with aluminum foil to protect the contents from light, and kept under refrigeration at −10°C until used. The essential oil was submitted to GC/MS analysis performed on Shimadzu QP5050A apparatus using a CBP-5 (Shimadzu) fused silica capillary column (30 m × 0.25 mm; 0.25 μm film thickness composed of 5% phenylmethylpolysiloxane) and programmed temperature as follows: 60°–240°C at 3°C/min, then to 280°C at 10°C/min, ending with 10 min at 280°C. The carrier gas was He at a flow rate of 1.0 mL/min and the split mode had a ratio of 1 : 20. Compounds were identified by computer search using digital libraries of mass spectral data [19] and by comparison of their retention indices and authentic mass spectra, relative to C8–C32 n-alkane series [20] in a temperature-programmed run.

3. Results and Discussion

The yield of *Lippia sidoides* essential oil was 0.8%. Within the identified components of the essential oil, the most abundant were oxygenated monoterpenes, followed by sesquiterpenes hydrocarbons (Table 1).

Table 1: Percentage of chemical constituents of essential oil from *Lippia sidoides* Cham. (Verbenaceae) leaves, cultivated in Hidrolândia, Goiás, Brazil.

Constituent	RI	%
Artemisia triene	929	1.71
Camphene	954	6.19
Sabinene	975	1.27
β-pinene	979	1.23
ρ-cymene	1024	0.38
Sylvestrene	1030	3.03
1,8 cineole	1031	26.67
Cis-sabinene hydrate	1070	0.50
Camphor	1146	1.60
Isoborneol	1160	14.60
Bornyl acetate	1288	10.77
α-cedrene	1411	1.75
(e)-caryophyllene	1419	1.09
Cis-thujopsene	1431	1.12
α-himachalene	1451	1.37
α-humulene	1454	5.66
Ar-curcumene	1480	1.83
β-selinene	1490	4.33
Cis-calamenene	1529	2.68
Zierone	1575	1.99
Rosifoliol	1600	4.53
Citronellyl pentanoate	1625	1.79
Alo-himachalol	1662	0.59
Oxygenated monoterpenes	—	53.64
Sesquiterpenes hydrocarbons	—	19.83
Monoterpene hydrocarbons	—	14.31
Oxygenated sesquiterpenes	—	8.90
Unidentified	—	3.32
Total identified (%)	—	96.68

RI: retention indices.

Altogether, 96.68% of the chemical constituents of the essential oil were identified. As described in Table 1 and by chromatogram showed in Figure 1, 1,8 cineole, an oxygenated monoterpene was mostly constituent (26.67%), followed by isoborneol (14.60%) and bornyl acetate (10.77%).

In *L. sidoides* cultivated in Minas Gerais, Brazil, the 1,8 cineole was also identified in lower concentrations (9.26%) than in this work. However, thymol and carvacrol were also

identified [21]. 1,8 cineole was also identified in other species of its kind, such as *Lippia microphylla* Cham. [22], *Lippia alba* (Mill.) N. E. Brown [6, 23, 24] and *Lippia schomburgkiana* Schauer [24].

The results found in this work for *L. sidoides*, cultivated in an area of anthropic bushland, differ from that presented in the literature, where the thymol and carvacrol appear as major components [11–13]. What can be understood when considering that the environment of which the plant develops are factors such as temperature, relative humidity, exposure to the sun and wind, which exert a direct influence on the chemical composition of volatile oils [2, 23, 25]. Alteration in the yield of the essential oils, as well as the quantity of chemical constituents can still be observed due to the different phases of the plant's development [2, 6, 18] and at different times of the year [4, 23].

Qualitative and quantitative variations in the composition of the oils can also be observed in species that have chemotypes or chemical races, where botanically identical plants produce different chemical compounds, irrespective of their environment, as registered in *L. alba*, where three chemotypes from different regions and cultivated under the same conditions produce citral, carvone, and linalool, confirming that the variations occur in function of infraspecific variation [6]. Moreover, depending on the liability of the constituents of volatile oils, the method used to extract the essential oils could affect the identification [2, 26].

4. Conclusion

The chemical composition of essential oil described in this paper differs from that described in the literature for *L. sidoides* found in its native environment, highlighting the need for further studies to assess the variation in chemical composition of vegetal species in different environments, especially those who may have biological activity.

Acknowledgments

The authors are grateful to Brazilian agencies CNPq and CAPES for financial support and to Professor Dr. Marcos José da Silva, do Departamento de Biologia Geral do Instituto de Ciências Biológicas/UFG, for identification of the plant.

References

[1] A. T. Henriques, C. A. Simões-Pires, and M. A. Apel, "Óleos essenciais: importância e perspectivas terapêuticas," in *Química de Produtos Naturais, Novos Fármacos e a Moderna Farmacognosia*, R. A. Yunes and V. Cechinel-Filho, Eds., pp. 219–256, Itajaí, Univale, Brazil, 2009.

[2] C. M. O. Simões and V. Spitzer, "Óleos voláteis," in *Farmacognosia: Da Planta Ao Medicamento*, C. M. O. Simões, E. P. Schenkel, G. Gosmann, J. C. P. Mello, L. A. Mentz, and P. R. Petrovick, Eds., pp. 467–496, UFRGS, Porto Alegre, Brazil, 5th edition, 2004.

[3] E. M. Costa-Neto and M. V. M. Oliveira, "The use of medicinal plants in the county of Tanquinho, State of Bahia, Northeastern Brazil," *Revista Brasileira de Plantas Medicinais*, vol. 2, no. 2, pp. 1–8, 2000.

[4] M. R. A. Santos, R. Innecco, and A. A. Soares, "Caracterização anatômica das estruturas secretoras e produção de óleo essencial de *Lippia alba* (Mill.) N. E. Br. em função do horário de colheita nas estações seca e chuvosa," *Revista Ciência Agronômica*, vol. 35, no. 2, pp. 377–383, 2004.

[5] J. S. Aguiar and M. C. C. D. Costa, "*Lippia alba* (Mill.) N. E. Brown (Verbenaceae): survey of the publications in the chemical, agronomical and pharmacological area, published between 1974 to 2004," *Revista Brasileira de Plantas Medicinais*, vol. 8, no. 1, pp. 79–84, 2005.

[6] E. S. Tavares, E. S. Julião, H. D. Lopes, H. R. Bizzo, C. L. S. Lage, and S. G Leitão, "Análise do óleo essencial de folhas de três quimiotipos de *Lippia alba* (Mill.) N. E. Br. (Verbenaceae) cultivados em condições semelhantes," *Brazilian Journal of Pharmacognosy*, vol. 15, no. 1, pp. 1–5, 2005.

[7] J. E. B. P. Pinto, J. C. W. Cardoso, E. M. Castro, S. K. Bertolucci, L. A. Melo, and S. Dousseau, "Aspectos morfo-fisiológicos e conteúdo de óleo essencial de plantas de alfazema-do-Brasil em função de níveis de sombreamento," *Horticultura Brasileira*, vol. 25, no. 2, pp. 210–214, 2007.

[8] S. Froelich, M. P. Gupta, K. Siems, and K. Jenett-Siems, "Phenylethanoid glycosides from *Stachytarpheta cayennensis* (Rich.) Vahl, Verbenaceae, a traditional antimalarial medicinal plant," *Brazilian Journal of Pharmacognosy*, vol. 18, no. 4, pp. 517–520, 2008.

[9] S. L. Goulart and C. R. Marcati, "Anatomia comparada do lenho em raiz e caule de *Lippia salviifolia* Cham. (Verbenaceae)," *Revista Brasileira de Botanica*, vol. 31, no. 2, pp. 263–275, 2008.

[10] E. R. Martins, D. M. Castro, D. C. Castelanni, and J. E. Dias, *Plantas Medicinais*, Universidade Federal de Viçosa, Viçosa, Brazil, 2000.

[11] L. M. A. Macambira, C. H. S. Andrade, F. J. A. Matos, A. A. Craveiro, and R. Braz Filho, "Naphthoquinoids from *Lippia sidoides*," *Journal of Natural Products*, vol. 49, no. 2, pp. 310–312, 1986.

[12] S. M. O. Costa, T. L. G. Lemos, O. D. L. Pessoa, J. C. C. Assunção, and R. Braz-Filho, "Constituintes químicos de *Lippia sidoides* (Cham.) Verbenaceae," *Brazilian Journal of Pharmacognosy*, vol. 12, supplement 1, pp. 66–67, 2002.

[13] R. S. Nunes, H. S. Xavier, P. J. Rolim Neto, D. P. Santana, and U. P. Albuquerque, "Botanical standardization of *Lippia sidoides* Cham. (Verbenaceae)," *Acta Farmaceutica Bonaerense*, vol. 19, no. 2, pp. 115–118, 2000.

[14] M. A. Botelho, V. S. Rao, C. B. M. Carvalho et al., "*Lippia sidoides* and *Myracrodruon urundeuva* gel prevents alveolar bone resorption in experimental periodontitis in rats," *Journal of Ethnopharmacology*, vol. 113, no. 3, pp. 471–478, 2007.

[15] M. A. Botelho, N. A. P. Nogueira, G. M. Bastos et al., "Antimicrobial activity of the essential oil from *Lippia sidoides*, carvacrol and thymol against oral pathogens," *Brazilian Journal of Medical and Biological Research*, vol. 40, no. 3, pp. 349–356, 2007.

[16] E. Lacoste, J. P. Chaumont, D. Mandin, M. M. Plumel, and F. J. A. Matos, "Antiseptic properties of the essential oil of *Lippia sidoides* Cham: application to the cutaneous microflora," *Annales Pharmaceutiques Francaises*, vol. 54, no. 5, pp. 228–230, 1996.

[17] F. P. Oliveira, E. O. Lima, J. P. Siqueira-Júnior, E. L. Souza, B. H. C. Santos, and H. M. Barreto, "Effectiveness of *Lippia sidoides* Cham. (Verbenaceae) essential oil in inhibiting the growth of *Staphylococcus aureus* strains isolated from clinical material," *Brazilian Journal of Pharmacognosy*, vol. 16, no. 4, pp. 510–516, 2006.

[18] L. K. A. M. Leal, V. M. Oliveira, S. M. Araruna, M. C. C. Miranda, and F. M. A. Oliveira, "Análise de timol por CLAE na tintura de *Lippia sidoides* Cham. (alecrim-pimenta) produzida em diferentes estágios de desenvolvimento da planta," *Brazilian Journal of Pharmacognosy*, vol. 13, supplement 1, pp. 9–11, 2003.

[19] National Institute of Standards and Technology, *PC Version of the NIST/EPA/NIH Mass Spectral Database*, U.S. Department of Commerce, Gaithersburg, Md, USA, 1998.

[20] R. P. Adams, *Identification of Essential Oil Components by Gas Chromatography/Mass Spectroscopy*, Allured, Carol Stream, Ill, USA, 4th edition, 2007.

[21] R. K. Lima, M. G. Cardoso, J. C. Moraes, S. M. Carvalho, V. G. Rodrigues, and L. G. L. Guimarães, "composição química e efeito fumigante do óleo essencial de *Lippia sidoides* cham. e monoterpenos sobre *Tenebrio molitor* (L.) (coleoptera: tenebrionidae)," *Ciencia e Agrotecnologia*, vol. 35, no. 4, pp. 664–671, 2011.

[22] F. F. G. Rodrigues, H. D. M. Coutinho, A. R. Campos, S. G. de Lima, and J. G. M. da Costa, "Atividade antibacteriana e composição química do óleo essencial de *Lippia microphylla* cham," *Acta Scientiarum*, vol. 33, no. 2, pp. 141–144, 2011.

[23] F. M. C. Barros, E. O. Zambarda, B. M. Heinzmann, and C. A. Mailmann, "Variabilidade sazonal e biossíntese de terpenóides presentes no óleo essencial de *Lippia alba* (Mill.) n. e. brown (Verbenaceae)," *Quimica Nova*, vol. 32, no. 4, pp. 861–867, 2009.

[24] J. G. S. Maia and E. H. A. Andrade, "Database of the amazon aromatic plants and their essential oils," *Quimica Nova*, vol. 32, no. 3, pp. 595–622, 2009.

[25] T. S. Fiuza, S. M. T. Sabóia-Morais, J. R. Paula et al., "Composition and chemical variability in the essential oils of *Hyptidendron canum* (Pohl ex Benth.) Harley," *Journal of Essential Oil Research*, vol. 22, no. 2, pp. 159–163, 2010.

[26] X. Gu, Z. Zhang, X. Wan, J. Ning, C. Yao, and W. Shao, "Simultaneous distillation extraction of some volatile flavor components frompu-erh Tea samples—comparison with steam distillation-liquid/liquid extraction and soxhlet extraction," *International Journal of Analytical Chemistry*, vol. 2009, Article ID 276713, 6 pages, 2009.

Hindawi Publishing Corporation
International Journal of Analytical Chemistry
Volume 2012, Article ID 259217, 7 pages
doi:10.1155/2012/259217

Research Article

Characterisation of Flavonoid Aglycones by Negative Ion Chip-Based Nanospray Tandem Mass Spectrometry

Paul J. Gates[1] and Norberto P. Lopes[2]

[1] *School of Chemistry, University of Bristol, Cantock's Close, Bristol BS8 1TS, UK*
[2] *Faculdade de Ciências Farmacêuticas de Ribeirão Preto, Universidade de São Paulo, Via do Café S/N, 14040-903 Ribeirão Preto, SP, Brazil*

Correspondence should be addressed to Paul J. Gates, paul.gates@bristol.ac.uk

Received 26 September 2011; Accepted 20 November 2011

Academic Editor: Michael Niehues

Flavonoids are one of the most important classes of natural products having a wide variety of biological activities. There is wide interest in a range of medical and dietary applications, and having a rapid, reliable method for structural elucidation is essential. In this study a range of flavonoid standards are investigated by chip-based negative ion nanospray mass spectrometry. It was found that the different classes of flavonoid studied have a combination of distinct neutral losses from the precursor ion $[M\text{-}H]^-$ along with characteristic low-mass ions. By looking only for this distinct pattern of product ions, it is possible to determine the class of flavonoid directly. This methodology is tested here by the analysis of a green tea extract, where the expected flavonoids were readily identified, along with quercetin, which is shown to be present at only about 2% of the most intense ion in the spectrum.

1. Introduction

Flavonoids are an important class of dietary natural products with a range of biological activities, such as antioxidant, UV-protection, antiparasitic, anti-inflammatory, and anti-fungal [1–6]. The flavonoids are subcategorised into eight different classes with some of the compounds also exhibiting possible beneficial properties such as health-promoting and anticancer activities [7]. The common C6-C3-C6 structural core for all flavonoids arises from the shikimate (C6-C3) and acetate (C6) biosynthetic pathways. In their review, Williams and Grayer pointed out that the theoretical number of possible flavonoid structures (with hydroxyl, methoxyl, methyl, isoprenyl benzyl, and sugar substituents) is enormous, and many new natural flavonoids are still to be isolated [8]. Until now, more than 9000 different flavonoids have been isolated. The majority were isolated and identified employing classical phytochemical procedures, and there is no doubt that many more new flavonoids remain to be discovered [8].

Many analytical methodologies have been developed to detect and quantify flavonoids, mostly using high-performance liquid chromatography with UV-VIS spectral detection. However, identification of flavonoids, as well as other natural products, through hyphenated systems (LC-UV) is limited since a complete chromatographic resolution for all chromophores is required to be sure that the correct conclusion is reached [9, 10]. Mass spectrometry (MS) with electrospray ionisation (ESI) has emerged as a complementary method for high sensitivity, selectivity, and fast analysis of natural products [11], such as sesquiterpene lactones [12] and alkaloids [13]. Among all mass spectrometry techniques, electrospray ionisation tandem mass spectrometry (ESI-MS/MS) using low-energy collision-induced dissociation (CID) has been the technique of choice for such studies through the technique's ability to analyse natural products with medium to high polarities [14].

Nanospray ionisation is an improvement over traditional ESI for the analysis of low volume low concentration samples [15]. With nanospray, it is possible to obtain mass spectra from picogram quantities of material with little sample clean-up being required. Standard nanospray uses disposable tips and as a result has problems with signal reproducibility between tips and difficulties with coupling to HPLC. With the development of automated "chip-based" nanospray

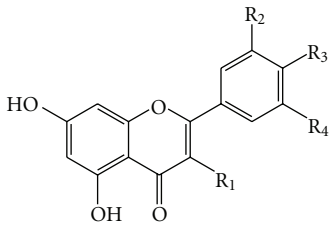

(a)

	R_1	R_2	R_3	R_4
(**1**)	OH	OH	OH	H
(**2**)	OH	OH	OH	OH
(**3**)	H	H	OH	H
(**4**)	H	OH	OH	H

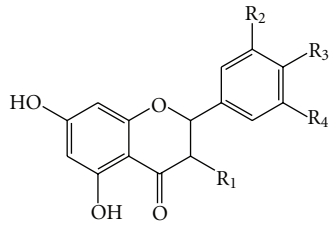

(b)

	R_1	R_2	R_3	R_4
(**5**)	H	H	OH	H
(**6**)	H	OH	OMe	H

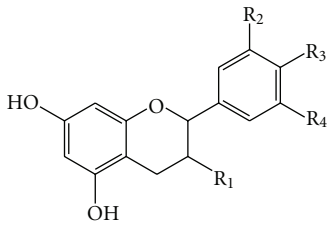

(c)

	R_1	R_2	R_3	R_4
(**7**)	OH	OH	OH	H
(**8**)	OH	OH	OH	OH

Figure 1: The structures of the flavonoids analysed. (**1**) Quercetin (molecular weight = 302); (**2**) Myricetin (molecular weight = 318); (**3**) Apigenin (molecular weight = 270); (**4**) Luteolin (molecular weight = 286); (**5**) Naringenin (molecular weight = 272); (**6**) Hesperetin (molecular weight = 302); (**7**) Catechin (molecular weight = 290) and (**8**) Epigallocatechin (molecular weight = 306).

systems, using arrays of uniform nanospray needles, the technique is becoming much more important [16]. In "chip-based" nanospray, the analyte solution is sprayed from a conductive pipette tip pressed against the rear of the chip using a small gas pressure and low voltage to create the spray. Each nanospray needle in the array is used only once to avoid contamination.

In recent years, nanospray ionisation has been applied to the analysis of natural products, but there are still some doubts about the applicability of the technique for the analysis of small molecules. Analysis of retinal, carotenoids, and xanthophylls showed some significant differences between the ions observed between nanospray and electrospray ionisation [14, 17, 18]. These results could be correlated to differences in the source design and ionisation conditions for nanospray and open up a new area of research in natural product chemistry. Based upon these previous studies and the increasingly recognised importance of flavonoids in the human diet along with the increase in metabolomic studies, the purpose of this study is to establish a sound basis for the ionisation and fragmentation of four aglycone flavonoid classes (Figure 1) in negative ion nanospray ionisation. The application and power of the technique to "real world" samples is exemplified with the identification of medium-polarity flavonoids from a simple extract of green tea without employing any prior sample preparation, clean-up, or chromatography.

2. Experimental

2.1. Materials. The flavonoid standards (Figure 1) were isolated as previously described [19] or obtained from Sigma-Aldrich (United Kingdom). Solutions of the analytes (approximetely 0.1 mg/mL) in 100% HPLC-grade methanol (Fisher Scientific) were prepared immediately prior to the analysis. The green tea sample was obtained from a local supermarket. A few grains were dissolved in 100% methanol with the sample centrifuged (13,000 rpm, 5 mins) prior to the analysis.

2.2. Instrumentation. Nanospray ionisation analyses were performed on a QStar-XL quadrupole-time-of-flight hybrid instrument (Applied Biosystems, Warrington, UK) using a NanoMate HD automatic chip-based nanospray system (Advion Biosciences, Norwich, UK). Instrument control, data acquisition, and data processing were performed through the Analyst QS version 1.1 software (Applied Biosystems, Warrington, UK). NanoMate control was through the ChipSoft software (Advion Biosciences, Norwich, UK). The NanoMate was set for 5 μL of solution to be aspirated and sprayed through a NanoMate 400 chip at 1.45 kV with a nitrogen back pressure of 0.4 psi. QStar acquisition parameters were ion source gas flow rate, 50; curtain gas flow rate, 20; ion spray voltage, 2700 V; declustering potential, 75 V; focusing potential, 280 V; declustering potential 2, 15 V. CID-MS/MS was performed at a collision energy in the range from -20 to -40 eV. The ion source gas, curtain gas, and collision gas were all nitrogen.

3. Results and Discussion

The compounds quercetin (flavonol, **1**), apigenin (flavone, **3**), naringenin (flavanone, **5**), and hesperetin (flavanone, **6**) (Figure 1) were used as standards to study their ability to produce high-intensity, stable-deprotonated molecule signals in negative ion mode nanospray ionisation. 100% HPLC methanol proved to be an excellent solvent for these studies with stable ion signals being produced for up to 20 minutes (Figure 2). This is essential as it allows for a number of tandem mass spectrometry (MS/MS) experiments to be performed on the same sample without any adjustments or tuning of the nanospray source. Use of methanol resulted in no observed methylation reactions as has previously been described for other natural products [20]. Over the range of source conditions used, all the aglycone flavonoids produced an intense and stable spray for at least 15 minutes from single 5 μL analyte solution aspirations. This demonstrates the possibility to work with more complex flavonoid samples and allows for setting up automatic MS/MS acquisitions from a batch analysis.

Following on from the ion formation studies, the systematic investigation was continued to determine the best

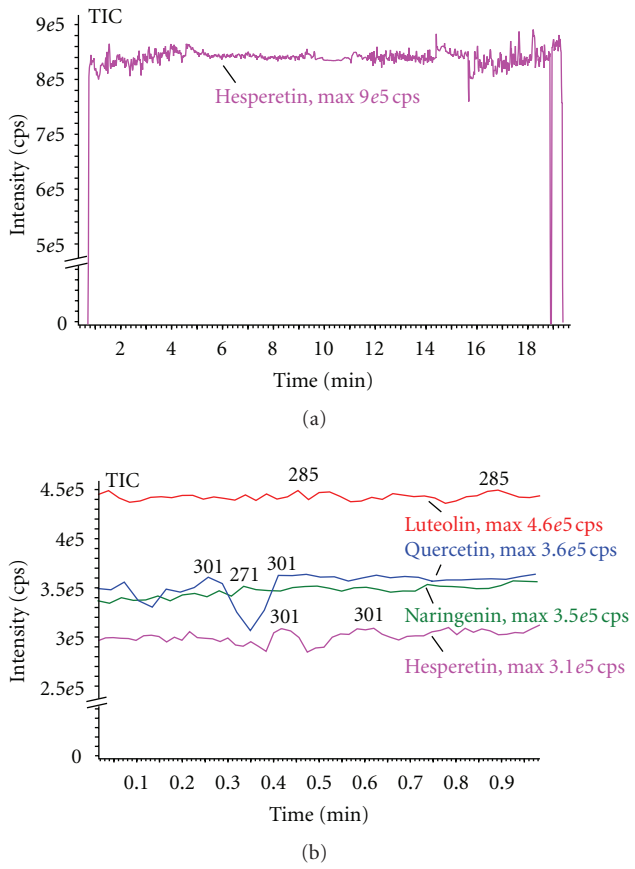

Figure 2: Demonstration of the stability of the chip-based nanospray infusion. The data shows plots of total ion count (from 5 μL aspirations) versus time for $[M\text{-}H]^-$ ions. Plot (a) is for hesperetin over a 20 minute run. The onset of nanospray is at about 30 s into the run with about 15 minutes of highly stable spray. After 15 minutes, the spray is less stable until the spray breaks down at about 19.5 minutes. Plot (b) is of luteolin, quercetin, naringenin, and hesperetin over a 1-minute run demonstrating intersample reproducibility.

CID collision energies required for effective product ion formation whilst eliminating unwanted gas-phase interactions. Collision energies from −20 to −40 eV resulted in good product ion spectra, with, as expected, more product ions being observed at higher voltages (more negative). A collision energy of around −35 eV was determined to result in the "best" product ion spectra (Figure 3). Examination of the spectra revealed high levels of complexity with many competing fragmentation routes. The main neutral molecules lost from the $[M\text{-}H]^-$ ions consisted of a combination of H_2O, CO, CO_2, and/or H_2CCO (Figure 3). A detailed analysis of all the spectra indicates that a combination of a specific order of neutral eliminations occurs along with the presence of a series of diagnostic low-mass product ions for each of the flavonoid classes analysed (Table 1 and Figure 3) resulting in the quick and reliable method for the identification of the flavonoid class. The diagnostic low-mass product ions result from ring contraction reactions which follow the same mechanisms as previously reported

Table 1: Table of the characteristic sequences of neutral losses, from their corresponding $[M\text{-}H]^-$ precursor ions and characteristic low-mass product ions, for the four flavonoid classes analysed in this study.

Flavonoid class	Characteristic neutral losses	Characteristic productions
Flavonols (**1** and **2**)	−28, −44, −18	151, 125, 107
Flavones (**3** and **4**)	−28, −44, −44, −28, −42	151, 121, 107
Flavanones (**5** and **6**)	−18, −44, −44, −18, −42	151, 125, 107
Flavanols (**7** and **8**)	−18, −44, −44, −18, −42	137, 125, 109

for flavonoids in negative mode ESI [21]. All of the flavonoids (except the flavanols) have the previously described ions at *m/z* 151 and 107 [21], whereas the flavanols catechin and epigallocatechin (with no oxidation at carbon 3, but following a similar ring contraction mechanism) result in the product ions at *m/z* 137 and 109. Also, all of the flavonoids except the flavones have an ion at *m/z* 125, and the flavones have an ion at *m/z* 121.

The flavanone hesperetin has a methoxyl substitution at the aromatic ring and showed elimination of a methyl radical ($^{\bullet}CH_3$) similar to that previously reported for mycosporine-like amino acids [22] and some other flavonoids [23]. Observation of this behaviour in nanospray allows the easy distinguishing of methoxylated flavonoids with identical molecular mass, for example, when screening plant extracts for flavonoid composition as previously report in ESI [23]. Increasing the collision energy for hesperetin results in an almost complete fragmentation of the radical ion, but allows for the observation of a loss of 16 mass units. An unusual CH_4 elimination has been previously described for heterocyclic aromatic amines which is proposed to be due to a gas-phase ion-molecule aromatic-nucleophilic substitution between β-carbolines and water vapour [24]. With hesperetin, the loss of 16 is suggested to be due to CH_4 elimination involving the methoxyl group and the *ortho*-hydroxyl group. Figure 4 shows the expansion of two product ion spectra of hesperetin at different collisional energies, clearly showing the competing losses of $^{\bullet}CH_3$ and CH_4. The mechanism for loss of $^{\bullet}CH_3$ proceeds through homolytic cleavage as previously described [22, 23]. The mechanism for water elimination from ortho-substituted aromatic esters is well known in electron ionisation. In this case we suggest that a similar cyclic rearrangement through homolytic cleavage is occurring, but involving the hydroxyl substitution, resulting in a stable quinonic ion (Figure 4). Both of these mechanisms, when taken together, are very useful for the structure elucidation of disubstituted flavonoids.

The analysis of a green tea extract in methanol was performed to demonstrate the utility of the technique. The analysis was performed without any chromatography or sample cleanup. The negative ion nanospray spectrum (Figure 5) is very complicated with a considerable number

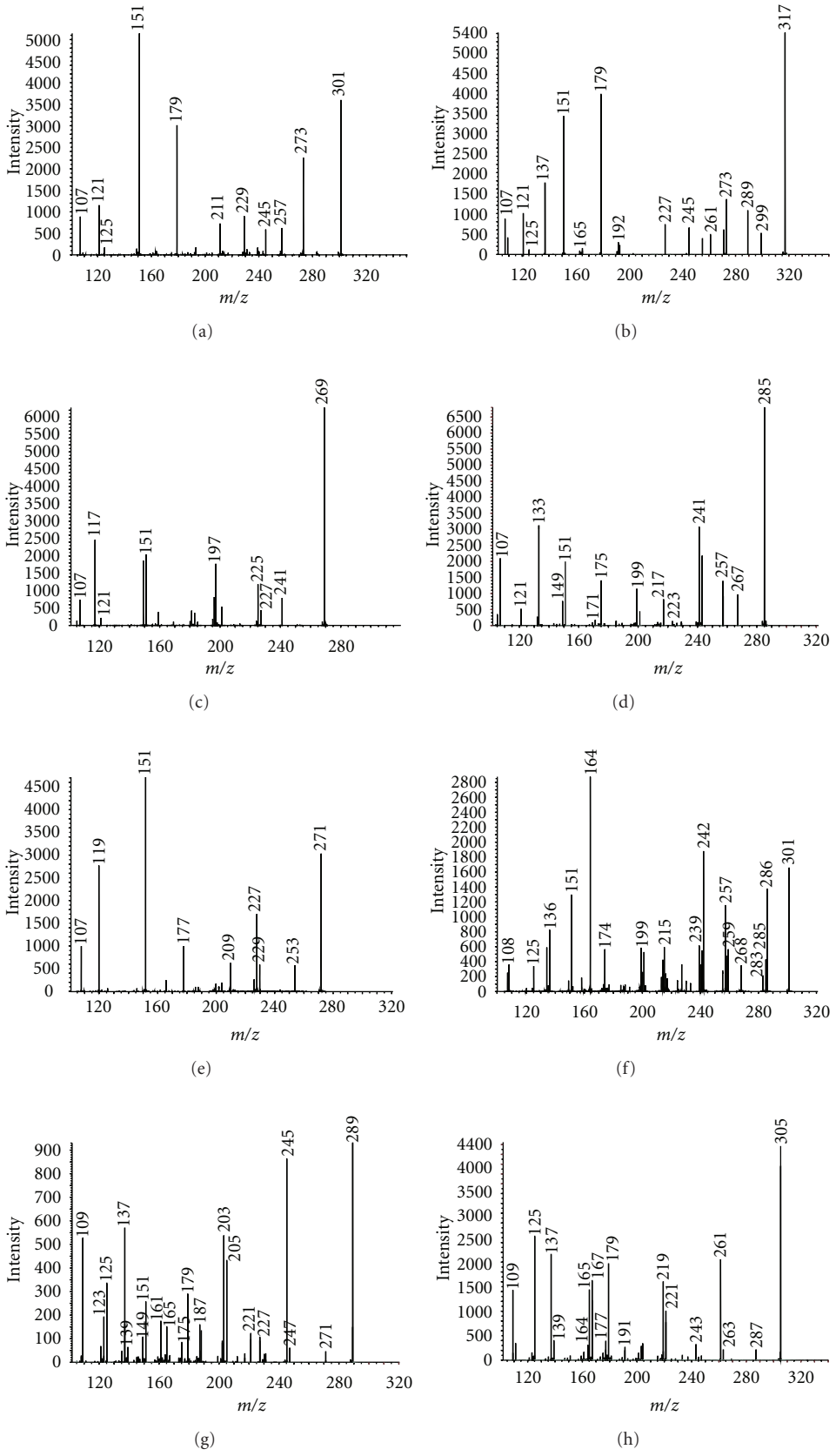

Figure 3: The negative ion nanospray product ion spectra of the eight flavonoids studied. Spectrum (a) is of quercetin, 1: (precursor ion (PI) *m/z* 301), (b) myricetin, 2: (PI *m/z* 317), (c) apigenin, 3: (PI *m/z* 269), (d) luteolin, 4: (PI *m/z* 285), (e) naringenin, 5: (PI *m/z* 271), (f) hesperetin, 6: (PI *m/z* 301), (g) catechin, 7: (PI *m/z* 289), and (h) epigallocatechin 8: (PI *m/z* 305).

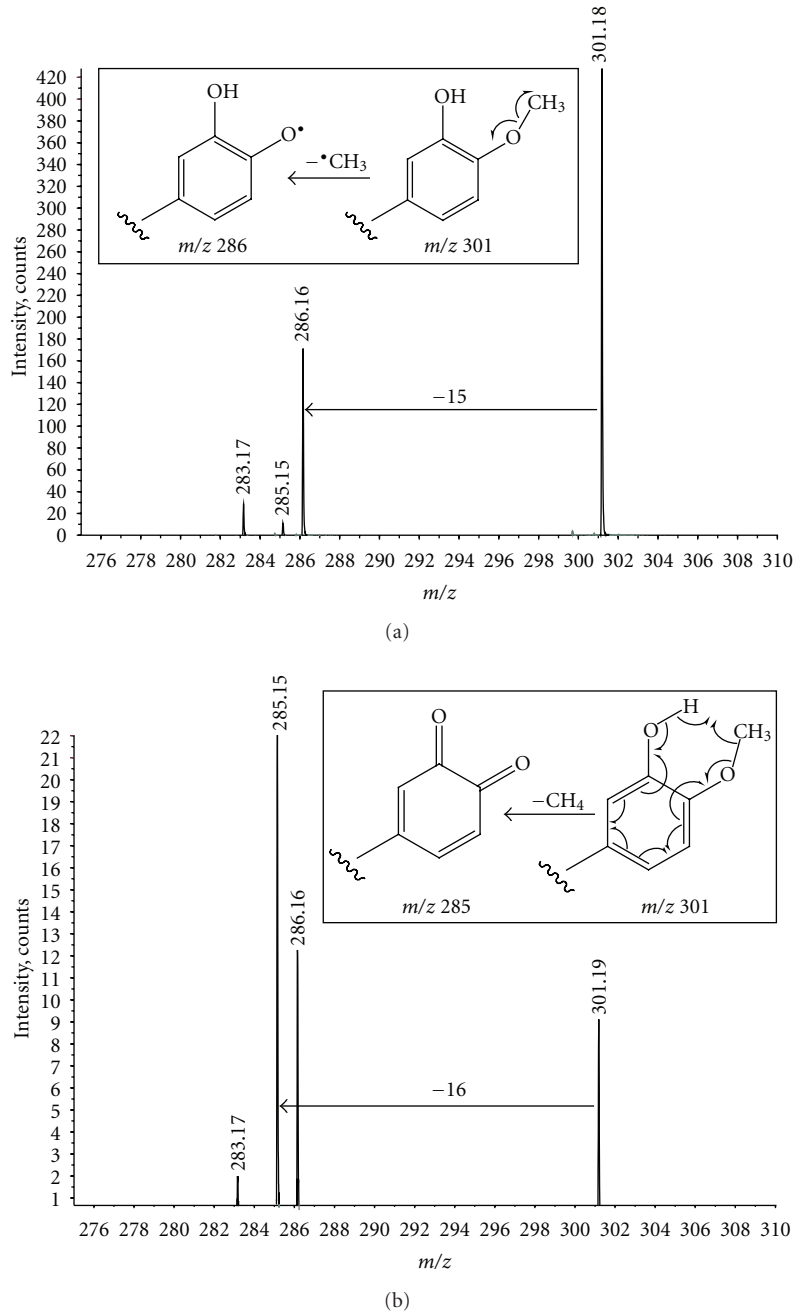

Figure 4: Enlargements of negative ion nanospray product ion spectra of hesperetin at low (a) and high (b) collision energies. The competition between losses of $^{\bullet}CH_3$ and CH_4 is clearly observed. At higher collision energy, the radical ion (*m/z* 286) has fragmented further to leave the quinonic ion (*m/z* 285) intact. The mechanism of formation of the two ions is shown in the inserts.

of ions over a wide mass range. Some of the observed masses (*m/z* 289, 305 and 317) match to the flavonoid standards already analysed in this study, and analysis of the MS/MS spectra (data not shown) of these proved them to be the expected flavonoids present in green tea: catechin, **7**, (flavanol), epigallocatechin, **8**, (flavanol) and myricetin, **2**, (flavonol). Other intense peaks (*m/z* 441 and 457) are gallate flavonoids not considered in this initial study. To test the detection limit of the technique, the peak at *m/z* 301 was studied further (see Figure 5). This peak occurs at approximately 2% of the most abundant ion in the spectrum, but performing MS/MS for about 1 minute still produced a good intensity product ion spectrum (Figure 5). A thorough study of this spectrum reveals an almost identical series of peaks to that of the flavonol quercetin, **1** (Figure 2). The differences between the two spectra are probably down to the different collision energies used. Quercetin is one of the most biologically active flavonoids and is more normally found in citrus fruits. The confirmation of the presence of quercetin in green tea (even at the low levels in this particular sample)

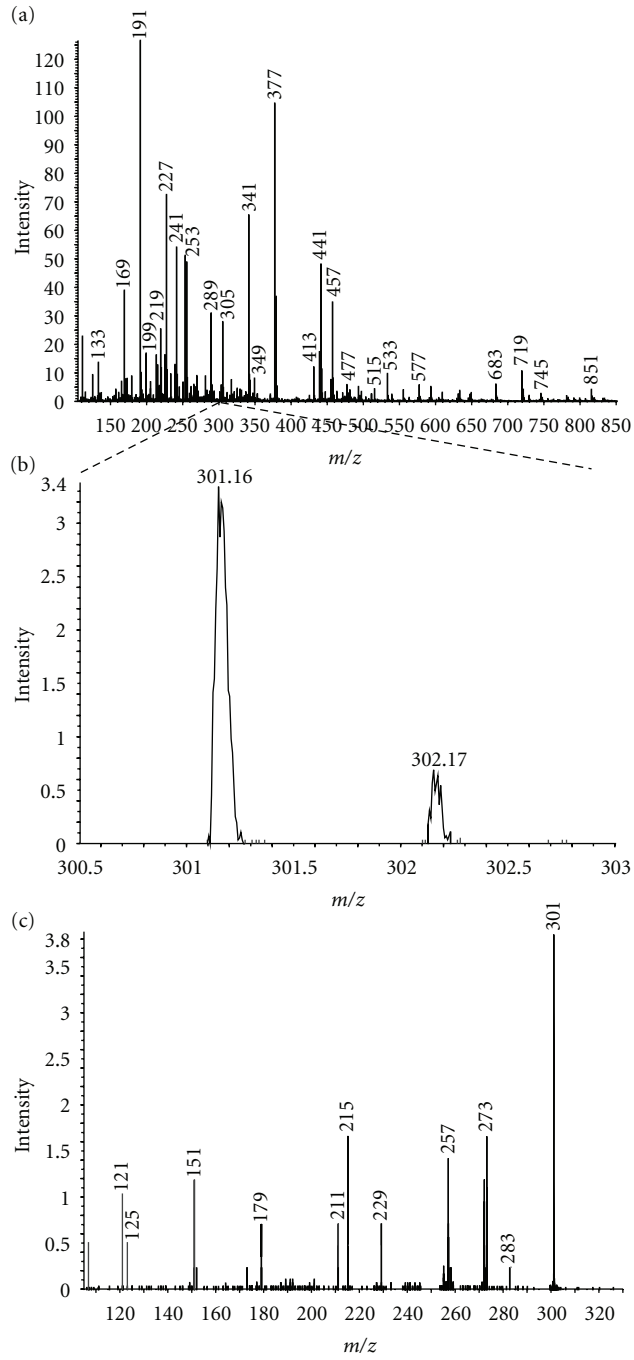

Figure 5: Negative ion nanospray spectra of the green tea extract. Spectrum (a) is the total extract recorded over a wide *m/z* range. Spectrum (b) is an enlargement of (a) to show the peak at *m/z* 301 at approximately 2% of the intensity of the most intense ion in spectrum (a). Spectrum (c) is the product ion spectrum of *m/z* 301 which clearly demonstrates the sensitivity of the technique.

is a highly significant result and a powerful demonstration of the sensitivity and application of this methodology.

4. Conclusions

In this initial study, the application of chip-based negative ion nanospray is demonstrated for the analysis of a series of flavonoid standards. The best spectra where produced from 100% HPLC methanol. MS/MS analysis of four of the classes of flavonoids have shown that they have a different, characteristic sequences of neutral losses from their corresponding $[M\text{-}H]^-$ precursor ions in combination with distinctive lower mass product ions. The application of this methodology is demonstrated for the analysis of a green tea extract where the expected flavonoids (catechin, epigallocatechin, and myricetin) were easily identified, along with the unexpected presence of quercetin (at approximately 2% of the most intense ion).

Acknowledgments

The authors thank Mark Allen of Advion BioSciences Ltd. (Norwich, UK) for helpful advice and discussions throughout this project. N. P. Lopes acknowledges FAPESP (São Paulo, Brazil) for financial support.

References

[1] A. Kanashiro, L. M. Kabeya, A. C. M. Polizello, N. P. Lopes, J. L. C. Lopes, and Y. M. Lucisano-Valim, "Inhibitory activity of flavonoids from *Lychnophora* sp. on generation of reactive oxygen species by neutrophils upon stimulation by immune complexes," *Phytotherapy Research*, vol. 18, no. 1, pp. 61–65, 2004.

[2] P. Chicaro, E. Pinto, P. Colepicolo, J. L. C. Lopes, and N. P. Lopes, "Flavonoids from *Lychnophora passerina* (Asteraceae): potential antioxidants and UV-protectants," *Biochemical Systematics and Ecology*, vol. 32, no. 3, pp. 239–243, 2004.

[3] R. Takeara, S. Albuquerque, N. P. Lopes, and J. L. C. Lopes, "Trypanocidal activity of *Lychnophora staavioides* Mart. (Vernonieae, Asteraceae)," *Phytomedicine*, vol. 10, no. 6-7, pp. 490–493, 2003.

[4] N. P. Lopes, P. Chicaro, M. J. Kato, S. Albuquerque, and M. Yoshida, "Flavonoids and lignans from *Virola surinamensis* twigs and their in vitro activity against *Trypanosoma cruzi*," *Planta Medica*, vol. 64, no. 7, pp. 667–669, 1998.

[5] L. Gobbo-Neto, M. D. Santos, A. Kanashiro et al., "Evaluation of the anti-inflammatory and antioxidant activities of di-*C*-glucosylflavones from *Lychnophora ericoides* (Asteraceae)," *Planta Medica*, vol. 71, no. 1, pp. 3–6, 2005.

[6] N. P. Lopes, M. J. Kato, and M. Yoshida, "Antifungal constituents from roots of Virolasurinamensis," *Phytochemistry*, vol. 51, no. 1, pp. 29–33, 1999.

[7] J. B. Harborne and C. A. Williams, "Anthocyanins and other flavonoids," *Natural Product Reports*, vol. 18, no. 3, pp. 310–333, 2001.

[8] C. A. Williams and R. J. Grayer, "Anthocyanins and other flavonoids," *Natural Product Reports*, vol. 21, no. 4, pp. 539–573, 2004.

[9] T. Guaratini, R. L. Vessecchi, F. C. Lavarda et al., "New chemical evidence for the ability to generate radical molecular ions of polyenes from ESI and HR-MALDI mass spectrometry," *Analyst*, vol. 129, no. 12, pp. 1223–1226, 2004.

[10] T. Guaratini, R. Vessecchi, E. Pinto, P. Colepicolo, and N. P. Lopes, "Balance of xanthophylls molecular and protonated molecular ions in electrospray ionization," *Journal of Mass Spectrometry*, vol. 40, no. 7, pp. 963–968, 2005.

[11] A. E. M. Crotti, R. Vessecchi, J. L. C. Lopes, and N. P. Lopes, "Electrospray ionization mass spectrometry: chemical processes invoeved in the ion formation from low molecular weight organic compounds," *Química Nova*, vol. 29, no. 2, pp. 287–292, 2006.

[12] A. E. M. Crotti, J. L. C. Lopes, and N. P. Lopes, "Triple quadrupole tandem mass spectrometry of sesquiterpene lactones: a study of goyazensolide and its congeners," *Journal of Mass Spectrometry*, vol. 40, no. 8, pp. 1030–1034, 2005.

[13] M. Pivatto, A. E. M. Crotti, N. P. Lopes et al., "Electrospray ionization mass spectrometry screening of piperidine alkaloids from *Senna spectabilis* (Fabaceae) extracts: fast identification of new constituents and co-metabolites," *Journal of the Brazilian Chemical Society*, vol. 16, no. 6, pp. 1431–1438, 2005.

[14] A. Fredenhagen, C. Derrien, and E. Gassmann, "An MS/MS library on an ion-trap instrument for efficient dereplication of natural products. Different fragmentation patterns for $[M + H]^+$ and $[M + Na]^+$ ions," *Journal of Natural Products*, vol. 68, no. 3, pp. 385–391, 2005.

[15] M. Wilm and M. Mann, "Analytical properties of the nanoelectrospray ion source," *Analytical Chemistry*, vol. 68, no. 1, pp. 1–8, 1996.

[16] G. A. Schultz, T. N. Corso, S. J. Prosser, and S. Zhang, "A fully integrated monolithic microchip electrospray device for mass spectrometry," *Analytical Chemistry*, vol. 72, no. 17, pp. 4058–4063, 2000.

[17] T. Guaratini, P. J. Gates, K. H. M. Cardozo, P. M. B. G. M. Campos, P. Colepicolo, and N. P. Lopes, "Letter: radical ion and protonated molecule formation with retinal in electrospray and nanospray," *European Journal of Mass Spectrometry*, vol. 12, no. 1, pp. 71–74, 2006.

[18] T. Guaratini, P. J. Gates, E. Pinto, P. Colepicolo, and N. P. Lopes, "Differential ionisation of natural antioxidant polyenes in electrospray and nanospray mass spectrometry," *Rapid Communications in Mass Spectrometry*, vol. 21, no. 23, pp. 3842–3848, 2007.

[19] P. A. dos Santos, J. L. C. Lopes, and N. P. Lopes, "Triterpenoids and flavonoids from *Lychnophoriopsis candelabrum* (Asteraceae)," *Biochemical Systematics and Ecology*, vol. 32, no. 5, pp. 509–512, 2004.

[20] N. P. Lopes, C. B. W. Stark, H. Hong, P. J. Gates, and J. Staunton, "A study of the effect of pH, solvent system, cone potential and the addition of crown ethers on the formation of the monensin protonated parent ion in electrospray mass spectrometry," *Analyst*, vol. 126, no. 10, pp. 1630–1632, 2001.

[21] N. Fabre, I. Rustan, E. de Hoffmann, and J. Quetin-Leclercq, "Determination of flavone, flavonol, and flavanone aglycones by negative ion liquid chromatography electrospray ion trap mass spectrometry," *Journal of the American Society for Mass Spectrometry*, vol. 12, no. 6, pp. 707–715, 2001.

[22] K. H. M. Cardozo, R. Vessecchi, V. M. Carvalho et al., "A theoretical and mass spectrometry study of the fragmentation of mycosporine-like amino acids," *International Journal of Mass Spectrometry*, vol. 21, pp. 3842–3848, 2008.

[23] U. Justesen, "Collision-induced fragmentation of deprotonated methoxylated flavonoids, obtained by electrospray ionization mass spectrometry," *Journal of Mass Spectrometry*, vol. 36, no. 2, pp. 169–178, 2001.

[24] N. P. Lopes, T. Fonseca, J. P. G. Wilkins, J. Staunton, and P. J. Gates, "Novel gas-phase ion-molecule aromatic nucleophilic substitution in β-carbolines," *Chemical Communications*, vol. 9, no. 1, pp. 72–73, 2003.

Hindawi Publishing Corporation
International Journal of Analytical Chemistry
Volume 2012, Article ID 260425, 9 pages
doi:10.1155/2012/260425

Review Article

Application of Monoclonal Antibodies against Bioactive Natural Products: Eastern Blotting and Preparation of Knockout Extract

Hiroyuki Tanaka,[1] Osamu Morinaga,[2] Takuhiro Uto,[2] Shunsuke Fuji,[3] Frederick Asare Aboagye,[4] Nguyen Huu Tung,[2] Xiao Wei Li,[5] Waraporn Putalun,[6] and Yukihiro Shoyama[2]

[1] *Graduate School of Pharmaceutical Science, Kyushu University, 3-1-1 Maidashi, Higashi-ku, Fukuoka 812-0855, Japan*
[2] *Faculty of Pharmaceutical Science, Nagasaki International University, 2827-7 Huis Ten Bosch, Sasebo 859-3298, Japan*
[3] *Faculty of Health Management, Nagasaki International University, 2827-7 Huis Ten Bosch, Sasebo 859-3298, Japan*
[4] *Phytochemistry Department, Centre for Scientific Research into Plant Medicine, University of Ghana, P.O. Box 73, Mampong-Akuapem, Ghana*
[5] *State Key Laboratory of Natural and Biomimetic Drugs, School of Pharmaceutical Sciences, Peking University, No.38 Xue-yuan Road, Haidian District, Beijing 100191, China*
[6] *Faculty of Pharmaceutical Science, Khon Kaen University, Khon Kaen 40002, Thailand*

Correspondence should be addressed to Yukihiro Shoyama, shoyama@niu.ac.jp

Received 30 August 2011; Accepted 18 October 2011

Academic Editor: Norberto Peporine Lopes

Matrix-assisted laser desorption/ionization (MALDI) tof mass spectrometry was used for the confirmation of hapten number in synthesized antigen. As application of MAb, the MAbs against ginsenosides and glycyrrhizin have been prepared resulting in the development of two new techniques that we named the eastern blotting method and the knockout extract preparation. In eastern blotting technique, glycosides like ginsenosides and glycyrrhizin separated by silica gel TLC were blotted to PVDF membrane that was treated with a $NaIO_4$ solution followed by BSA resulted in glycoside-BSA conjugate on a PVDF membrane. The blotted spots were stained by MAb. Double staining of eastern blotting for ginsenosides using antiginsenoside Rb_1 and Rg_1 MAbs promoted complete identification of ginsenosides in *Panax* species. The immunoaffinity concentration of glycyrrhizin was determined by immunoaffinity column conjugated with antiglycyrrhizin MAb resulting in the glycyrrhizin-knockout extract, which was determined by the synergic effect with glycyrrhizin on NO production using the cell line.

1. Introduction

Immunoassay systems using monoclonal antibody (MAb) against drugs and small molecular weight bioactive compounds have become an important tool for studies on receptor binding analysis, enzyme assay, and quantitative and/or qualitative analytical techniques in animals or plants. The immunoblotting method is based on the western blotting technique that utilizes the antigen-antibody binding properties and provides a specific and sensitive detection of higher molecule analytes like peptides and proteins. In our ongoing study on MAb, previously we prepared various kinds of MAb against natural products like forskolin [1], solamargine [2], crocin [3], marihuana compounds [4], opium alkaloids [5], ginsenosides [6, 7], berberine [8], sennosides [9], paeoniflorin [10], glycyrrhizin [11, 12], ginkgolic acid [13], aconitine alkaloid [14], baicalin [15], and so on and developed individual competitive enzyme-linked immunosorbent assay (ELISA) as a highly sensitive, specific, and simple methodology.

The confirmation of hapten number in synthesized antigens is most important in the first stage of MAb preparation. Therefore, its determination method will be discussed first of all. As an application of MAb, the MAb against ginsenosides and glycyrrhizin has been prepared resulting in the development of two new techniques that we have named

the eastern blotting method [12] and the knockout extract preparation [16]. They will be introduced in this paper.

2. Preparation of MAb against Natural Products

Various methods have been employed for the determination of natural products. They include spectral methods such as infrared (IR), nuclear magnetic resonance (NMR), and circular dichroism (CD) and other chromatographic methods such as ion chromatography (IC), capillary electrophoresis (CE), and high-speed counter current chromatography (HSCCC), and so on. Compared to TLC, GLC and HPLC methods, the ELISA method was more sensitive and selective. Moreover, it is possible to study a large number of natural products. Since natural product extracts consist of various chemical constituents (e.g., licorice contains 470 components or more), in general, some pretreatment is necessary for HPLC and other chromatographic analysis methods. ELISA, however, can determine the concentration of components directly without any pretreatment. Therefore, ELISA was used to measure the concentration of ginsenoside Rb_1 in ginseng and traditional Chinese medicines (TCMs).

2.1. Analytical Method for Determination of Hapten Number in Antigen, Hapten-Carrier Protein Conjugate. For production of MAb, synthesis of hapten, which is derived from an immune antigen and linker bridge, and the carrier protein conjugate is necessary. There had been no direct and appropriate methods for the determination of haptens conjugated with carrier proteins without differential UV analysis, radiochemical, or chemical methods. Therefore, immunization by the injection of hapten-carrier protein conjugate was unreliable. Wengatz et al. [17] determined the hapten density of immunoconjugates by matrix-assisted UV laser desorption/ionization mass spectrometry. We also reported the direct analytical method of hapten and carrier protein conjugates by a matrix-assisted laser desorption/ionization mass spectrometry (MALDI) tof mass spectrometry using an internal standard [18–20].

Figure 1 shows the MALDI tof mass spectrum of the most pharmacologically active marihuana compound, tetrahydrocannabinolic acid (THCA)-bovine serum albumin (BSA) conjugate, and BSA used as an internal standard [20]. This shows only the singly, doubly, and triply ionized molecule ions of the intact conjugate. The sharp peak at m/z 66,465 is the $[M + H]^+$ peak of BSA. A small $[M + H]^+$ peak of the THCA-BSA conjugate is at m/z 70,792, indicating that the calculated molecular mass of the THCA-BSA conjugate is 70,581 using a calculated molecular mass of 66,267 for BSA. The calculated molecule mass of the THCA moiety is 4,314. From this result, 12.7 molecules of THCA are combined with BSA [20]. Since this method is suitable for small molecule natural products, we had been analyzing the hapten number of all natural products for MAbs including glycosides like ginsenosides and glycyrrhizin.

2.2. Preparation of MAb against Ginsenosides and ELISA as an Assay System. Ginseng, the crude drug of *Panax ginseng*, is one of the most important natural medicines in many countries. It has been used to enhance stamina and capacity to cope with fatigue and physical stress and as a tonic against cancers, disturbances of the central nervous system (memory, learning, and behavior), hypothermia, carbohydrate and lipid metabolism, immune function, the cardiovascular system, and radioprotection [21]. It contains more than 30 kinds of dammarane and oleanane saponins considered to be pharmacologically active components. Ginsenoside Rb_1 is the main saponin in ginseng. However, since the concentration in the ginseng root or the root extract varies depending on the method of extraction, subsequent treatment, or even the season of its collection [22], standardization of quality is required. For this purpose, we have prepared anti-ginsenoside Rb_1 [6] and Rg_1 MAbs [7]. The immunoassay system using MAb is not frequently used for naturally occurring smaller molecular weight bioactive compounds. Preparation of MAbs is difficult, but is one of the most important steps for the analysis of natural products. As a typical natural product, the preparation of MAb against the ginseng saponin ginsenoside Rb_1 will be discussed.

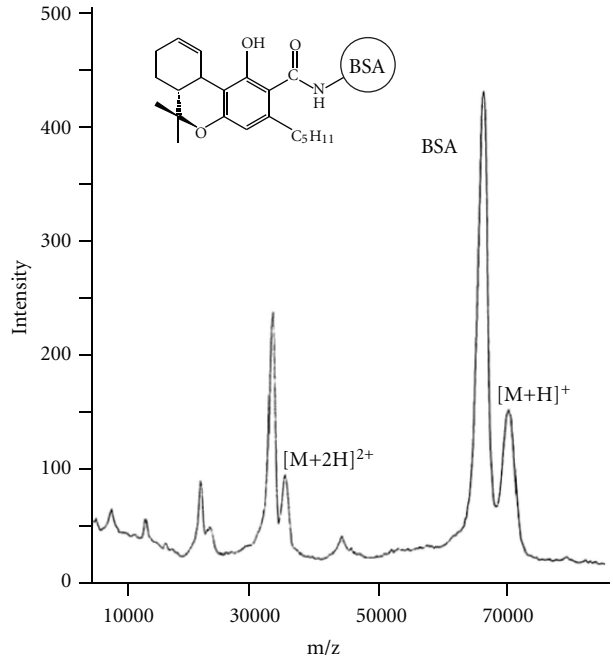

Figure 1: Matrix-assisted laser desorption/ionization tof mass spectrometry of tetrahydrocannabinolic-acid-BSA conjugate. [M + H] indicates the molecular weight of the conjugate, from which the hapten number can be calculated.

A hybridoma-producing MAb reactive to ginsenoside Rb_1 was obtained by the general procedure and classified into IgG2b which had κ light chains. The reactivity of IgG type MAb, 9G7 was tested by varying antibody concentration and by performing a dilution curve. The antibody concentration was selected for competitive ELISA. The free MAb following competition is bound to polystyrene microtiter plates precoated with ginsenoside Rb_1-HSA. Under these conditions, the full measurement range of the assay extends from 20 to 400 ng/mL [6].

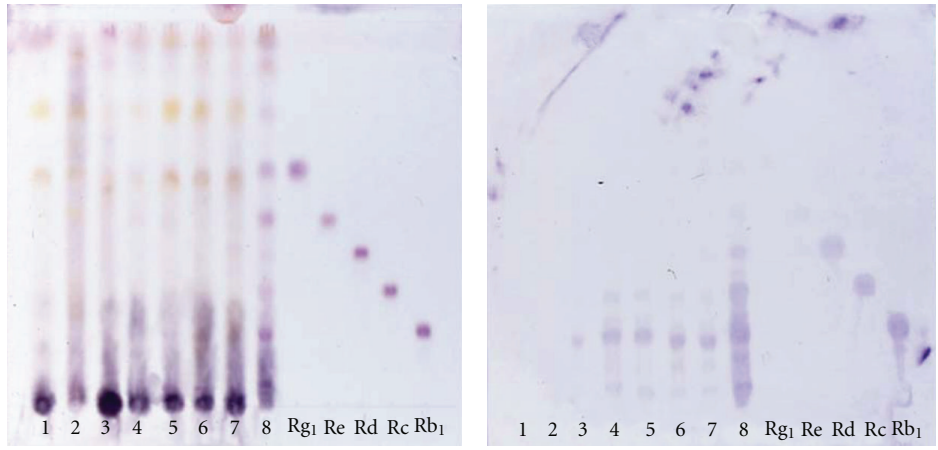

(a) TLC (b) Eastern blotting

Figure 2: Eastern blotting of ginsenosides in traditional Chinese medicine formulas using anti-ginsenoside Rb1 MAb. Samples (1) Jigengtang, (2) Dahuanggancaotang, (3) Nenshenyangyongtang, (4) Sijunzitang, (5) Nenshentang, (6) Buanxiaxiexintang, (7) Xiaocaihutang, and (8) Crude ginseng extract. Lanes 1 and 2 do not contain ginseng. Standard of ginsenosides indicated, ginsenosidr-Rg_1, -Re, -Rd, -Rc, and -Rb_1, respectively, from the upper spot.

Cross-reactivity is the most important factor in determining the value of an antibody. Since the ELISA for ginsenoside Rb_1 was established for phytochemical investigations involving crude plant extracts, the assay specificity was checked by determining the cross-reactivity of the MAb with various related compounds. The cross-reactivity data of MAb that was obtained were examined by competitive ELISA and calculated using picomole amounts of ginsenoside Rb_1. The cross-reactivity of ginsenoside Rc and Rd, which possess a diglucose moiety attached to the C-3 hydroxy group, was weak compared to ginsenoside Rb_1 (0.024 and 0.020%, resp.). Ginsenoside Re and Rg_1 showed no cross-reactivity (less than 0.005%). It is evident that the MAb reacted only with a small number of structurally related ginsenoside Rb_1 molecules, and very weakly, and did not react with other steroidal compounds like glycyrrhizin, digitoxin, tigogenin, tigonin, and solamargine.

In our ongoing studies on MAbs against ginseng saponins, anti-ginsenoside Rg_1 MAb [7] and Re [23] have been prepared and their ELISA was set up. Anti-ginsenoside Rg_1 MAb was also highly specific like anti-ginsenoside Rb_1. On the other hand, anti-ginsenoside Re MAb showed wide cross-reactivity. Therefore, the MAb can be used for the analysis for the total ginsenoside concentration.

2.3. Application of MAb in the Natural Products Field. Although western blotting is a common assay methodology for high-molecular-weight-substances, this method has not been employed for small molecules, as direct immunostaining of such compounds on a TLC plate is as yet unknown. Therefore, a new method for such small-molecular compounds is required. Moreover, if small molecules can be blotted to a membrane, fixing them also requires a new methodology. Previously, we succeeded in separating small-molecule compounds such as solasodine glycosides into a part of an epitope and fixing on the membrane [24], as follows.

2.3.1. New Staining Method for Ginsenosides, "Eastern Blotting". Figure 2 shows the H_2SO_4 staining and eastern blotting of ginsenoside standards and TCM using anti-ginsenoside Rb_1 MAb. It is impossible to determine the ginsenosides by TLC staining by H_2SO_4 as indicated in Figure 2(a). On the other hand, clear staining of ginsenoside Rb_1 occurred by eastern blotting, as indicated in Figure 2(b). Furthermore, it became evident that Jigengtang and Dahuanggancaotang prescriptions that did not contain ginseng, as indicated by the absence of a ginsenoside Rb_1band. The eastern blotting method was considerably more sensitive than that of H_2SO_4 staining. The H_2SO_4 staining detected all standard compounds. The eastern blotting indicated only limited staining of ginsenoside Rb_1, Rc, and Rd, whose cross-reactivities were under 0.02% as shown in Figure 2(b). We suggest that an aglycone, protopanaxadiol, and a part of the sugars may be of importance to the immunization and may function as an epitope for the structure of ginsenosides. In addition, it is suggested that the specific reactivity of sugar moieties in the ginsenoside molecule against anti-ginsenoside Rb_1 MAb may be modified by the $NaIO_4$ treatment of ginsenosides on the PVDF membrane, causing ginsenoside Rc and Rd to become detectable by eastern blotting.

Application of the eastern blotting method for the detection of glycyrrhizin in the serum samples was investigated. In general, it is difficult to detect glycyrrhizin in serum due to the large amount of impurities. The developed bands of impurities lapped over the band of glycyrrhizin, and we failed to find a proper developing solvent system that could separate glycyrrhizin and the impurities apart from each other clearly on the TLC plate. Figure 3 shows the detection of glycyrrhizin by the eastern blotting technique in the rat serum samples. Glycyrrhizin could not be identified on the TLC plate stained by H_2SO_4through many bands that were detected (Figure 3(a)). On the other hand, eastern blotting clearly shows the band of glycyrrhizin even after 1 h

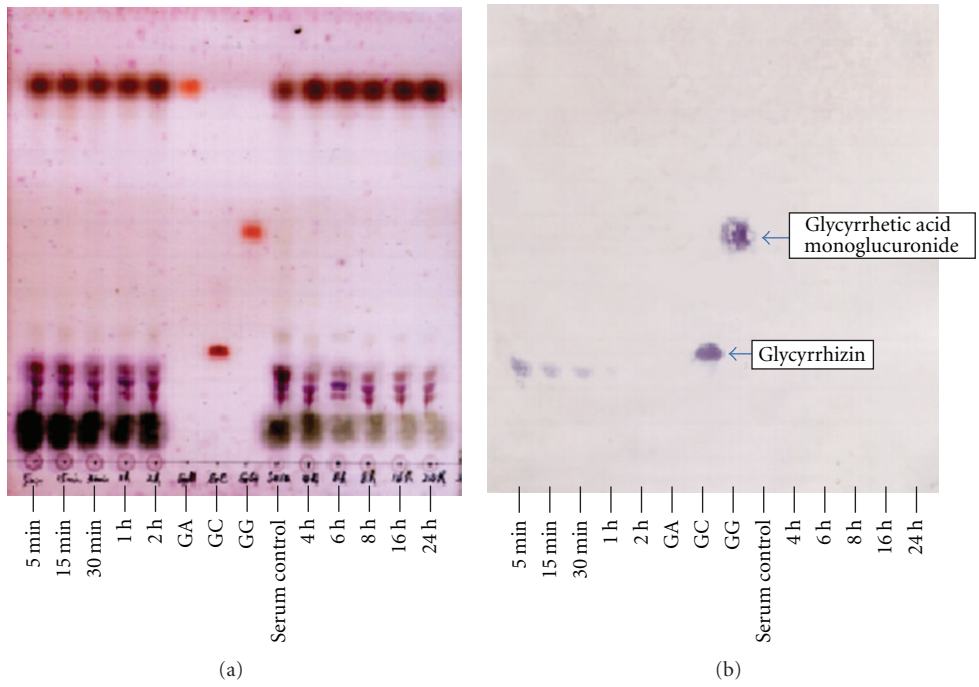

Figure 3: Eastern blotting profile of glycyrrhizin in rat serum after injection of glycyrrhizin (a) TLC of rat-serum-injected glycyrrhizin TLC was developed with *n*-BuOH-H_2O-AcOH (7 : 2 : 1). Spots were detected by 10% H_2SO_4. (b) Eastern blotting of rat-serum-injected glycyrrhizin; the band of glycyrrhizin was detected until 1 h after injection. GA: glycyhrrhetinic acid, GC: glycyrrhizin, and GG: glycyrrhetinic acid monoglucuronide.

(Figure 3(b)). Although the sensitivity of the eastern blotting method was greatly affected by the impurities, the detection limit was still at the nanogram level. The results proved that the eastern blotting technique could be a unique method for identifying glycyrrhizin against a background of a large amount of impurities.

When the mixture of anti-ginsenoside Rb_1 and Rg_1 MAbs and the pair of substrates were tested for staining for ginsenosides, all ginsenosides, ginsenoside Rb_1 , -Rc, -Rd, -Re, and -Rg_1 were stained blue although the purple color staining for ginsenoside Rg_1 was expected because 3-amino-9-ethylcarbazole and 4-chloro-1-naphotol might be different. Therefore, we performed successive staining of the membrane using anti-ginsenoside Rg_1 and then anti-ginsenoside Rb_1. Finally, we performed the double staining of ginsenosides indicating that ginsenoside Rg_1 and ginsenoside Re were stained purple and the other blue, as indicated in Figure 4. From this result, both antibodies can distinguish the individual aglycones, protopanaxatriol, and protopanaxadiol. For this application, the crude extract of various *Panax* species was analyzed by the newly developed double staining system. Major ginsenosides can be determined clearly by the double staining method, as indicated in Figure 4.

Therefore, it is suggested that the staining color shows the pharmacological activity. As shown in Figure 4(b), the purple bands indicate ginsenosides which have protopanaxatriol as an aglycone and stimulation activity for the central nervous system (CNS). On the other hand, the blue color indicates ginsenosides containing protopanaxadiol as an aglycone that possess a depression effect on the CNS. Moreover, the Rf value of ginsenosides roughly suggests the number of sugars attached to the aglycone. Both analyses make it possible to jointly identify which aglycone attaches and how many sugars it possesses, leading to the structure of the ginsenosides. In fact, three kinds of ginsenosides possessing protopanaxadiol-ginsenoside Rh_1, -Rf, and 20-*O*-glucoginsenoside Rf in *P. ginseng* root were determined by coloring and Rf value by comparing them with the structures reported in the previous paper [25].

Figure 5(a) indicates immunolocalization of glycyrrhizin in a licorice root slice using anti-glycyrrhizin MAb as another application of the eastern blotting method. The phloem (⟷) contained a higher concentration of glycyrrhizin than the xylem and cork part [26]. On the other hand, no staining occurred on ginseng (Figure 5(c)).

In the earlier experiments, we carried out the blotted staining on PVDF membrane using MAb on solasodine glycosides and called it western blotting [24]. Now we have applied this new methodology to licorice glycoside, glycyrrhizin and named it eastern blotting [12] for studying ginsenosides [23], saikosaponin [27], and so on.

2.3.2. Immunoaffinity Concentration and One-Step Purification of Ginsenoside Rb_1 by Immunoaffinity Column. A crude extract of *P. ginseng* roots was loaded onto the immunoaffinity column and washed with the washing solution of phosphate buffer. Figure 6 shows the fraction 1–8 containing

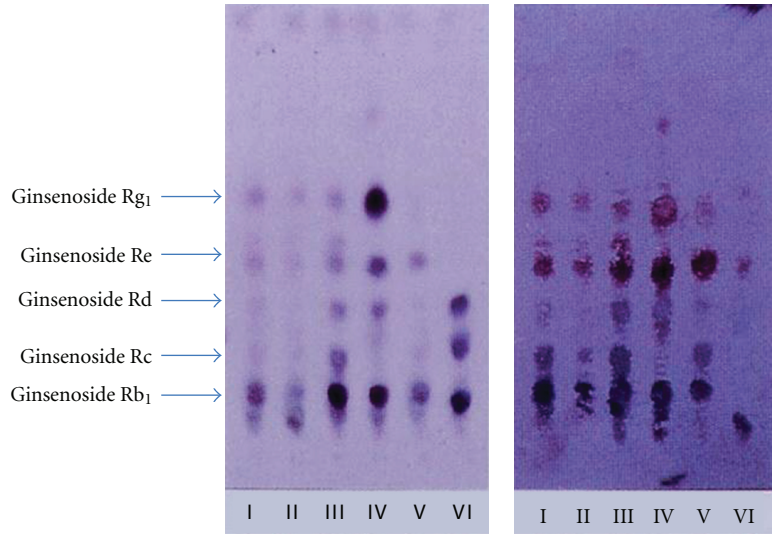

Figure 4: Double Eastern blotting staining of ginsenosides contained in various ginseng samples using anti-ginseenoside-Rb1 and anti-ginsenoside-Rg_1 MAbs. (a) TLC profile stained by sulfuric acid. (b) Eastern blotting by anti-ginsenoside-Rb_1 and anti-ginseside-Rg_1 monoclonal antibodies I, II, III, IV, V, and VI indicated white ginseng, red ginseng, fibrous ginseng (*P. ginseng*), *P. notoginseng*, *P. quinquefolius* and *P. japonicus*, respectively. Upper purple color spots and lower blue color spots were stained by anti-ginsenoside-Rg_1, and anti-ginsenoside-Rb_1 monoclonal antibodies, respectively.

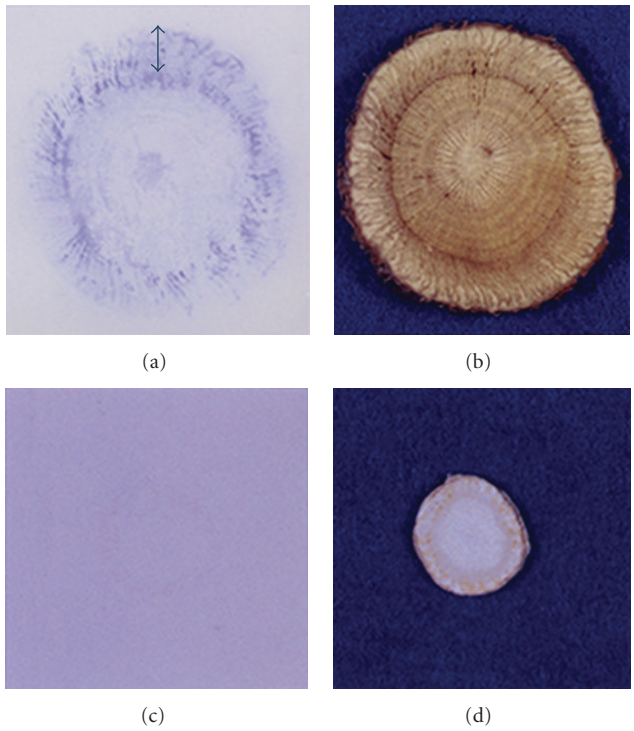

Figure 5: Immunocytolocalization of glycyrrhizin in fresh licorice root using anti-glycyrrhizin MAb. (a) Eastern blotting of fresh licorice slice, (b) fresh licorice slice, (c) Eastern blotting of fresh ginseng slice, and (d) fresh ginseng slice.

overloaded ginsenoside Rb_1. The other ginsenosides Rg_1, Rc, Re. and Rd were also detected in these fractions by eastern blotting (data not shown). A sharp peak appeared around fraction 20–24 eluted by acetate buffer containing KSCN and methanol to give pure ginsenoside Rb_1.

Overloaded ginsenoside Rb_1 was repeatedly immunoaffinity column choromatographed to separate ginsenoside Rb_1 completely [28]. The antibody was stable when exposed to the eluent, and the immunoaffinity column showed almost no decrease in capacity after repeated use more than 10 times under the same conditions, as was reported for a one-step separation of forskolin from a crude extract of *Coleus forskohlii* root [29]. This methodology is effective for the rapid and simple purification of ginsenoside Rb_1 and may open up a wide field of comparable studies with other families of saponins for which an acceptable method for one-step separation has not yet been developed. Furthermore, to separate the total ginseng saponins, a wide cross-reactive MAb against ginsenoside like anti-ginsenoside Re MAb could be designed, as was done for the total solasodine glycosides by an immunoaffinity column using an anti-solamargine MAb [30]. A combination of immunoaffinity column chromatography, Eastern blotting and ELISA could be used to survey low concentrations of ginsenoside Rb_1 of plant origin and/or in experimental animals and humans. In fact, we have succeeded in the isolation of ginsenoside Rb_1 from a different plant, *Kalopanax pictus* Nakai, which was not known previously to contain ginsenosides, using this combination of methods [31].

2.3.3. Newly Established Knockout Extract for Glycyrrhizin. Glycyrrhizin has been reported to possess numerous pharmacological effects like anti-inflammation [32], antiulcer [33], antitumor [34], antiallergy [35], and hepatoprotective

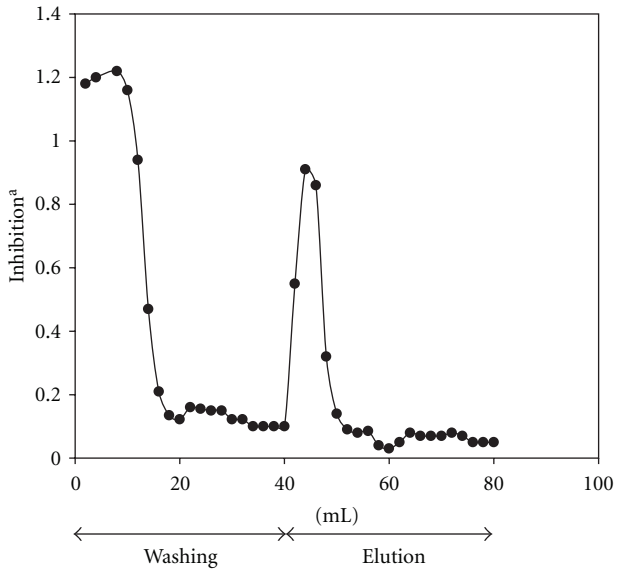

Figure 6: Elution profile of *Panax ginseng* crude extract on immunoaffinity column monitoring by ELISA using anti-ginsenoside-Rb_1 MAb. The column was washed by phosphate buffer and then eluted by HOAc buffer containing KSCN and MeOH. Individual fractions (2 mL) were assayed by ELISA using anti-ginsenoside-Rb_1 MAb.

activities [36]. Although glycyrrhizin is supposed to be a major active principle in licorice crude extract, a large number of studies have demonstrated that the licorice extract is rich in bioactive compounds other than glycyrrhizin such as triterpenes, flavonoids, and their aglycones [37]. In order to confirm the effect of glycyrrhizin in TCM, previously we purified glycyrrhizin from TCM using an immunoaffinity column conjugated with anti-glycyrrhizin MAb [38]. In this section, one-step purification of glycyrrhizin and its function in the licorice crude extract have been indicated as previously discussed about ginsenoside Rb_1.

To eliminate glycyrrhizin from licorice extract, 12 mg of licorice extract (glycyrrhizin content: 1275.0 μg) in loading buffer was applied on the anti-glycyrrhizin MAb immunoaffinity column, and then the loading buffer was continuously circulated through the column to enhance the binding efficiency. After overnight circulation at 4°C, the unbound column fraction was collected. The column was washed, and then bound column fraction was eluted by elution solvent. Glycyrrhizin concentration of bound column fraction was 1269.26 μg of glycyrrhizin (99.5% of the loading glycyrrhizin). On the other hand, glycyrrhizin content of unbound fraction was 3.50 μg (0.27% of the loading glycyrrhizin). These data indicated that anti-glycyrrhizin MAb immunoaffinity column could eliminate glycyrrhizin from licorice crude extract with high efficiency. From this evidence, we named this fraction knockout extract [16, 39].

To further characterize glycyrrhizin knockout extract, the TLC analysis and eastern blotting were performed. As shown in Figure 7(a), several spots including glycyrrhizin were detected in licorice extract. However, the spots of glycyrrhizin were undetected in glycyrrhizin-knockout extract, although all other spots were clearly detected (Figure 7(a), lane 2). eastern blotting by anti-glycyrrhizin MAb demonstrated that glycyrrhizin was detected in licorice extract, but the spot of glycyrrhizin was invisible in unbound fraction (Figure 7(b), lane 2). Therefore, these data suggest that glycyrrhizin was specifically eliminated from licorice extract by anti-glycyrrhizin MAb binding immunoaffinity column.

This technique is useful approach to clarify the multicomponent interaction with the specific protein such as enzymes, but it is unsuitable to investigate the interaction between one principal component and other components in herbal medicines. To investigate the role of one principal compound in the crude extract, we prepared knockout extract by removing target compound from the crude extract using high-specific MAb immunoaffinity column. By using this approach, it may become possible to determine the potential function of one natural compound on the crude extract or TCM by *in vitro* and *in vivo* assays.

Nitric oxide (NO) is free radical with multiple physiological functions, such as vasodilatation, neurotransmission, and inflammation [40]. During inflammatory process, large amount of NO is produced by inducible nitric oxide synthase (iNOS) by inflammatory cytokines and/or bacterial lipopolysaccharide (LPS) in various cell types including macrophages [41]. Overproduction of NO by iNOS triggers the pathogenesis of septic shock and organ destruction in certain inflammatory and autoimmune diseases [42–44]. Therefore, the inhibition of NO production by blocking iNOS expression may be useful strategy for the treatment of various inflammatory diseases.

To determine whether licorice crude extract inhibits NO production in LPS-stimulated mouse RAW264 macrophages, cells were treated with various concentrations of licorice extract for 30 min and then stimulated with LPS. LPS caused a dramatic increase in NO production, and this induction was inhibited in a dose-dependent manner by treatment with licorice extract.

We next investigated the inhibitory effect of glycyrrhizin-knockout extract and the combined treatment with glycyrrhizin-knockout extract and glycyrrhizin on NO production. Since 100 μg/mL of licorice extract contains 10.6 μg of glycyrrhizin, the cells were pretreated with licorice extract (100 μg/mL), glycyrrhizin-knockout extract (89.4 μg/mL), or combination of glycyrrhizin-knockout extract (89.4 μg/mL) and glycyrrhizin (10.6 μg/mL). Figure 8(a) indicated that treatment of licorice extract leads to a marked suppression of NO production as compared to LPS treatment [inhibition ratio (IR) = 57.7%]. Interestingly, although glycyrrhizin alone could not block NO production, the inhibitory effect of glycyrrhizin-knockout extract was decreased compared with licorice extract (IR = 17.8%). Moreover, the combined treatment with glycyrrhizin-knockout extract and glycyrrhizin significantly improved the inhibition of NO production (IR = 33.5%). To determine whether the combinational effect of glycyrrhizin-knockout extract and glycyrrhizin was related to iNOS expression, we performed western blotting (Figure 8(b)). Although the licorice extract strongly

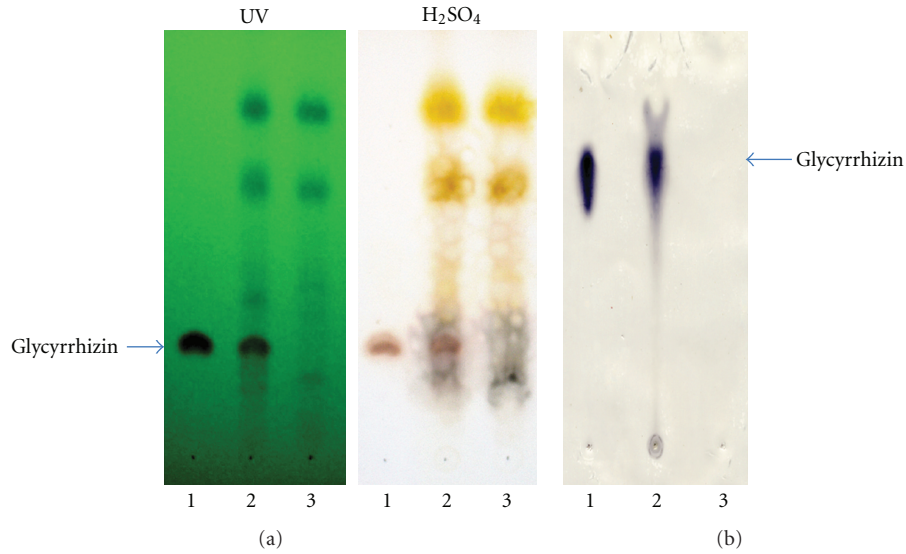

Figure 7: Preparation of knock-out extract eliminated glycyrrhizin from licorice crude extract using immunoaffinity column conjugated with anti-glycyrrhizin MAb. Lines 1, 2, and 3 indicate glycyrrhizin, crude extract, and knock-out extract, respectively.

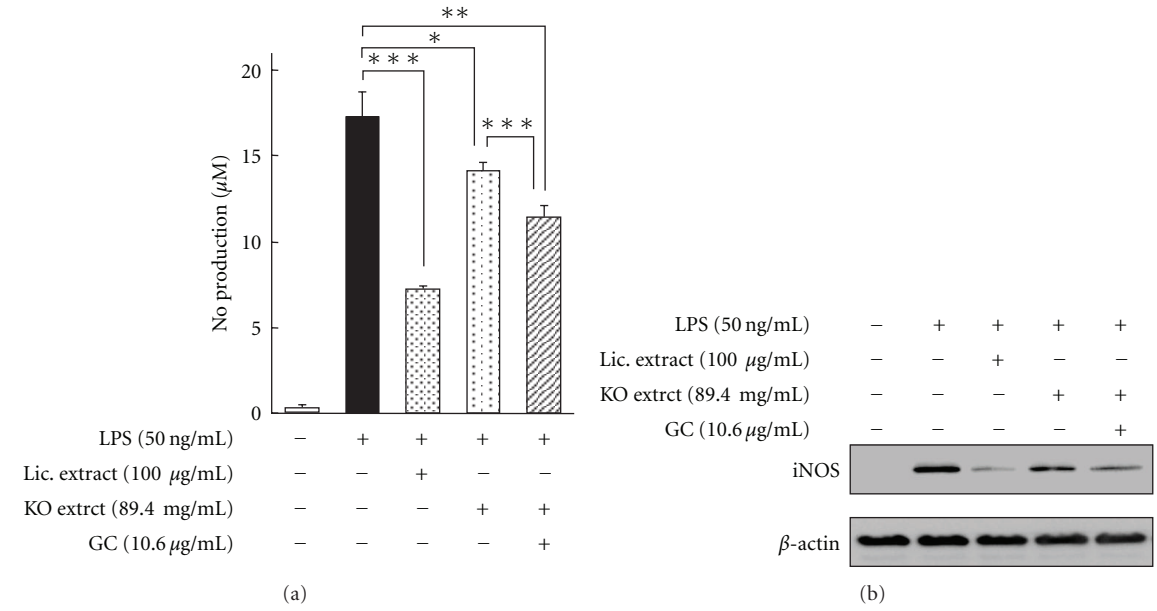

Figure 8: Effects of glycyrrhizin-knockout extract and the combination of glycyrrhizin-knockout extract and glycyrrhizin on LPS-induced NO production (a) and iNOS protein expression (b). $^{*}P < 0.05$, $^{**}P < 0.01$, $^{***}P < 0.001$.

suppressed LPS-induced iNOS expression, treatment of glycyrrhizin-knockout extract reduced this effect [45].

3. Conclusions

Two unique applications using MAb, eastern blotting and knockout extract have been introduced in this paper. The eastern blotting method has great potential applications for the wide range of natural products, especially glycosides like ginsenosides of ginseng and glycyrrhizin in licorice. When two kinds of MAbs, against ginsenoside Rb_1 and Rg_1 can be used, the double staining that enhanced the separate staining of ginsenosides having protopanaxatriol or protopanaxadiol in a molecule, occurred. The staining color can be used to monitor the pharmacological activity suggesting that the purple spots contain protopanaxatriol as an aglycone indicating central nervous system (CNS) stimulatory activity [46]. On the other hand, the blue color indicates ginsenosides having protopanaxadiol which possess a depression effect on the CNS [37]. Furthermore, the Rf value of ginsenosides

suggests the number of sugars attached to the aglycone. Both evidences make it possible to confirm which aglycone is attached and how many sugars are combined with the aglycone.

We demonstrated that knockout extract prepared by anti-natural compound-specific MAb immunoaffinity column is a useful approach for determination of potential function of natural compound on *in vitro* and *in vivo* assays. The pharmacological analysis by knockout extract might be directly applicable to both other crude extracts and various TCMs to clarify the real pharmacologically active components.

A ginsenoside Rb_1 knockout extract can be prepared using an immunoaffinity column conjugated with anti-ginsenoside Rb_1 MAb. In this extract, all compounds except only ginsenoside Rb_1 are contained. Furthermore, glycyrrhizin-knockout extract prepared from licorice crude extract using an immunoaffinity column conjugated with anti-glycyrrhizin MAb. These knockout extracts may be able to support the pharmacological investigation for finding out a really active component in a crude drug and/or TCM. In fact, addition of glycyrrhizin to glycyrrhizin-knockout extract could improve the inhibition of iNOS expression resulting that glycyrrhizin may exert combinational inhibition of iNOS expression when coexisting with the other constituents contained in licorice extract.

References

[1] R. Sakata, Y. Shoyama, and H. Murakami, "Production of monoclonal antibodies and enzyme immunoassay for typical adenylate cyclase activator, forskolin," *Cytotechnology*, vol. 16, no. 2, pp. 101–108, 1994.

[2] M. Ishiyama, Y. Shoyama, H. Murakami, and H. Shinohara, "Production of monoclonal antibodies and development of an ELISA for solamargine," *Cytotechnology*, vol. 18, no. 3, pp. 153–158, 1996.

[3] L. Xuan, H. Tanaka, Y. Xu, and Y. Shoyama, "Preparation of monoclonal antibody against crocin and its characterization," *Cytotechnology*, vol. 29, no. 1, pp. 65–70, 1999.

[4] H. Tanaka, Y. Goto, and Y. Shoyama, "Monoclonal antibody based enzyme immunoassay for marihuana (cannabinoid) compounds," *Journal of Immunoassay*, vol. 17, no. 4, pp. 321–342, 1996.

[5] Y. Shoyama, T. Fukada, and H. Murakami, "Production of monoclonal antibodies and ELISA for thebaine and codeine," *Cytotechnology*, vol. 19, no. 1, pp. 55–61, 1995.

[6] H. Tanaka, N. Fukuda, and Y. Shoyama, "Formation of monoclonal antibody against a major ginseng component, ginsenoside Rb1 and its characterization," *Cytotechnology*, vol. 29, no. 2, pp. 115–120, 1999.

[7] N. Fukuda, H. Tanaka, and Y. Shoyama, "Formation of monoclonal antibody against a major ginseng component, ginsenoside Rg1 and its characterization: monoclonal antibody for a ginseng saponin," *Cytotechnology*, vol. 34, no. 3, pp. 197–204, 2000.

[8] J. S. Kim, H. Tanaka, and Y. Shoyama, "Immunoquantitative analysis for berberine and its related compounds using monoclonal antibodies in herbal medicines," *Analyst*, vol. 129, no. 1, pp. 87–91, 2004.

[9] O. Morinaga, S. Nakajima, H. Tanaka, and Y. Shoyama, "Production of monoclonal antibodies against a major purgative component, sennoside B, their characterization and use in ELISA," *Analyst*, vol. 126, no. 8, pp. 1372–1376, 2001.

[10] Z. Lu, O. Morinaga, H. Tanaka, and Y. Shoyama, "A quantitative ELISA using monoclonal antibody to survey paeoniflorin and albiflorin in crude drugs and traditional Chinese herbal medicines," *Biological and Pharmaceutical Bulletin*, vol. 26, no. 6, pp. 862–866, 2003.

[11] H. Tanaka and Y. Shoyama, "Formation of a monoclonal antibody against glycyrrhizin and development of an ELISA," *Biological and Pharmaceutical Bulletin*, vol. 21, no. 12, pp. 1391–1393, 1998.

[12] S. Shan, H. Tanaka, and Y. Shoyama, "Enzyme-linked immunosorbent assay for glycyrrhizin using anti-glycyrrhizin monoclonal antibody and an eastern blotting technique for glucuronides of glycyrrhetic acid," *Analytical Chemistry*, vol. 73, no. 24, pp. 5784–5790, 2001.

[13] P. Loungratana, H. Tanaka, and Y. Shoyama, "Production of monoclonal antibody against ginkgolic acids in Ginkgo biloba Linn," *American Journal of Chinese Medicine*, vol. 32, no. 1, pp. 33–48, 2004.

[14] K. Katsumi, K. Edakuni, O. Morinaga, H. Tanaka, and Y. Shoyama, "An enzyme-linked immunosorbent assay for aconitine-type alkaloids using an anti-aconitine monoclonal antibody," *Analytica Chimica Acta*, vol. 616, no. 1, pp. 109–114, 2008.

[15] K. Kido, O. Morinaga, Y. Shoyama, and H. Tanaka, "Quick analysis of baicalin in Scutellariae Radix by enzyme-linked immunosorbent assay using a monoclonal antibody," *Talanta*, vol. 77, no. 1, pp. 346–350, 2008.

[16] H. Tanaka, N. Fukuda, and Y. Shoyama, "Eastern blotting and immunoaffinity concentration using monoclonal antibody for ginseng saponins in the field of traditional Chinese medicines," *Journal of Agricultural and Food Chemistry*, vol. 55, no. 10, pp. 3783–3787, 2007.

[17] I. Wengatz, R.-D. Schmid, S. Kreissig et al., "Determination of the hapten density of immuno-conjugates by matrix-assisted UV laser desorption/ionization mass spectrometry," *Analytical Letters*, vol. 25, pp. 1983–1997, 1992.

[18] Y. Shoyama, T. Fukada, T. Tanaka, A. Kusai, and K. Nojima, "Direct determination of opium alkaloid-bovine serum albumin conjugate by matrix-assisted laser desorption/ionization mass spectrometry," *Biological and Pharmaceutical Bulletin*, vol. 16, no. 10, pp. 1051–1053, 1993.

[19] Y. Shoyama, R. Sakata, R. Isobe, H. Murakami, A. Kusai, and K. Nojima, "Direct determination of forskolin-bovine serum albumin conjugate by matrx-assisted laser desorption ionization mass spectrometry," *Organic Mass Spectrometry*, vol. 28, pp. 987–988, 1993.

[20] Y. Goto, Y. Shima, S. Morimoto et al., "Determination of tetrahydrocannabinolic acid-carrier protein conjugate by matrix-assisted laster desorption/Ionization mass spectrometry and antibody formation," *Organic Mass Spectrometry*, vol. 29, pp. 668–671, 1994.

[21] The Society for Korean Ginseng, In *Understanding of Korean Ginseng*, The Society for Korean Ginseng, Seoul, Korea, 1995.

[22] I. Kitagawa, T. Taniyama, M. Yoshikawa, Y. Ikenishi, and Y. Nakagawa, "Chemical studies on crude drug processing. VI. (1)) Chemical structures of malonyl-Ginsenosides Rb1, Rb2, Rc, and Rd isolated from the root of Panax ginseng C.A. Meyer," *Chemical and Pharmaceutical Bulletin*, vol. 37, no. 11, pp. 2961–2970, 1989.

[23] O. Morinaga, H. Tanaka, and Y. Shoyama, "Detection and quantification of ginsenoside Re in ginseng samples by a chromatographic immunostaining method using monoclonal antibody against ginsenoside Re," *Journal of Chromatography B*, vol. 830, no. 1, pp. 100–104, 2006.

[24] H. Tanaka, W. Putalun, C. Tsuzaki, and Y. Shoyama, "A simple determination of steroidal alkaloid glycosides by thin-layer chromatography immunostaining using monoclonal antibody against solamargine," *FEBS Letters*, vol. 404, no. 2-3, pp. 279–282, 1997.

[25] N. Fukuda, S. Shan, H. Tanaka, and Y. Shoyama, "New staining methodology: eastern blotting for glycosides in the field of Kampo medicines," *Journal of Natural Medicines*, vol. 60, no. 1, pp. 21–27, 2006.

[26] S. Yokota, Y. Onohara, and Y. Shoyama, "Immunofluorescence and immunoelectron microscopic localization of medicinal substance, Rb1, in several plant parts of Panax ginseng," *Current Drug Discovery Technologies*, vol. 8, no. 1, pp. 51–59, 2011.

[27] O. Morinaga, S. Zhu, H. Tanaka, and Y. Shoyama, "Visual detection of saikosaponins by on-membrane immunoassay and estimation of traditional Chinese medicines containing Bupleuri radix," *Biochemical and Biophysical Research Communications*, vol. 346, no. 3, pp. 687–692, 2006.

[28] N. Fukuda, H. Tanaka, and Y. Shoyama, "Isolation of the pharmacologically active saponin ginsenoside Rb1 from ginseng by immunoaffinity column chromatography," *Journal of Natural Products*, vol. 63, no. 2, pp. 283–285, 2000.

[29] H. Yanagihara, R. Sakata, H. Minami, H. Tanaka, Y. Shoyama, and H. Murakami, "Immunoaffinity column chromatography against forskolin using an anti-forskolin monoclonal antibody and its application," *Analytica Chimica Acta*, vol. 335, no. 1-2, pp. 63–70, 1996.

[30] W. Putalun, H. Tanaka, and Y. Shoyama, "Rapid separation of solasodine glycosides by an immunoaffinity column using anti-solamargine monoclonal antibody," *Cytotechnology*, vol. 31, no. 1-2, pp. 151–156, 1999.

[31] H. Tanaka, N. Fukuda, S. Yahara, S. Isoda, C. S. Yuan, and Y. Shoyama, "Isolation of ginsenoside Rb1 from Kalopanax pictus by eastern blotting using anti-ginsenoside Rb1 monoclonal antibody," *Phytotherapy Research*, vol. 19, no. 3, pp. 255–258, 2005.

[32] S. Amagaya, E. Sugishita, and Y. Ogihara, "Comparative studies of the stereoisomers of glycyrrhetinic acid on anti-inflammatory activities," *Journal of Pharmacobio-Dynamics*, vol. 7, no. 12, pp. 923–928, 1984.

[33] R. Doll and I.-D. Hill, "Triterpenoid liquorice compound in gastric and duodenal ulcer," *The Lancet*, vol. 280, no. 7266, pp. 1166–1167, 1962.

[34] Z. Y. Wang and D. W. Nixon, "Licorice and cancer," *Nutrition and Cancer*, vol. 39, no. 1, pp. 1–11, 2001.

[35] T. Kuroyanagi and M. Saito, "Effect of prednisolone and glycyrrhizin on passive transfer in experimental allergic encephalomyelitis," *Japanese Journal of Allergology*, vol. 15, no. 2, pp. 67–74, 1966.

[36] T. Nakamura, T. Fujii, and A. Ichihara, "Enzyme leakage due to change of membrane permeability of primary cultured rat hepatocytes treated with various hepatotoxins and its prevention by glycyrrhizin," *Cell Biology and Toxicology*, vol. 1, no. 4, pp. 285–295, 1985.

[37] M. N. Asl and H. Hosseinzadeh, "Review of pharmacological effects of glycyrrhiza sp. and its bioactive compounds," *Phytotherapy Research*, vol. 22, no. 6, pp. 709–724, 2008.

[38] J. Xu, H. Tanaka, and Y. Shoyama, "One-step immunochromatographic separation and ELISA quantification of glycyrrhizin from traditional Chinese medicines," *Journal of Chromatography B*, vol. 850, no. 1-2, pp. 53–58, 2007.

[39] C.-Z. Wang and Y. Shoyama, "Herbal medicine: identification, and evaluation strategies," in *Text Book of Complementary and Alternative Medicine*, C.-S. Yuan, E.-J. Bieber, and B.-A. Bauer, Eds., pp. 51–70, Informa Healthcare, Minnesota, Minn, USA, 2nd edition, 2006.

[40] S. Moncada, R. M. J. Palmer, and E. A. Higgs, "Nitric oxide: physiology, pathophysiology, and pharmacology," *Pharmacological Reviews*, vol. 43, no. 2, pp. 109–142, 1991.

[41] C. Nathan and Q. W. Xie, "Regulation of biosynthesis of nitric oxide," *Journal of Biological Chemistry*, vol. 269, no. 19, pp. 13725–13728, 1994.

[42] K. M. Naseem, "The role of nitric oxide in cardiovascular diseases," *Molecular Aspects of Medicine*, vol. 26, no. 1-2, pp. 33–65, 2005.

[43] T. J. Guzik, R. Korbut, and T. Adamek-Guzik, "Nitric oxide and superoxide in inflammation and immune regulation," *Journal of Physiology and Pharmacology*, vol. 54, no. 4, pp. 469–487, 2003.

[44] S. B. Abramson, A. R. Amin, R. M. Clancy, and M. Attur, "The role of nitric oxide in tissue destruction," *Best Practice and Research: Clinical Rheumatology*, vol. 15, no. 5, pp. 831–845, 2001.

[45] T. Uto, O. Morinaga, H. Tanaka, and Y. Shoyama, "Analysis of the synergistic effect of glycyrrhizin and other constituents in licorice extract on lipopolysaccharide-induced nitric oxide production using knock-out extract," *Biochemical and Biophysical Research Communications*, vol. 417, no. 1, pp. 473–478, 2012.

[46] K. Hashimoto, K. Satoh, P. Murata et al., "Components of *Panax* ginseng that improve accelerated small intestinal transit," *Journal of Ethnopharmacology*, vol. 84, no. 1, pp. 115–119, 2003.

Hindawi Publishing Corporation
International Journal of Analytical Chemistry
Volume 2012, Article ID 407274, 8 pages
doi:10.1155/2012/407274

Research Article

Concentration of Inorganic Elements Content in Benthic Seaweeds of Fernando de Noronha Archipelago by Synchrotron Radiation Total Reflection X-Ray Fluorescence Analysis (SRTXRF)

Leandro De Santis Ferreira,[1] Rosana Peporine Lopes,[2] Mabel Norma Costas Ulbrich,[2] Thais Guaratini,[3] Pio Colepicolo,[4] Norberto Peporine Lopes,[1] Ricardo Clapis Garla,[5] Eurico Cabral Oliveira Filho,[6] Adrian Martin Pohlit,[7] and Orghêda Luiza Araújo Domingues Zucchi[1]

[1] *Departamento de Física e Química, Faculdade de Ciências Farmacêuticas de Ribeirão Preto, Universidade de São Paulo, 14040-903 Ribeirão Preto, SP, Brazil*
[2] *Instituto de Geociências, Universidade de São Paulo, 05508-080 São Paulo, SP, Brazil*
[3] *Lychnoflora Pesquisa e Desenvolvimento em Produtos Naturais LTDA, Incubadora SUPERA, Campus da USP, 14040-900 Ribeirão Preto, SP, Brazil*
[4] *Instituto de Química, Universidade de São Paulo, 05513-970 São Paulo, SP, Brazil*
[5] *Departamento de Botânica, Ecologia e Zoologia, Centro de Biociências, Universidade Federal do Rio Grande do Norte, 59072-970 Natal, RN, Brazil*
[6] *Instituto de Biociências, Universidade de São Paulo, 05508-090 São Paulo, SP, Brazil*
[7] *Coordenação de Pesquisa em Produtos Naturais, Instituto Nacional de Pesquisa da Amazônia, 69060-001 Manaus, AM, Brazil*

Correspondence should be addressed to Leandro De Santis Ferreira, leansf@fcfrp.usp.br

Received 31 August 2011; Accepted 13 October 2011

Academic Editor: Ricardo Vessecchi

SRTXRF was used to determine As, Ba, Br, Ca, Co, Cr, Cs, Cu, Dy, Fe, K, Mn, Mo, Ni, Pb, Rb, Sr, Ti, V, and Zn in eleven seaweed species commonly found in Fernando de Noronha: *Caulerpa verticillata* (J. Agardh) (Chlorophyta), *Asparagopsis taxiformis* (Delile), *Dictyurus occidentalis* (J. Agardh), *Galaxaura rugosa* (J. Ellis & Solander) J. V. Lamouroux, *G. obtusata* (J. Ellis & Solander) J. V. Lamouroux, *G. marginata* (J. Ellis & Solander) J. V. Lamouroux (Rhodophyta), *Dictyota cervicornis* (Kützing), *Dictyopteris justii* (J. V. Lamouroux), *Dictyopteris plagiogramma* (Montagne) Vickers, *Padina gymnospora* (Kützing) Sonder, and a *Sargassum* sp. (Phaeophyta). Data obtained were compared to those from the analysis of other parts of the world seaweeds using different analytical techniques and were found to be in general agreement in terms of major and minor elemental components. Results provide baseline information about the absorption and accumulation of these elements by macroalgae in the area.

1. Introduction

In the South Atlantic Ocean is located Fernando de Noronha archipelago around 540 km of the northeastern Brazilian coast. This archipelago is composed by one large island and 20 small adjacent islets that represent a mountain chain top developed along an east-west fracture zone of the ocean floor and was built up by volcanic and subvolcanic essentially alkaline and subsaturated rocks [1].

The marine flora of Fernando de Noronha was first studied by Dickie [2]. Most of the investigations carried out since then were taxonomic studies [3–5]. Also, the families Dictyotaceae and Sargassaceae of brown algae, the green algae *Caulerpa verticillata*, and the red algae *Galaxaura* spp. are among the most abundant macroalgae on the rocky and reef shores of the archipelago [5, 6]. Their predominance is probably related to the production of secondary metabolites that inhibit herbivore predation [7].

Seaweeds require various mineral ions for photosynthesis and growth. Also, it has long been established that marine and estuarine macroalgae accumulate metals to levels many times those found in the surrounding waters [7], and several algae have been used for monitoring concentrations of elements [8–12]. This study provides baseline information for further investigations of the absorption and accumulation of 20 elements by eleven macroalgae species commonly found in Fernando de Noronha archipelago. The concentrations of the elements in the seaweeds were determined using Synchrotron Radiation Total Reflection X-Ray Fluorescence Analysis (SRTXRF).

2. Experimental

2.1. Chemicals Reagents and Solutions. All the reagents were purchased from Merck (Darmstadt, HE, Germany) and Synth (Diadema, SP, Brazil). The multielementary solution was prepared using monoelementary solutions purchased from Acros Organics (Geel, ANT, Belgium and New Jersey, NJ, USA), and ultrapure (deionized) water was obtained using a deionizer from Microtec (Ribeirão Preto, SP, Brazil).

2.2. Sampling. Eleven species of seaweeds commonly found in Fernando de Noronha archipelago were studied: *Caulerpa verticillata* (Chlorophyta), *Asparagopsis taxiformis*, *Dictyurus occidentalis*, *Galaxaura rugosa*, *G. obtusata*, *G. marginata* (Rhodophyta), *Dictyota cervicornis*, *Dictyopteris justii*, *Dictyopteris plagiogramma*, *Padina gymnospora,* and a *Sargassum* sp. (Phaeophyta) Samples were collected in February and March, 2006 at Caieiras Beach (3°50′18.8″S, 32°23′57.3″W) and Sueste Bay (3°52′1.2″S, 32°25′19.7″W) which are on the main island (Figure 1; Table 1). The IBAMA authorization to collect algae was registered with the number 050/2006. Seaweed specimens were collected randomly, that is, some individuals in a population were collect without a rule or defined sequence. Whole plants were uprooted and placed in labeled plastic bags. Seaweed samples were frozen and sent to the laboratory where they arrived 48 h after harvesting. The algae were identified by Prof. Dr. Eurico Cabral de Oliveira Filho. Residual sediment, epiphytes, and animals were removed, and the algae were washed with distilled water to remove seawater and air dried in a circulating air oven at 40°C for 48 h. After drying, around 5 g of each seaweed species was powdered by a triturating process in a grail after freezing the samples with liquid nitrogen. The powdered seaweeds were kept in a freezer until analysis was performed.

2.3. Sample and Calibration Solution Preparation. Samples of 250 mg of each algae species were placed in pyrex test tubes and digested according to a procedure described by Ward et al. [13] . Briefly, 6.0 mL of nitric acid (65%) and hydrogen peroxide (30%) were added to each test tube and homogenized. Test tubes were then placed on a digestion block overnight (*ca.* 12 hours) and heated at 130 ± 5°C until a translucid, particle-free, and fully digested solution was obtained. 5.00 mL of ultrapure water were transferred to the digested (sample) solution using a pyrex volumetric pipette, and the resulting solution was homogenized. The blank was a mixture of nitric acid, hydrogen peroxide, and deionized water and was done using the same procedure performed to the samples. Then 1.00 mL of this solution was removed using a pyrex volumetric pipette and to this aliquot was added 10 μL of Ga (1.0 μL mL^{-1}) as an internal standard [14]. Calibration solutions of multielements that emit X-K and X-L rays were prepared, and Ga element was added as internal standard as above. 5.0 μL of each sample were placed on a perspex support (polished quartz, 28 × 22 mm). The same procedure was done for 5.0 μL of calibration solution. Drying for 1 h under, a 150 W infrared lamp (Phillips model 7, Amsterdam, NH, Netherlands) gave rise to a thin layer of approximately 5 mm diameter. Sample and calibration solutions were irradiated as described below.

Table 1: Classification and sampling for eleven macroalgae studied in Fernando de Noronha archipelago, of northeastern Brazil.

Divisions and species	Site
Chlorophyta	
Caulerpa verticillata (J. Agardh, 1847)	S
Rhodophyta	
Asparagopsis taxiformis (Delile) Trevisan de Saint-Léon, 1845	S
Dictyurus occidentalis (J. Agardh, 1847)	C
Galaxaura rugosa (J. Ellis & Solander) J. V. Lamouroux, 1816	C
Galaxaura obtusata (J. Ellis & Solander) J. V. Lamouroux, 1816	C
Galaxaura marginata (J. Ellis & Solander) J. V. Lamouroux, 1816	C
Phaeophyta	
Dictyota cervicornis (Kützing, 1859)	S
Dictyopteris justii (J. V. Lamouroux, 1809)	S
Dictyopteris plagiogramma (Montagne) Vickers, 1905	C
Padina gymnospora (Kützing) Sonder, 1871	C
Sargassum sp. (C. Agardh, 1820)	S

S: Sueste; C: Caieiras.

2.4. Instrumentation and Analysis Conditions. The equipment used was an X-ray fluorescence beamline constructed at the National Synchrotron Light Laboratory—LNLS (Campinas, São Paulo State, Brazil). For the total reflection of radiation, a series of mirrors are adjusted to allow that the synchrotron radiation hit the sample in small angle. The sample and calibration solutions were analyzed (three replicates of each) for 100 s each with a white synchrotron radiation beam using 0.5 mm of Al as absorber, 1.0 mm of Ta as collimator in the detector, a sample-to-detector distance of 1.1 mm, a height of 1 mm under total reflection conditions, and an angle of incidence of 1 mrad. The characteristic X-rays were detected with the aid of a Ge hyperpure semiconductor detector (resolution of 145 eV for energy of 5.9 keV).

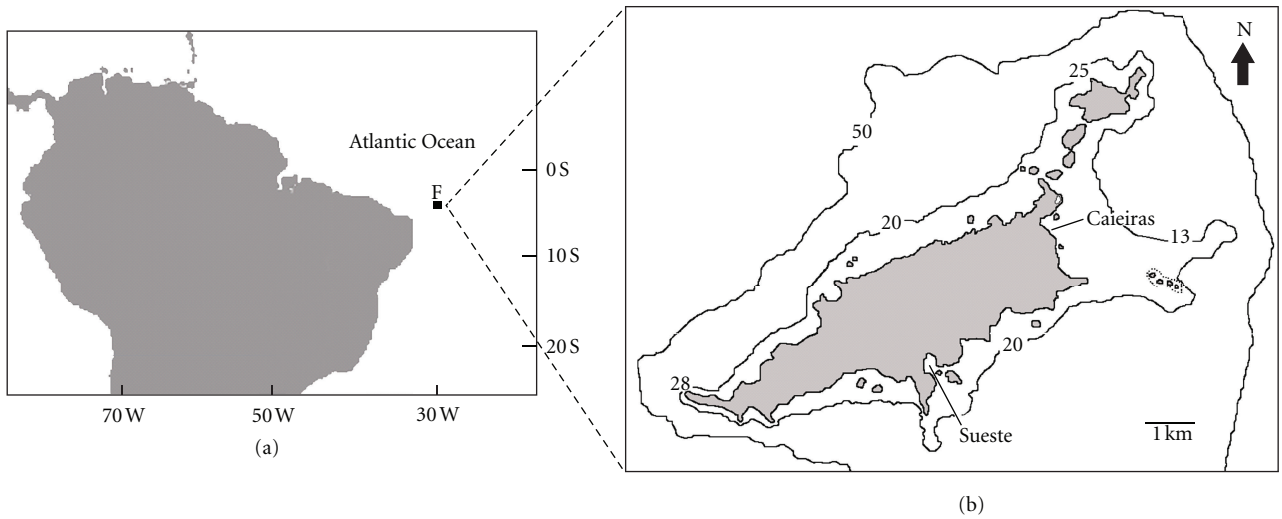

Figure 1: Geographical localization of study sites (Caieiras and Sueste) at the main island of Fernando de Noronha archipelago, off northeastern Brazil, where seaweeds were collected.

2.5. Quantitative Analysis for X-Ray Fluorescence. Energy peaks detected in specters of the calibration samples were determined on the spectrometer, and the energy-emitting elements were identified from their X-ray characteristics (analytical lines). The liquid intensities for characteristic X-rays emitted were calculated with a mathematic adjustment in which the contribution of interfering lines on the analytical line (spectral interference) was considered including the escape peak and the addition peak. Mathematical adjustments were calculated with the software AXIL [15].

In quantitative analysis, the fluorescent intensity of the characteristic line is related to the concentration by the expression $I_i = S_i \times C_i \times A_i$, where I_i = fluorescent intensity of element i (cps), S_i = elemental sensitivity of element i (cps μg^{-1} mL), C_i = concentration of element i ($\mu g\,mL^{-1}$), and A = absorption factor.

Given the tiny thickness of the prepared samples, the absorption and/or intensification effects (matrix effect) of the analytical line are negligible. Thus, there is no need to consider the absorption factor [16], and the relation is $I_i = S_i \times C_i$.

To correct like geometry and X-ray flow variation errors during excitation, Ga was used as internal standard. Ga is not present in the macroalgae samples. Referencing to internal standard yields the expression $(I_i/I_{Ga}) = (S_i/S_{Ga}) \times (C_i/C_{Ga})$, where I_{Ga} = fluorescent intensity of Ga (cps), S_{Ga} = elemental sensitivity of Ga (cps μg^{-1} mL), and C_{Ga} = concentration of Ga ($\mu g\,mL^{-1}$).

If we define $S_i' = S_i/S_{Ga}$ and $R_i = C_{Ga} \times (I_i/I_{Ga})$, where S_i' = relative sensitivity for element i (unidimensional) and R_i = product of relative intensity and C_{Ga} ($\mu g\,mL^{-1}$), then

$$R_i = S_i' \times C_i. \quad (1)$$

In the calibration solutions, R_i is directly proportional to C_i; therefore, the angular coefficient of the calibration curve for the element i is its relative sensitivity. If S_i' is known for the elements present in the calibration solutions, then the following function is obtained:

$$\ln S_i' = a + bZ_i + cZ_i^2 + dZ_i^3, \quad (2)$$

where a, b, c, and d are parameters that can be determinated by variance analyses, and Z_i is the atomic number for element i.

The relative sensitivity for any X-K or X-L ray emitting elements present in the samples can thus be calculated. The SANEST program was used to test significance of the parameters at 5% probability for inclusion in the model which was used to determine the above (2) [17]. The concentrations ($\mu g\,mL^{-1}$ or $\mu g\,g^{-1}$) for any inorganic element present in different samples were obtained from (1) after obtaining the experimental limits of detection (LD)(3)

$$LD_i = \frac{3 \cdot \sqrt{BG_i/t} \cdot C_{Ga}}{I_{Ga} \cdot S_i'}, \quad (3)$$

where BG_i = background (cps), t = detection time (s), and other variables are defined above [18, 19].

From the calculation of the experimental LD values, it was established that the values of LD are a polynomial function of the atomic number of the elements present, $LD_i = f(Z_i)$. Thus, using this formula, it is possible to calculate the LD for the elements which are not present in the sample.

3. Results and Discussion

Calibration curves ($\ln S_i' = f(Z_i)$) with significant parameters at 5% level were obtained for all X-K (Table 2, Figure 2) and X-L ray (Table 3, Figure 3) emitting elements through the multielementary calibration solutions. For the SRTXRF technique, the maximum S_i' value obtained is for the internal standard which was the element Ga ($Z = 31$) in this

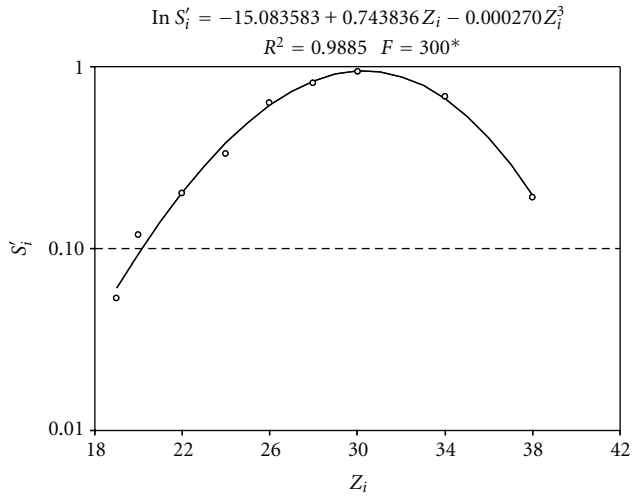

Figure 2: Experimental and calculated relative sensitivity for chemical elements emitting X-K rays for $19 \leq Z_i \leq 38$.

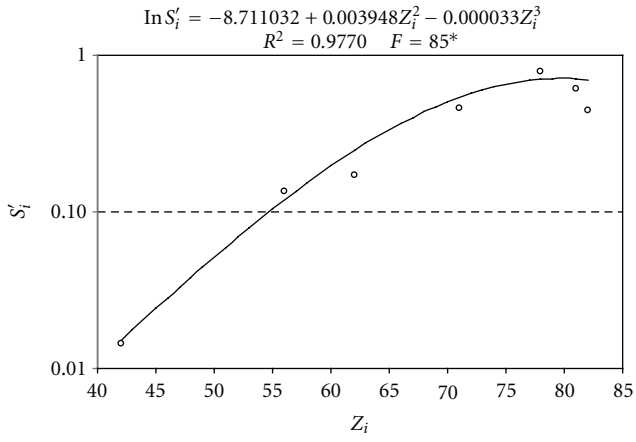

Figure 3: Experimental and calculated relative sensitivity for chemical elements emitting X-L rays for $42 \leq Z_i \leq 82$.

experiment. The functions increase for $Z < 31$ until $Z = 31$ and decreasing for $Z > 31$. Theoretically, $S'_{Ga} = 1.0$; however, the experimental value of Ga was 0.93. It is important to correct for this difference in the calculation of the other elements. In this case, if the experimental data were used without experimental correction, an error of 6.6% can be observed for all the elements. Some authors attribute the need to perform these corrections to obtain the values close to true net intensities [20].

The minimum detection limits for X-K and X-L ray emitting elements are presented in Table 4. The lowest recorded detection limit for X-K ray emitting elements was LD = 0.01 ppm for Zn ($Z = 30$) and Ni ($Z = 28$) and the highest detection limit value was LD = 1.72 ppm for K ($Z = 19$). Lowest and highest detection limit values for X-L ray emitting elements were, respectively, 0.01 ppm for Cu ($Z = 29$) and 1.57 ppm for Mo ($Z = 42$). After determining the experimental detection limits, the concentration of each chemical element was estimated (Table 5). The results of the

Table 2: Experimental and calculated mean relative sensitivity, S_i', and mean standard deviation for chemical elements emitting X-K rays for $19 \leq Z_i \leq 38$.

Element	Z_i	S_i' (experimental)	$s(m)$[a]	S_i'(calculated)
K	19	0.053007	0.004082	0.060650
Ca	20	0.118720	0.006506	0.093774
Ti	22	0.200669	0.015206	0.203081
Cr	24	0.329118	0.017632	0.381365
Fe	26	0.632468	0.027613	0.613014
Ni	28	0.810042	0.030792	0.832589
Zn	30	0.930767	0.025492	0.943175
Se	34	0.665939	0.051780	0.666817
Sr	38	0.190190	0.019045	0.195293

[a] $s(m)$ = standard deviation = S_i' (exprimental)/$\sqrt{n}$, $n = 9$.

Table 3: Experimental and calculated mean relative sensitivity, S_i', and mean standard deviation for chemical elements emitting X-L rays for $42 \leq Z_i \leq 82$.

Element	Z_i	S_i' (experimental)	$s(m)$[a]	S_i'(calculated)
Mo	42	0.014521	0.001182	0.015121
Ba	56	0.135400	0.008366	0.119381
Sm	62	0.170940	0.007042	0.246660
Lu	71	0.457106	0.014518	0.537822
Pt	78	0.789765	0.060052	0.743550
Tl	81	0.612795	0.047333	0.707681
Pb	82	0.445363	0.012872	0.697799

[a] $s(m)$ = standard deviation = S_i' (exprimental)/$\sqrt{n}$, $n = 9$.

analysis of algae (Table 5) and the chemical composition of the alkaline rocks where the algae were collected (Table 6) were compared.

Essential elements Ca, Fe, K, Mn, and Zn were found in all algae samples as were relevant species CaO, Fe_2O_3, K_2O, MnO, and Zn in the rocks upon which these algae grew. Interestingly, *G. marginata* had little Fe (75.27 ppm) while *D. plagiogramma* had over 150 times that amount (11936.65 ppm). *P. gymnospora* (3028.40 ppm) had the least values of Ca while *G. marginata* and *A. taxiformis* had the highest Ca levels detected (82606.32 and 88908.21 ppm, resp.). Relatively little K was found in *C. verticillata* (504.13 ppm) while the levels of K in *D. occidentalis* were almost 100 times this amount (49523.34 ppm). Also, the *P. gymnospora* had large amounts of Zn (274.44 ppm) whereas five algae species had levels of Zn in the range of 2–7 ppm Also, Sr was found in all rocks analyzed (*ca*. 950–1750 ppm) and was absorbed by all algae species and in relatively large abundance (*ca*. 500–6000 ppm). In contrast, Ba was generally abundant in rock samples (*ca*. 20–1350 ppm) from where the algae were collected, but Ba was only detected in *D. justii*. While Br was detected in several species, it was most concentrated in *A. taxiformis* (257.10 ppm).

The results obtained by SRTXRF analysis of algae are comparable to those obtained for algae from other parts of the world using other analytical methods. For example,

Table 4: Minimum detection limits values (ppm) for X-K and X-L ray emitting elements.

Species	As	Ba	Br	Ca	Co	Cr	Cs	Cu	Dy	Fe	K	Mn	Mo	Ni	Pb	Rb	Sr	Ti	V	Zn
Chlorophyta																				
C. verticillata	0.02	—	0.03	0.29	—	0.03	—	—	—	0.02	0.36	0.02	—	—	—	—	0.09	0.05	0.04	0.01
Rhodophyta																				
A. taxiformis	—	—	0.08	0.90	—	0.09	—	—	0.12	0.07	1.12	0.08	—	—	0.06	—	0.21	0.18	0.13	0.03
D. occidentalis	0.02	—	—	0.22	—	0.03	0.12	0.01	0.03	0.02	1.72	0.03	0.43	—	—	0.05	0.08	—	—	0.01
G. rugosa	—	—	0.02	0.25	—	0.02	0.14	—	0.03	0.02	0.37	0.02	0.49	—	0.02	—	0.07	—	—	0.01
G. obtusata	—	—	—	0.40	—	—	0.22	—	0.05	0.03	0.60	0.04	0.86	—	—	—	0.11	—	—	0.01
G. marginata	—	—	—	0.87	—	—	0.46	—	0.12	0.07	1.35	0.08	1.57	—	—	—	0.23	—	—	0.02
Phaeophyta																				
D. cervicornis	—	—	0.07	0.73	—	0.08	—	—	—	0.06	1.26	0.07	—	—	0.06	—	0.21	0.18	0.11	0.03
D. justii	0.02	0.16	0.03	0.30	0.02	—	—	—	—	0.02	0.48	0.03	—	0.01	—	—	0.10	—	0.04	0.01
D. plagiogramma	—	—	—	0.83	—	0.08	0.30	—	0.13	0.08	1.16	0.08	—	0.05	0.07	0.16	0.25	0.11	—	0.05
P. gymnospora	0.01	—	0.02	0.09	0.01	—	0.06	0.01	—	0.01	0.21	0.01	—	0.01	—	0.03	0.04	—	—	0.01
Sargassum sp.	0.03	—	0.03	0.25	0.02	—	—	0.01	—	0.02	0.50	0.03	—	0.01	—	0.06	0.09	—	0.04	0.01

—: not calculated.

Table 5: Mean values of elemental composition (ppm) of eleven species of seaweeds collected in Fernando de Noronha Archipelago, off northeastern Brazil and their respective CV, coefficient of variation (%).

Species	As	Ba	Br	Ca	Co	Cr	Cs	Cu	Dy	Fe	K	Mn	Mo	Ni	Pb	Rb	Sr	Ti	V	Zn
Chlorophyta																				
C. verticillata	10.82 (11.26)	—	8.60 (13.63)	20639.78 (0.93)	—	11.91 (12.51)	—	—	—	2559.68 (0.47)	504.13 (5.08)	21.43 (6.40)	—	—	—	—	511.19 (1.80)	108.86 (3.66)	14.06 (8.37)	11.44 (3.83)
Rhodophyta																				
A. taxiformis	—	—	257.10 (2.64)	88908.21 (1.95)	—	25.87 (10.30)	—	—	108.47 (10.46)	4108.09 (1.77)	1988.31 (3.22)	77.14 (9.75)	—	—	12.18 (9.48)	—	2121.10 (1.79)	224.55 (4.35)	39.63 (5.53)	17.35 (1.61)
D. occidentalis	12.03 (8.43)	—	—	15366.59 (0.30)	—	6.26 (7.96)	62.98 (17.10)	1.55 (11.38)	6.12 (15.43)	915.92 (1.15)	49523.34 (1.29)	10.33 (4.35)	465.94 (14.12)	—	—	13.78 (10.85)	718.43 (2.12)	—	—	3.21 (18.63)
G. rugosa	—	—	1.65 (17.96)	22949.59 (1.63)	—	5.28 (2.41)	192.80 (5.05)	—	21.66 (15.51)	513.81 (2.55)	1092.76 (3.99)	15.64 (1.90)	832.84 (12.86)	—	2.00 (9.25)	—	1735.42 (3.63)	—	—	2.36 (12.17)
G. obtusata	—	—	—	41500.55 (6.75)	—	—	358.28 (7.76)	—	39.57 (14.48)	245.12 (5.92)	2611.29 (6.96)	23.58 (23.38)	671.37 (9.99)	—	—	—	3002.25 (9.42)	—	—	3.80 (16.81)
G. marginata	—	—	—	82606.32 (0.88)	—	—	736.05 (3.21)	—	54.34 (9.56)	75.27 (7.73)	15655.44 (0.62)	39.79 (5.66)	836.71 (7.84)	—	—	—	5957.57 (1.53)	—	—	5.70 (18.02)
Phaeophyta																				
D. cervicornis	—	—	20.21 (8.44)	44313.30 (1.04)	—	19.53 (5.43)	—	—	—	3621.88 (0.88)	40527.54 (1.21)	60.85 (4.33)	—	—	27.22 (1.73)	—	2272.40 (0.61)	181.51 (5.68)	44.39 (10.78)	25.54 (2.92)
D. justii	17.35 (2.37)	21.39 (14.88)	3.56 (12.04)	18394.89 (4.26)	3.53 (4.81)	—	—	—	—	1410.02 (4.05)	7370.06 (4.41)	30.33 (3.94)	—	5.35 (16.12)	—	—	3046.38 (4.15)	—	33.87 (3.00)	22.50 (1,67)
D. plagiogramma	—	—	—	56397.66 (2.17)	—	53.64 (7.44)	289.32 (15.38)	—	46.31 (19.97)	11936.65 (2.62)	10593.50 (2.35)	78.34 (6.44)	—	15.15 (5.23)	17.56 (16.64)	47.58 (12.20)	1521.78 (0.91)	537.01 (7.26)	—	24.58 (3.78)
P. gymnospora	15.20 (2.28)	—	8.03 (10.63)	3028.40 (0.55)	1.93 (17.99)	—	148.77 (2.46)	1.10 (11.52)	—	251.77 (0.73)	9910.06 (0.51)	7.04 (6.41)	—	1.91 (13.19)	—	12.75 (17.70)	881.64 (1.21)	—	—	274.44 (0.33)
Sargassum sp.	117.92 (0.10)	—	16.63 (5.92)	14035.01 (0.70)	5.35 (7.23)	—	—	1.61 (9.72)	—	172.12 (1.91)	27196.26 (0.84)	21.53 (5.85)	—	2.68 (8.54)	—	36.43 (9.32)	1453.50 (0.77)	—	14.13 (6.20)	6.15 (5.63)
Average	34.67	21.39	45.11	37103.66	3.60	20.41	298.03	1.42	46.08	2346.40	15179.33	35.09	701.71	6.27	14.74	27.63	2111.06	262.98	29.22	36.10

—: not detected.

Table 6: Representative chemical composition of alkaline rocks from Caieiras (1 to 5) and Sueste (6 to 8).

	Caieiras					Sueste			
	1	2	3	4	5	6	7	8	Average
K_2O[a]	1.45	4.85	4.86	2.92	1.83	2.21	5.16	3.67	3.37
CaO[a]	11.2	5.80	4.10	6.81	12.5	10.5	0.58	5.73	7.15
TiO_2[a]	3.19	2.36	1.18	2.40	3.86	3.37	0.17	2.26	2.35
MnO[a]	0.18	0.18	0.15	0.21	0.16	0.21	0.19	0.12	0.18
Fe_2O_{3total}[a]	12.9	5.99	4.57	7.71	12.5	13.2	2.23	4.79	7.99
V[b]	275.1	164.0	71.0	171.8	239.9	257.0	13.0	187.4	172.40
Cr[b]	505.1	229.0	—	37.3	303.5	303.0	—	—	275.58
Co[b]	55.0	19.1	8.00	15.8	48.2	44.6	—	8.77	28.50
Ni[b]	358.9	23.6	17.9	62.4	295.5	309.6	—	19.6	155.36
Cu[b]	53.3	7.90	4.20	—	51.3	53.1	—	—	33.96
Zn[b]	57.5	97.0	95.3	94.3	122.5	114.1	181.0	80.0	105.21
Rb[b]	53.0	142.0	142.5	80.5	47.1	49.1	322.0	96.5	116.59
Sr[b]	960.9	820.8	1329	1620	1744	1023	—	1520	1288.24
Mo[b]	2.14	—	7.00	6.07	2.57	2.00	—	3.82	3.93
Cs[b]	1.20	1.90	2.40	3.67	0.55	1.00	—	4.33	2.15
Ba[b]	510.2	946.0	1191	1070	906.4	558.0	19.0	1330	816.33
Dy[b]	5.96	7.10	6.60	5.94	8.11	6.90	—	6.90	6.79
Pb[b]	—	13.3	14.7	14.5	5.21	7.20	32.0	11.9	14.12

—: not detected; [a]wt %; [b]ppm, —not analyzed . Using the procedure described in Janasi et al. [21], major, minor, and trace elements were determined by inductively coupled plasma-mass spectrometer (ICP-MS).

Hou and Yan [22] studied elements present in 35 species of marine algae from the coast of China by neutron activation analysis in a miniature neutron source reactor (MNSR). They observed that, in brown, red, and green algae, the levels of individual elements were (averages, resp., in parentheses): As (159/<0.36/12.2 ppm), Ba (76.2/109.6/174 ppm), Br (3426/6157/596 ppm), Ca (22.7/29.7/11.2 ppt), Co (0.93/1.15/1.04 ppm), Cr (4.02/4.84/6.33 ppm), Cs (1.11/1.02/0.95 ppm), Fe (1892/2511/3716 ppm), K (67.5/48.4/29.0 ppt), Mn (857/89.4/90.6 ppm), Rb (29.4/21.5/25.8 ppm), Sr (892/313/161 ppm), and Zn (21.7/28.3/23.3 ppm). Besides this study, in another work about 26 marine benthic algae species found in Karachi Coast, Pakistan, the levels (averages for the 26 species are in parentheses) of Ca (26.75 ppt), Co (5.88 ppm), Cr (5.13 ppm), Cu (11.87 ppm), Fe (2.41 ppt), K (69.5 ppt), Pb (13.43 ppm), and Zn (53.28 ppm) were established using flame atomic absorption spectrometry (AAS) [23]. As in the algae in these previous studies, the algae of Fernando de Noronha were found to contain large amounts of Ca, K, and Fe (in parts per thousand, ppt) and small or trace amounts of As, Ba, Co, Cr, Cs, Cu, Pb, Rb, and Zn. Since data on the composition of the surfaces where algae in these previous studies grew was not reported, it is not possible to ascertain the contributions of these surface substrates to the composition of the algae. The similar compositional trends in principle and trace elements present in algae from these previous studies and those of Fernando de Noronha lends support to the usefulness of the SRTXRF technique in the analytical arsenal.

Low numbers of algae species contained Rb (4 algae species, 12–48 ppm), Ti (4 species, 109–537 ppm), and V (5 species, 14–44 ppm) which may be related to geological characteristics of the alkaline rocks present in the study sites. Low concentrations of As (5 species, range 11–118 ppm), Co (3 species, 1.9–5.4 ppm), Cr (6 species, range 5.3–54 ppm), Cu (3 species, range 1.1–1.6 ppm), Ni (4 species, range 1.9–15 ppm), and Pb (4 species, range 2.0–27 ppm) were observed in most of the algae species, except for *Sargassum* sp. which had a higher concentration of As (118 ppm) compared to the other species. These elements may have been absorbed from the seawater through natural weathering and lixiviation of rocks and soil.

An interesting finding was the detection of Dy which is a rare earth metal present in rocks of both collection sites in *A. taxiformis, D. occidentalis, G. rugosa, G. obtusa, G. marginata,* and *D. plagiogramma*. Thus, these algae absorb and store this rare chemical element which is present in rocks in relatively low abundance.

4. Conclusion

The SRTXRF technique proved to be adequate for the determination of 20 chemical elements present in eleven species of common macroalgae of Fernando de Noronha archipelago providing baseline information for the accumulation of metals in two sites. The results indicate a relationship among the metals present in the seaweeds and the rocks present in this area. Besides, the concentrations of common

macro- and microelements obtained are comparable to those obtained by other authors using different analytical methods. However, multielement capability in a single analysis, high-sensitivity and precision, short analysis time, and easy sample preparation are some advantages of SRTXRF when compared to other elemental determination techniques such as AAS or ICP-MS.

Acknowledgments

The authors thank the Laboratório Nacional de Luz Síncrotron (LNLS-Campinas, SP) for allowing the use of beam line facilities and for CNPq, FAPESP, and CAPES for financial support. The authors declare that they do not have any conflict of interests.

References

[1] U. G. Cordani, M. N. Ulbrich, E. A. Menor, and R. P. Lopes, "Cenozoic alkaline volcanism of Fernando de Noronha island," in *South American Symposium on Isotope Geology, Field Trip Guide*, pp. 1–24, CBPM/IRD, Salvador, 2003.

[2] G. Dickie, "Enumeration of algae collected at Fernando de Noronha by H. M. Moseley, N. A. naturalist to H. M. S. "Challenger"," *Journal Linnean Society*, vol. 14, pp. 363–365, 1874.

[3] F. Pinheiro-Vieira and M. M. Ferreira-Correia, "Quarta contribuição ao inventário das algas marinhas bentônicas do nordeste brasileiro," *Arquivos de Ciências do Mar*, vol. 10, pp. 189–192, 1970.

[4] E. C. de Oliveira Filho, "An annotated list of the Brazilian seaweeds in Dickie's herbarium," *Botanical Journal of the Linnean Society*, vol. 69, no. 3, pp. 229–238, 1974.

[5] Pedrini A. G., Y. Ugadim, M. R. A. Braga, and S. M. B. Pereira, "Algas marinhas bentônicas do Arquipélago de Fernando de Noronha, Brasil," *Boletim de Botânica da USP*, vol. 13, pp. 93–101, 1992.

[6] V. R. Eston, A. E. Migotto, E. C. O. Filho, S. A. Rodrigues, and J. C. Freitas, "Vertical distribution of benthic marine organisms on rocky coasts of the Fernando de Noronha Archipelago (Brazil)," *Boletim do Instituto Oceanográfico de São Paulo*, vol. 34, pp. 37–53, 1986.

[7] C. S. Lobban and P. J. Harrison, *Seaweed Ecology and Physiology*, Cambridge University, Cambridge, UK, 1997.

[8] G. M. Amado-Filho, L. T. Salgado, M. F. Rebelo, C. E. Rezende, C. S. Karez, and W. C. Pfeiffer, "Heavy metals in benthic organisms from Todos os Santos Bay, Brazil," *Brazilian Journal of Biology*, vol. 68, no. 1, pp. 95–100, 2008.

[9] G. W. Bryan, "The effects of heavy metals (other than mercury) on marine and estuarine organisms," *Proceedings of the Royal Society of London. Series B*, vol. 177, no. 48, pp. 389–410, 1971.

[10] G. W. Bryan and L. G. Hummerstone, "Indicators of heavy metal contamination in the Looe Estuary (Cornwall) with particular regard to silver and lead," *Journal of the Marine Biological Association of the United Kingdom*, vol. 57, pp. 75–92, 1977.

[11] Y. Serfor-Armah, B. J. B. Nyarko, E. K. Osae, D. Carboo, S. Anim-Sampong, and F. Seku, "Rhodophyta seaweed species as bioindicators for monitoring toxic element pollutants in the marine ecosystem of Ghana," *Water, Air, and Soil Pollution*, vol. 127, no. 1-4, pp. 243–253, 2001.

[12] M. Rajfur, A. Kłos, and M. Wacławek, "Sorption properties of algae Spirogyra sp. and their use for determination of heavy metal ions concentrations in surface water," *Bioelectrochemistry*, vol. 80, no. 1, pp. 81–86, 2010.

[13] A. F. Ward, L. F. Marciello, L. Carrara, and V. J. Luciano, "Simultaneous determination of major, minor and trace elements in agricultural and biological samples by inductively coupled argon plasma spectrometry," *Spectroscopy Letters*, vol. 13, pp. 803–831, 1980.

[14] O. L. A. D. Zucchi, S. Moreira, M. J. Salvador, and L. L. Santos, "Multielement analysis of soft drinks by x-ray fluorescence spectrometry," *Journal of Agricultural and Food Chemistry*, vol. 53, no. 20, pp. 7863–7869, 2005.

[15] P. van Espen, H. Nullens, and F. Adams, "A computer analysis of X-ray fluorescence spectra," *Nuclear Instruments and Methods*, vol. 142, no. 1-2, pp. 243–250, 1977.

[16] R. Klockenkämper and A. von bohlen, "Determination of the critical thickness and the sensitivity for thin-film analysis by total reflection X-ray fluorescence spectrometry," *Spectrochimica Acta Part B*, vol. 44, no. 5, pp. 461–469, 1989.

[17] E. P. Zonta and A. Machado, *SANEST: Sistema de Análise Estatística para Microcomputadores*, CIAGRI-ESALQ-USP, São Paulo, Brazil, 1993.

[18] L. A. Currie, "Limits for qualitative detection and quantitative determination: application to radiochemistry," *Analytical Chemistry*, vol. 40, no. 3, pp. 586–593, 1968.

[19] W. Ladisich, R. Rieder, P. Wobrauschek, and H. Aiginger, "Total reflection X-ray fluorescence analysis with monoenergetic excitation and full spectrum excitation using rotating anode X-ray tubes," *Nuclear Instruments and Methods in Physics Research*, vol. 330, no. 3, pp. 501–506, 1993.

[20] M. J. Salvador, D. A. Dias, S. Moreira, and O. L. A. D. Zucchi, "Analysis of medicinal plants and crude extracts by synchrotron radiation total reflection X-ray fluorescence," *Journal of Trace and Microprobe Techniques*, vol. 21, no. 2, pp. 377–388, 2003.

[21] V. A. Janasi, S. Andrade, and H. H. G. J. Ulbrich, "A correção do drift instrumental em ICP-AES com espectrômetro seqüencial e a análise de elementos maiores, menores e traços em rochas," *Boletim do Instituto de Geociências da USP: Série Científica*, vol. 26, pp. 45–58, 1995.

[22] X. Hou and X. Yan, "Study on the concentration and seasonal variation of inorganic elements in 35 species of marine algae," *Science of the Total Environment*, vol. 222, no. 3, pp. 141–156, 1998.

[23] M. A. Rizvi and M. Shameel, "Pharmaceutical biology of seaweeds from the Karachi coast of Pakistan," *Pharmaceutical Biology*, vol. 43, no. 2, pp. 97–107, 2005.

Hindawi Publishing Corporation
International Journal of Analytical Chemistry
Volume 2012, Article ID 850969, 7 pages
doi:10.1155/2012/850969

Research Article

Development of a Novel Biosensor Using Cationic Antimicrobial Peptide and Nickel Phthalocyanine Ultrathin Films for Electrochemical Detection of Dopamine

Maysa F. Zampa,[1,2] Inês Maria de S. Araújo,[2,3] José Ribeiro dos Santos Júnior,[3] Valtencir Zucolotto,[4] José Roberto de S. A. Leite,[2] and Carla Eiras[2]

[1] *Instituto Federal de Educação, Ciência e Tecnologia do Piauí (IFPI), Campus Parnaíba, 64210260 Parnaíba, PI, Brazil*
[2] *Biotec, Núcleo de Pesquisa em Biodiversidade e Biotecnologia, Universidade Federal do Piauí (UFPI), Campus Ministro Reis Velloso (CMRV), 64202020 Parnaíba, PI, Brazil*
[3] *Departamento de Química, Centro de Ciências da Natureza (CCN), Universidade Federal do Piauí (UFPI), 64049550 Teresina, PI, Brazil*
[4] *Grupo de Biofísica Molecular Sérgio Mascarenhas, Instituto de Física de São Carlos (IFSC), USP, 13560970 São Carlos, SP, Brazil*

Correspondence should be addressed to Carla Eiras, carla.eiras.ufpi@gmail.com

Received 5 September 2011; Accepted 3 October 2011

Academic Editor: Ricardo Vessecchi

The antimicrobial peptide dermaseptin 01 (DS 01), from the skin secretion of *Phyllomedusa hypochondrialis* frogs, was immobilized in nanostructured layered films in conjunction with nickel tetrasulfonated phthalocyanines (NiTsPc), widely used in electronic devices, using layer-by-layer technique. The films were used as a biosensor to detect the presence of dopamine (DA), a neurotransmitter associated with diseases such as Alzheimer's and Parkinson's, with detection limits in the order of 10^{-6} mol L^{-1}. The use of DS 01 in LbL film generated selectivity in the detection of DA despite the presence of ascorbic acid found in biological fluids. This work is the first to report that the antimicrobial peptide and NiTsPc LbL film exhibits electroanalytical activity to DA oxidation. The selectivity in the detection of DA is a fundamental aspect for the development of electrochemical sensors with potential applications in the biomedical and pharmaceutical industries.

1. Introduction

Nanomaterials are causing a great impact on electrochemical biosensors development. Nanotechnology brings new possibilities for biosensors construction and for developing novel electrochemical bioassays [1].

Due to the increased use of organic molecules, the LbL technique has been widely employed in manufacturing ultrathin films with potential application as biosensors [2–6]. The ultrathin films' technique has many advantages, since it allows the construction of structures that present different chemical properties than those encountered in the originating materials [4–6].

A key feature for LbL films, in particular, is the incorporation of sulfonated groups to metallic phthalocyanines [7–9]. The electrodes modified with PAH/FeTsPc LbL films displayed electroactivity but were not suitable for dopamine detection. The development of voltammetric sensors for the detection of neurotransmitters, as dopamine (DA), in the extracellular fluid of the central nervous system has received much attention in the past few decades due to role in Parkinson disease [10, 11]. The electrochemical methods have advantages over others because they allow the detection of neurotransmitters in living organisms [12].

However, the coexistence of ascorbic acid (AA) with a concentration of 100–1000 times higher than that of DA greatly challenges the electrochemical strategy for DA detection. It was observed that AA could be easily oxidized at a potential close to the DA and the species formed could lead to oxidation of AA, as well as the reaction sites on the

electrode surface could be easily blocked by the product of AA oxidation [13].

The electrochemical analysis of serum with a traditional solid electrode, such as glassy carbon, suffers from the problem of an overlapped oxidation potential between AA and DA. Moreover, there is no reversible electrochemical kinetics, so the fouling effect on the electrode surface by the oxidized AA could result in poor selectivity and reproducibility. Therefore, direct quantification of the AA concentration by the electrochemical method is difficult [14, 15].

Amphibian skin is an important source of gene-encoded AMPs, with more than half of ~900 eukaryotic peptides described to date isolated from South American Hylidae or European, Asian, or North American Ranidae [16]. The dermaseptins are a superfamily of AMPs that are produced in the skin of Hylidae and Ranidae frogs [17]. These peptides share a signature pattern consisting of a conserved Trp residue at position 3 and an AA(A/G)KAAL(G/N)A consensus motif in the midregion, which gives these molecules a cationic characteristic.

In this work we used a dermaseptin called DS 01, collected from the skin of *Phyllomedusa oreades* and *P. hypochondrialis* frogs. This molecule has demonstrated highly antibacterial activity against gram-negative and gram-positive bacteria as well as against many protozoans [17, 18]. The cationic features mainly refer to the ability of dermaseptins to exploit differences in lipid composition of the protozoan plasma membrane (PM). The PM of prokaryotes and lower eukaryotes is characterized by the presence of anionic phospholipids (PLs) at the outer leaflet, by the presence of certain sterols and to a lesser extent by a distinctive plasma membrane potential [19].

Zampa et al. first demonstrated the immobilization of AMPs in electroactive thin films while maintaining bioactivity as shown in the enhanced detection of *Leishmania* by cyclic voltammetry [20].

In the present paper, we prepared stably assembled films using LbL method based on electrostatic interaction between the positively charged AMP layer, called dermaseptin 01 (DS 01), and negatively charged nickel tetrasulfonated phthalocyanine (NiTsPc) layer. We studied the electron transfer of DA and AA and further explored possible applications of this films for determination of DA in the presence of AA.

2. Experimental

2.1. Peptide Synthesis. The amidated DS 01 was synthesized on a Pioneer Synthesis System from Applied Biosystems (Framingham, MA, USA). Fmoc-amino acids and Fmoc PAL-PEG-PS resin were purchased from Applied Biosystems (Framingham, MA, USA). In order to purify the peptide, the use of a preparative C18 column (Vydac 218 TP 1022, Hesperia, CA, USA) on a HPLC system Class LC-10VP (Shimadzu Corp., Kyoto City, Japan) was required. Molecular mass (2793.6 Da) and sample purity were checked by MALDI-TOF MS. The final purification step of this synthetic peptide was performed by RP-HPLC on a Vydac 218 TP 54 (Hesperia, CA, USA) analytical column.

2.2. Solutions for LbL Depositions. The DS 01 solution used to construct the LbL films was prepared at a concentration of 3.58×10^{-6} mol L^{-1} in Milli-Q water, and the resulting solution had pH set at 5.6. Already NiTsPc, purchased from Aldrich Co. and used without further purification, was used at a concentration of 5.11×10^{-4} mol L^{-1} in HCl (pH 2.5) solution. The Figures 1(a) and 1(b) show the structures of NiTsPc and DS 01, respectively. DA and AA stock solutions were prepared at 10^{-3} mol L^{-1} concentrations, both commercially purchased from Aldrich Co..

2.3. Multilayer Deposition. DS 01-containing films were produced combining the AMP with NiTsPc. At pH 5.6, DS 01 bears a positive net charge, in a way that interactions between the anionic NiTsPc and cationic DS 01 were primarily electrostatic. Immobilization was carried out in a LbL fashion upon the alternate immersion of ITO (indium tin oxide-(ITO)-covered glass plates) in solutions containing DS 01 and NiTsPc, respectively, for 5 min followed by immersion in the washing solution (HCl pH 2.5). An illustration showing film fabrication and immobilization is shown in Figure 2. After each immersion step, the film was dried using a nitrogen gas flow. The architecture investigated was ITO/(DS 01/NiTsPc)$_3$ where 3 is the number of bilayers. For comparison effect, ITO modified with one monolayer of NiTsPc was studied.

2.4. Cyclic Voltammetry. Cyclic voltammograms were collected with LbL films deposited onto ITO using a potentiostat Autolab PGSTAT 30 Eco Chemie and a three-electrode electrochemical cell. A 1.0 cm^2 platinum foil was used as auxiliary electrode, and the reference electrode was an Hg/HgCl/KCl (sat.) (SCE). All the potentials were referred to SCE. The LbL films deposited on ITO plates were employed as working electrodes. Experiments were carried out using a solution of H_2SO_4 0.05 mol L^{-1} at room temperature. Cyclic voltammetry was also employed for DA detection, with DA being added in the electrolytic solution in a concentration range from 0 to 1.96×10^{-5} mol L^{-1}.

3. Results and Discussion

To test the possibility of synergism between the molecules of DS 01 and NiTsPc, we compared the electrochemical profile of a NiTsPc monolayer (ITO/(NiTsPc)$_1$) and the film containing three bilayers (ITO/(DS 01/NiTsPc)$_3$), as shown in Figure 3. The electrical response signal of NiTsPc monolayer was detected. It is assumed that this low response in the electrical signal is a result of a small amount of NiTsPc electroactive molecules adsorbed in the unique monolayer on ITO surface.

The anodic process observed around +0.5 V may be related to the oxidation of nickel metal center [Ni(II)/Ni(III) + e^-] [21, 22], and the corresponding reduction process can be detected at +0.3 V. Figure 3 also illustrates the cyclic voltammogram of the ITO/(DS 01/NiTsPc)$_3$ film, which shows two reduction processes at +0.3 V and +0.7 V, while the latter may be related to the reduction of the

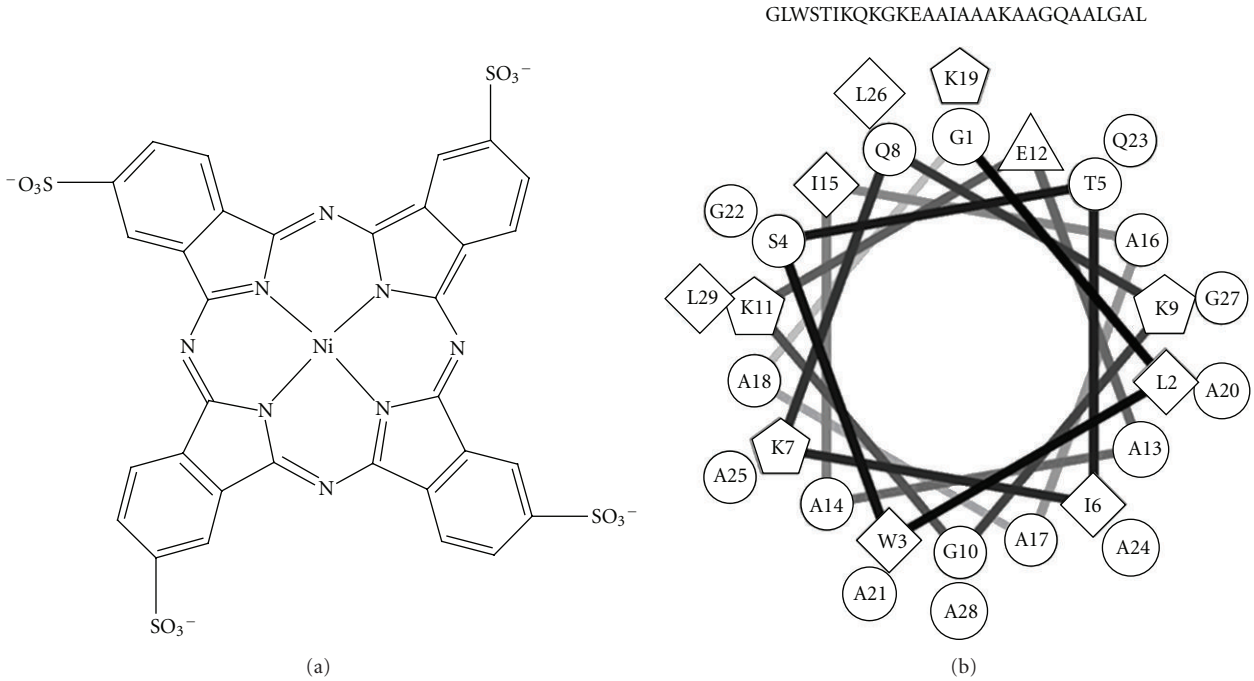

Figure 1: Chemical structures of materials used in LbL films: (a) nickel tetrasulfonated phthalocyanine (NiTsPc) and (b) amino acid sequence and helix-wheel plots of the antimicrobial peptide (DS 01) showing the amphiphilic character of the molecule.

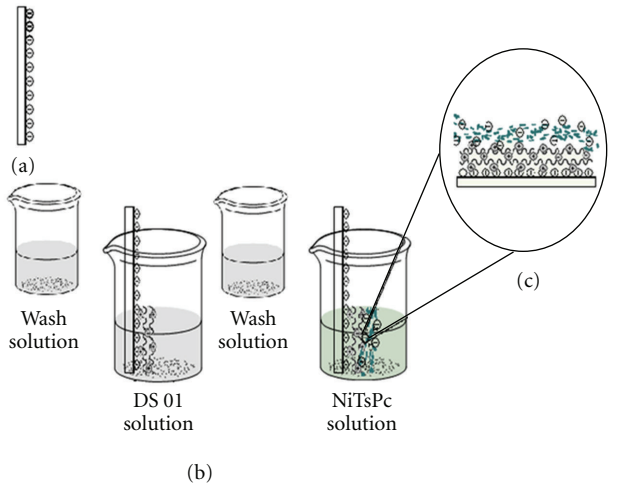

Figure 2: LbL film assembly process: scheme of film formation according to the LbL technique: (a) bare substrate, (b) deposition of the first layer of DS 01 AMP, (c) first bilayer formed (ITO/(DS 01/NiTsPc)$_1$).

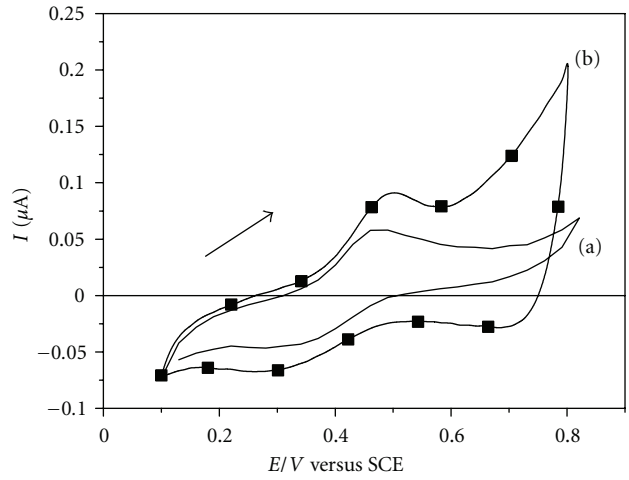

Figure 3: Electrochemical profiles of the films: cyclic voltammograms of (a) NiTsPc monolayer onto ITO substrate and (b) ITO/(DS 01/NiTsPc)$_3$ film. Electrolyte solution H_2SO_4 0.05 mol L^{-1}, at 25 mVs^{-1}.

phthalocyanine macrocycle. The film shows a new electrochemical profile, different from that observed for the NiTsPc monolayer, suggesting that materials interact at the molecular level and displays new properties.

Voltammetric experiments demonstrated the stability of ITO/(DS 01/NiTsPc)$_3$ film, which after successive scanning cycles continued to exhibit redox processes at the same level of electrical current (data not shown).

The study of electrochemical activity of the film at different scan speeds is important to identify the mechanism that governs the redox process of the material. To perform this experiment, scanning cycles were recorded in scan speeds ranging between 10 and 100 mV s^{-1}, as observed in cyclic voltammograms in Figure 4.

The linear relationship between anodic peak current and scan rate, which could be expressed by $I_p(\mu A) = (0.0030 \pm 0.0002) \times 10^3 \nu\ (V\,s^{-1}) + (0.044 \pm 0.008)$ ($r = 0.992$, $n = 8$), indicates that the reaction is governed by a mechanism of charge transfer between neighboring redox centers and the surface of ITO substrate, called electron hopping. This

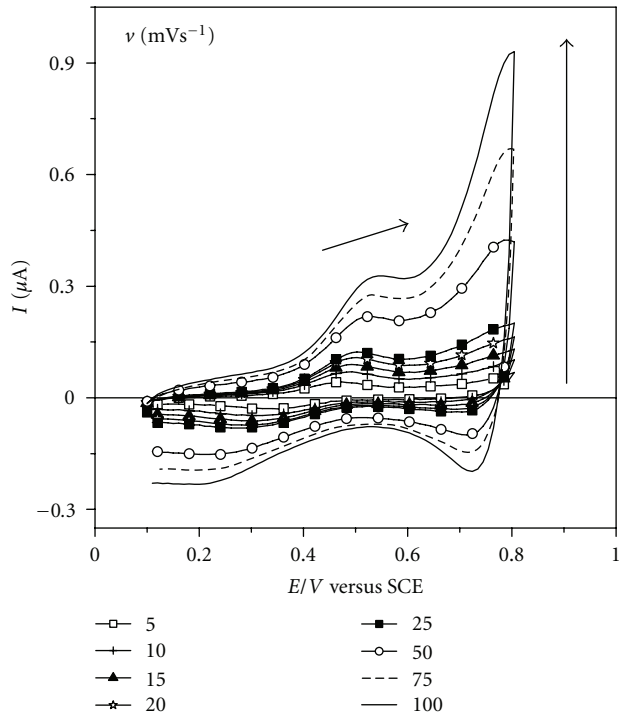

Figure 4: Study of the redox process of the film: cyclic voltammograms for ITO/(DS 01/NiTsPc)$_3$ film at different scanning speeds. Electrolyte solution H_2SO_4 0.05 mol L^{-1}.

electron transfer process is associated with the existence of molecules immobilized on the substrate surface [23, 24].

The identification of important features of ITO/(DS 01/NiTsPc)$_3$ film, such as electrochemical profile, stability, and the mechanism that governs the electronic charges, led to the application experimenting of DA detection and its interferent AA, testing the use of the film as an electrochemical biosensor.

Figure 5(a) reports the voltammograms obtained for ITO/(DS 01/NiTsPc)$_3$ film after successive additions of aliquots of DA stock solution. The concentration of DA in the electrochemical cell ranged from 0 to 1.96×10^{-5} mol L^{-1}. It was observed that DA oxidation occurred at +0.64 V, and the electrical signal response increased linearly with the increase of analyte concentration in the electrolyte solution (Figure 5(b)). The linear regression equation was $I_p(\mu A) = (1.40 \pm 0.04) \times 10^5 C$ (mol L^{-1}) + (0.12 ± 0.05) ($r = 0.997$, $n = 10$).

Using the information above, we calculated the detection limit (DL) which was 1.665×10^{-6} mol L^{-1} [25]. The DL indicates the lowest concentration of analyte that can be detected by the biosensor without interference from noise caused by current equipment. The results of this work indicate that the biosensor is able to detect DA concentrations in a limit employed by the industry, for example, the pharmaceutical field.

Another important study was to assess whether DA permanently binds to active sites of the film after the detection test. Figure 6 shows the cyclic voltammogram of the film at the maximum concentration of DA (1.9608×10^{-5} mol L^{-1}) in electrolyte solution. Then, the film was applied to potential scans in the electrolyte solution free of DA. The electrochemical profile of ITO/(DS 01/NiTsPc)$_3$ film in this condition was shown in Figure 6 and indicates that the DA oxidation process at +0.64 V is no longer observed. Thus, the results suggest that the DA does not bind to the biosensor active sites permanently, because, after washing the biosensor in the electrolyte solution, there is no evidence of DA presence there.

As discussed above, it is necessary to study the electrochemical profile of the film in the presence of the analyte, DA, and its interferent AA, at the same time. Figure 7 illustrates the cyclic voltammograms obtained for ITO/(DS 01/NiTsPc)$_3$ film in the presence of DA and AA simultaneously in the following proportions C_{DA}/C_{AA}: 1 : 1, 1 : 2, and 1 : 3. It is observed that the voltammograms are identical, independent of AA concentration tested, exhibiting only a single oxidation process at +0.64 V and the same response level of electric current.

In this last stage of tests, the capability/ability of the biosensor in detecting only the presence of the interferent AA was studied. In this case, the experiments were conducted in an electrolyte solution without DA. Figure 8 shows the cyclic voltammograms of the film after AA successive additions to the electrolytic solution, and there is no variation in electrical response signal; that is, the proposed biosensor does not detect AA alone. According to the results, it appears that the ITO/(DS 01/NiTsPc)$_3$ film detects DA presence in the electrolytic medium which also contains the two analytes (AA and DA); however, the film is unable to detect the concentrations of DA and AA. It is assumed that AA probably adsorbs on electroactive film sites, blocking the electrical signal response of DA.

According to these discussions, the biosensor can be considered selective for DA, since the selectivity is the ability of a method to determine the analyte reliably in the presence of other substances that may interfere in the determination. Selectivity is an important parameter for the electroanalytical method validation.

Previous results observed for LbL films of POMA or gum containing NiTsPc [26, 27] indicated the overlapping oxidation processes of DA and AA, yielding in the tested films the characteristic of not being selective.

Zampa et al. [28] built biosensors for DA detection using the natural chicha gum (*Sterculia striata*) in tetralayers fashion with LD at approximately 10^{-5} mol L^{-1}. The process of DA detection in this biosensor was considered irreversible and governed by a diffusional process. No tests were performed to detect DA in the presence of AA.

In the present study, the biosensor ITO/(DS 01/NiTsPc)$_3$ showed an even lower LD, about 10^{-6} mol L^{-1}, emphasizing that the presence of the DS 01 AMP along with NiTsPc was a decisive factor to confer the observed selectivity in DA and AA detection. The behavior of the film studied as a biosensor encourages the advance of application research of this nanostructured system in the biomedical and pharmaceutical areas.

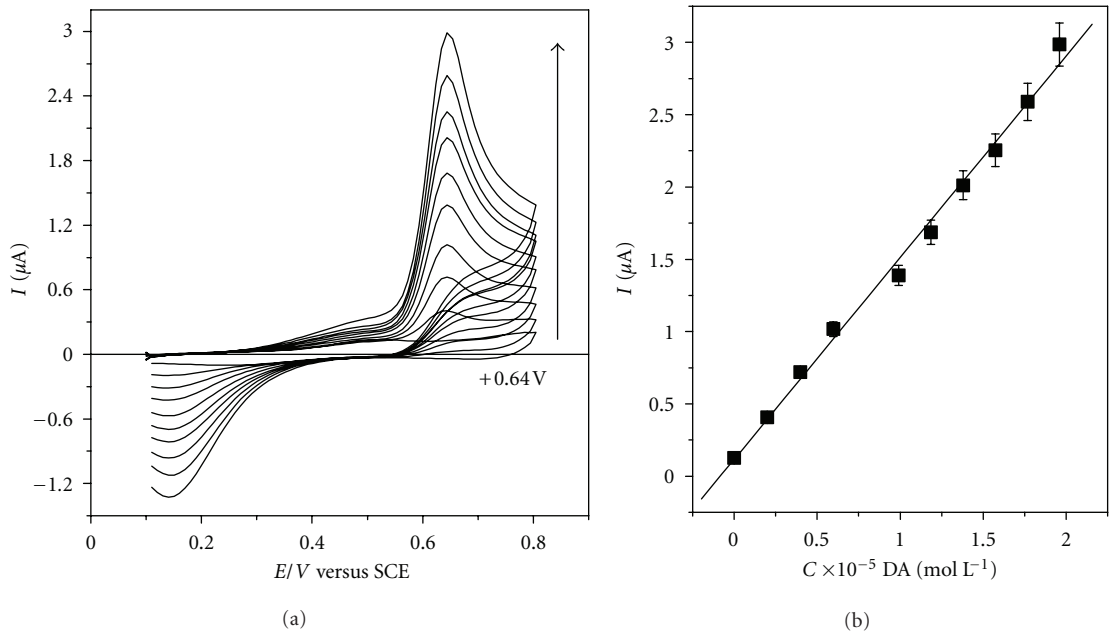

Figure 5: Dopamine detection test: (a) cyclic voltammograms for DA detection at concentrations ranging from 0 to 1.96×10^{-5} mol L^{-1}, in H_2SO_4 0.05 mol L^{-1} at 25 mVs^{-1}, for ITO/(DS 01/NiTsPc)$_3$ film. (b) Calibration curve (I versus C) for DA detection.

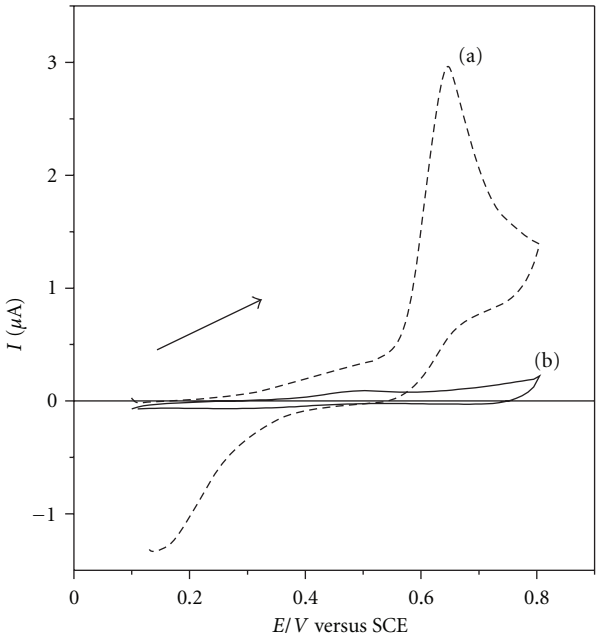

Figure 6: Study of the interaction between dopamine and film active sites: comparison between the electrochemical profile of ITO/(DS 01/NiTsPc)$_3$ film in (a) presence of DA (1.9608×10^{-5} mol L^{-1}) and in (b) DA absence, electrolyte solution H_2SO_4 0.05 mol L^{-1}, at 25 mVs^{-1}.

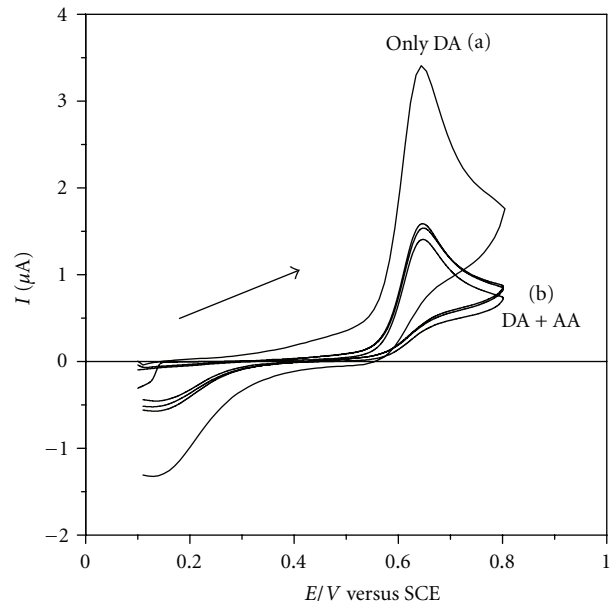

Figure 7: Interferent detection test: cyclic voltammograms for ITO/(DS 01/NiTsPc)$_3$ film in (a) 1.9608×10^{-5} mol L^{-1} of DA and (b) in presence of DA (1.9608×10^{-5} mol L^{-1}) and AA simultaneously, in different proportions C_{DA}/C_{AA}: 1 : 1, 1 : 2, and 1 : 3. Electrolyte solution H_2SO_4 0.05 mol L^{-1}, at 25 mVs^{-1}.

4. Conclusions

Employing the LbL technique, a film containing the DS 01 AMP and NiTsPc macromolecules was constructed. DS 01 AMP is a biological material studied for prospective drugs while NiTsPc is a conductive material broadly utilized in researches in electronic devices. The ITO/(DS 01/NiTsPc)$_3$ film was characterized as a stable system, able to detect DA in array bounds of 10^{-6} mol L^{-1} besides being an selective electrode for AA. A selective electrode had not yet been

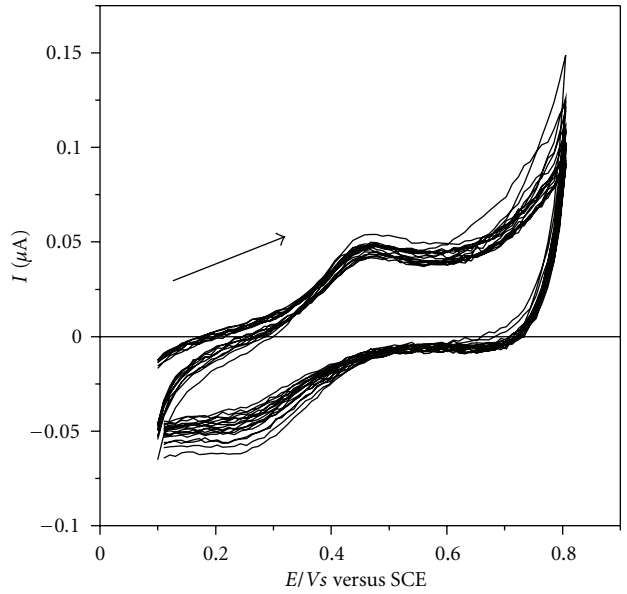

Figure 8: Ascorbic acid detection test: cyclic voltammograms for ITO/(DS 01/NiTsPc)$_3$ film after successive additions of stock solution containing AA aliquots, in concentrations ranging from 1.235 $\times$ 10^{-5} to 20.000 $\times$ 10^{-5} mol L^{-1}. Electrolyte solution H_2SO_4 0.05 mol L^{-1}, at 25 mVs^{-1}.

developed by this research group. According to these results, it is expected that these films become objects of study in the important field of electrochemical biosensors.

Acknowledgments

The authors thank the financial support from the Brazilian funding agencies FAPEPI (Fluxo Contínuo Program 2009—process number 20.203.0637/2008), CAPES (Nanobiomed Network), and CNPq (Jovens Pesquisadores/Nanotecnologia 2008—process number 577355/2008-2, Universal 476700/2009-4 and Consolidação Novos *Campi* 503495/2009-3 and 501874/2009-7) and IFPI (ProAgrupar 2010). The authors are grateful for the English revision done by our dear friend Mrs. Claudia Hissette.

References

[1] M. Pumera, S. Sánchez, I. Ichinose, and J. Tang, "Electrochemical nanobiosensors," *Sensors and Actuators, B*, vol. 123, no. 2, pp. 1195–1205, 2007.

[2] F. Gambinossi, P. Baglioni, and G. Caminati, "Hybrid LbL/LB films as molecular OLEDs: an acoustic shear wave attenuation and Brewster angle microscopy study," *Materials Science and Engineering C*, vol. 27, no. 5–8, pp. 1056–1060, 2007.

[3] Q. Sheng and J. Zheng, "Bienzyme system for the biocatalyzed deposition of polyaniline templated by multiwalled carbon nanotubes: a biosensor design," *Biosensors and Bioelectronics*, vol. 24, no. 6, pp. 1621–1628, 2009.

[4] G. Decher, J. D. Hong, and J. Schmitt, "Buildup of ultrathin multilayer films by a self-assembly process: III. Consecutively alternating adsorption of anionic and cationic polyelectrolytes on charged surfaces," *Thin Solid Films*, vol. 210-211, no. 2, pp. 831–835, 1992.

[5] F. Caruso, H. Lichtenfeld, M. Giersig, and H. Mohwald, "Electrostatic self-assembly of silica nanoparticle-polyelectrolyte multilayers on polystyrene latex particles," *Journal of the American Chemical Society*, vol. 120, no. 33, pp. 8523–8524, 1998.

[6] A. A. Mamedov, N. A. Kotov, M. Prato, D. M. Guldi, J. P. Wicksted, and A. Hirsch, "Molecular design of strong single-wall carbon nanotube/polyelectrolyte multilayer composites," *Nature Materials*, vol. 1, no. 3, pp. 190–194, 2002.

[7] H. Ding, X. Zhang, M. K. Ram, and C. Nicolini, "Ultrathin films of tetrasulfonated copper phthalocyanine-capped titanium dioxide nanoparticles: fabrication, characterization, and photovoltaic effect," *Journal of Colloid and Interface Science*, vol. 290, no. 1, pp. 166–171, 2005.

[8] V. Zucolotto, M. Ferreira, M. R. Cordeiro, C. J. L. Constantino, W. C. Moreira, and O. N. Oliveira Jr., "Nanoscale processing of polyaniline and phthalocyanines for sensing applications," *Sensors and Actuators, B*, vol. 113, no. 2, pp. 809–815, 2006.

[9] P. Bertoncello and M. Peruffo, "An investigation on the self-aggregation properties of sulfonated copper(II) phthalocyanine (CuTsPc) thin films," *Colloids and Surfaces A*, vol. 321, no. 1–3, pp. 106–112, 2008.

[10] K. A. Maguire-Zeiss, D. W. Short, and H. J. Federoff, "Synuclein, dopamine and oxidative stress: co-conspirators in Parkinson's disease?" *Molecular Brain Research*, vol. 134, no. 1, pp. 18–23, 2005.

[11] S. Arreguin, P. Nelson, S. Padway, M. Shirazi, and C. Pierpont, "Dopamine complexes of iron in the etiology and pathogenesis of Parkinson's disease," *Journal of Inorganic Biochemistry*, vol. 103, no. 1, pp. 87–93, 2009.

[12] S. M. Chen and W. Y. Chzo, "Simultaneous voltammetric detection of dopamine and ascorbic acid using didodecyldimethylammonium bromide (DDAB) film-modified electrodes," *Journal of Electroanalytical Chemistry*, vol. 587, no. 2, pp. 226–234, 2006.

[13] M. Zhang, K. Gong, H. Zhang, and L. Mao, "Layer-by-layer assembled carbon nanotubes for selective determination of dopamine in the presence of ascorbic acid," *Biosensors and Bioelectronics*, vol. 20, no. 7, pp. 1270–1276, 2005.

[14] J. Chen and C. S. Cha, "Detection of dopamine in the presence of a large excess of ascorbic acid by using the powder microelectrode technique," *Journal of Electroanalytical Chemistry*, vol. 463, no. 1, pp. 93–99, 1999.

[15] P. C. Nien, P. Y. Chen, and K. C. Ho, "On the amperometric detection and electrocatalytic analysis of ascorbic acid and dopamine using a poly(acriflavine)-modified electrode," *Sensors and Actuators, B*, vol. 140, no. 1, pp. 58–64, 2009.

[16] P. Nicolas and C. El Amri, "The dermaseptin superfamily: a gene-based combinatorial library of antimicrobial peptides," *Biochimica et Biophysica Acta*, vol. 1788, no. 8, pp. 1537–1550, 2009.

[17] G. D. Brand, J. R. S. A. Leite, S. M. de Sá Mandel et al., "Novel dermaseptins from Phyllomedusa hypochondrialis (Amphibia)," *Biochemical and Biophysical Research Communications*, vol. 347, no. 3, pp. 739–746, 2006.

[18] G. D. Brand, J. R. S. A. Leite, L. P. Silva et al., "Dermaseptins from Phyllomedusa oreades and Phyllomedusa distincta: anti-trypanosoma cruzi activity without cytotoxicity to mammalian cells," *The Journal of Biological Chemistry*, vol. 277, no. 51, pp. 49332–49340, 2002.

[19] L. Rivas, J. R. Luque-Ortega, and D. Andreu, "Amphibian antimicrobial peptides and Protozoa: lessons from parasites,"

Biochimica et Biophysica Acta, vol. 1788, no. 8, pp. 1570–1581, 2009.

[20] M. F. Zampa, I. M. S. Araújo, V. Costa et al., "Leishmanicidal activity and immobilization of dermaseptin 01 antimicrobial peptides in ultrathin films for nanomedicine applications," *Nanomedicine*, vol. 5, no. 3, pp. 352–358, 2009.

[21] F. Lanças, *Validação de Métodos Cromatográficos de Análise*, Rima, São Carlos, Brazil, 2004.

[22] J. T. S. Irvine, B. R. Eggins, and J. Grimshaw, "The cyclic voltammetry of some sulphonated transition metal phthalocyanines in dimethylsulphoxide and in water," *Journal of Electroanalytical Chemistry*, vol. 271, no. 1-2, pp. 161–172, 1989.

[23] C. C. Leznoff and A. B. P. Lever, *Phthalocyanines Properties and Applications*, vol. 1–4, John Wiley & Sons, New York, NY, USA, 1989.

[24] F. N. Crespilho, V. Zucolotto, O. N. Oliveira Jr., and F. C. Nart, "Electrochemistry of layer-by-layer films: a review," *International Journal of Electrochemical Science*, vol. 1, pp. 194–214, 2006.

[25] J. R. Siqueira, L. H. S. Gasparotto, F. N. Crespilho, A. J. F. Carvalho, V. Zucolotto, and O. N. Oliveira Jr., "Physicochemical properties and sensing ability of metallophthalocyanines/chitosan nanocomposites," *Journal of Physical Chemistry B*, vol. 110, no. 45, pp. 22690–22694, 2006.

[26] A. C. Santos, V. Zucolotto, C. J. L. Constantino, H. N. Cunha, J. R. Dos Santos, and C. Eiras, "Electroactive LbL films of metallic phthalocyanines and poly(0-methoxyaniline) for sensing," *Journal of Solid State Electrochemistry*, vol. 11, no. 11, pp. 1505–1510, 2007.

[27] C. Eiras, A. C. Santos, M. F. Zampa et al., "Natural polysaccharides as active biomaterials in nanostructured films for sensing," *Journal of Biomaterials Science, Polymer Edition*, vol. 21, no. 11, pp. 1533–1543, 2010.

[28] M. F. Zampa, A. C. F. de Brito, I. L. Kitagawa et al., "Natural gum-assisted phthalocyanine immobilization in electroactive nanocomposites: physicochemical characterization and sensing applications," *Biomacromolecules*, vol. 8, no. 11, pp. 3408–3413, 2007.

Hindawi Publishing Corporation
International Journal of Analytical Chemistry
Volume 2012, Article ID 508945, 7 pages
doi:10.1155/2012/508945

Research Article

Preliminary Assessment of the Chemical Stability of Dried Extracts from *Guazuma ulmifolia* Lam. (Sterculiaceae)

Gisely C. Lopes,[1] Renata Longhini,[1] Paulo Victor P. dos Santos,[2] Adriano A. S. Araújo,[3] Marcos Luciano Bruschi,[1] and João Carlos P. de Mello[1]

[1] *Programa de Pós-Graduação em Ciências Farmacêuticas, Departamento de Farmácia, Universidade Estadual de Maringá, Avenida Colombo, 5790, 87020-900 Maringá, PR, Brazil*
[2] *Student of Pharmacy, Universidade Estadual de Maringá, Avenida Colombo, 5790, 87020-900 Maringá, PR, Brazil*
[3] *Departamento de Fisiologia, Universidade Federal de Sergipe, Avenida Marechal Rondon, s/n, Cidade Universitária, 49100-000 São Cristóvão, SE, Brazil*

Correspondence should be addressed to João Carlos P. de Mello, mello@uem.br

Received 29 August 2011; Accepted 29 September 2011

Academic Editor: Ricardo Vessecchi

We report the results of a preliminary estimation of the stability of the dried extract from bark of *Guazuma ulmifolia* Lam. ("Mutamba"), with and without added colloidal silicon dioxide (CSD). The physical and chemical properties and the compatibility of CSD in the extract were evaluated for 21 days of storage under stress conditions of temperature (45 ± 2°C) and humidity (75 ± 5%). Thermogravimetry (TG) was supplemented using selective high-performance liquid chromatography (HPLC) for determination of stability of the characteristic constituents (chemical markers), namely, procyanidin B2 (PB2) and epicatechin (EP). The results showed that PB2 is an appropriate compound to be used as a chemical marker in the quality control of dried extracts of *G. ulmifolia*. The stress study showed that there was no significant difference between the two formulations. However, considering the TG data and the high temperatures involved, the results suggest that CSD increases the stability of the dried extract of *G. ulmifolia*.

1. Introduction

The reasons for the determination of stability of pharmaceuticals are based on concern for public health. The World Health Organization (WHO) defines the stability of drugs and medicines as the ability of a pharmaceutical product to maintain its chemical, physical, microbiological, and biopharmaceutical properties within specified limits throughout the duration of product usage [1].

Several studies reported on the stability of drugs and medicines [2–4]. To the best of our knowledge, the number of stability studies of plant extracts is not the same [5–7]. Measuring the chemical stability of extracts is challenging because of their chemical complexity, which may include hundreds of different compounds. Moreover, the presence of enzymes such as glycosidases, esterases, or oxidases plays an important role in the breakdown of secondary plant metabolites.

Assessment of the chemical stability of plant extracts, many of which are promising candidates for phytomedicines, plays an important role in the process of new drug development. A variety of environmental conditions, such as light, heat, humidity, and the freeze/thaw cycle, can significantly affect the chemical stability of drugs during storage and handling. Identification of stability-affecting factors facilitates the selection of packaging material and the definition of storage and handling conditions [8].

Guazuma ulmifolia Lam. (Sterculiaceae), popularly known as "Mutamba", is a tropical American plant found from Mexico to southern South America. In the popular medicine of several Latin-American countries, it is used for the treatment of burns, diarrhea, inflammations, and

alopecia. Polysaccharides, epicatechin (EP), and procyanidin oligomers, such as procyanidins B2 (PB2) and B5, three trimers [procyanidin C1; epicatechin-(4β ⟶6)-epicatechin-(4β ⟶8)-epicatechin; epicatechin-(4 β ⟶8)-epicatechin-(4β ⟶6)-epicatechin], and one tetramer [9, 10] have been isolated and identified from its extract. The antidiabetic properties [11, 12], hypotensive and vasorelaxant activity [13, 14], antiulcer [15, 16], antibacterial activities [17, 18], and antiviral activity [19] of the bark, aerial parts, fruits, crude extract, and fractions have been attributed to the presence of proanthocyanidins.

However, there are no studies on the stability of the constituents of *G. ulmifolia* dried extracts. The determination of proanthocyanidins in bark of *G. ulmifolia* was carried out using HPLC, and it was observed that PB2 and EP compounds can be used as chemical markers for routine quality control analysis (Figure 1) [20].

The stability of the constituents in the extract of *G. ulmifolia* is important because the pharmacological properties depend on the chemical viability of the extract. As pointed out above, the procyanidins are pharmacologically active constituents of *G. ulmifolia*; however, they are unstable condensed tannins [21]. Their stability is affected by several factors such as pH, storage, temperature, chemical structure, concentration, light, oxygen, solvents, flavonoids, proteins, metallic ions, and the presence of enzymes [21]. A compatibility study of excipients is essential to develop a stable pharmaceutical dosage form, especially when the active agent is unstable.

The aim of the present study was to evaluate the chemical stability of the dried extract from the bark of *Guazuma ulmifolia* Lam. (Sterculiaceae), with and without an added pharmaceutical excipient.

2. Experimental

2.1. Plant Material. Bark of *Guazuma ulmifolia* Lam., Sterculiaceae, was collected in August 2005 in the city of Jataizinho, state of Paraná, Brazil (S 23°18′26.1″; W 050°58′19.4″; 377 m altitude; Garmin v.2.24). The species was identified by Professor Dr. Cássia Mônica Sakuragui. Voucher specimens are deposited in the herbarium of the Department of Biology of the State University of Maringá under number HUEM 12.051.

2.2. Chemicals and Reagents. All reagents and solvents were of analytical and HPLC grade, including ethyl acetate and trifluoroacetic acid (TFA) (Merck, Darmstadt, Germany). Ultra-pure water obtained by a Milli-Q UF-Plus apparatus (Millipore, Bedford, USA) with conductivity of 18.2 MΩ·cm at 25°C was used in all experiments. Epicatechin (EP) (Sigma, USA) and procyanidin B2 (PB2) (isolated and certified by spectroscopic methods at the Pharmacognosy Laboratory of Maringá State University) of the highest grade (purity > 99.0%) were used as standards. Colloidal silicon dioxide (CSD) was purchased from Degussa (Essen, Germany). All other solvents and chemicals were of analytical grade.

2.3. Preparation of Extracts. Air-dried stem bark (900 g) was exhaustively extracted with 9.0 L of Me_2CO-H_2O (7 : 3) by turbo-extraction (Ultra-Turrax model UTC115KT; IKA; USA) for 20 min at ≤40°C. The extractive dispersion was filtered and evaporated under reduced pressure to 1.0 L and freeze-dried (Christ model Alpha 1-2, Germany), yielding 120 g of crude extract (CE). One gram of CE was dissolved in a mixture of 10 mL water and 400 mg of CSD was added [22]. This mixture (CEA) was freeze-dried under the same conditions described for CE.

2.4. Stability Study. CE and CEA were evaluated for thermal stability under accelerated conditions for 21 days [23]. Samples of the CE and CEA were weighed (200 mg) and packaged in opaque white polyethylene flasks with a capacity of 10 g. The CE and CEA samples were stored in a climate chamber (BINDER, model KBF 240, USA) with a constant relative humidity of 75 ± 5% and maintained at 45 ± 2°C, without direct light. Samples were analyzed at the initial time (t_0) and 2, 7, 14, and 21 days after exposure to the atmospheric conditions described above.

2.5. HPLC Analysis. Accurately weighed 50 mg of CE and 70 mg of CEA were dissolved in 500 μL water, mixed in a tube shaker, and extracted with 500 μL of ethyl acetate, in a microtiter shaker at 1800 rpm (Minishaker, model MS1, IKA, USA) for 3 min (n = 9). Tubes were placed in a refrigerated microcentrifuge (model 5415R, Eppendorf, USA) at 4000 rpm, for 4 min at 5°C, for the total separation of the phases. The ethyl-acetate phase was separated. After evaporation of the solvent and drying under air flow, the residue was reconstituted to 10 mL with methanol : water (1 : 1) (test solution-SS). The sample was filtered through a 0.5 μm membrane filter (Millipore, Bedford, USA).

The analyses were carried out using a HPLC system (Gilson, USA) consisting of a solvent delivery pump (Model 321), a variable wavelength UV/VIS detector (Model 156), a manual injection valve (Rheodyne, USA) with a 20 μL loop, degasser (Model 184), and a thermostated column compartment (Model 831). Data collection and analyses were performed using UniPoint LC System software (Gilson, Villiers-le-Bel, France). A gradient was eluted on a Phenomenex Gemini C-18 column (250 mm × 4.6 mm) (Phenomenex International, USA), 5 μm particle size, Phenomenex SecurityGuard (C-18 cartridge) (20 mm × 4.6 mm). The mobile phase consisted of water (0.05% TFA) as solvent A and acetonitrile (0.05% TFA) as solvent B, and both were degassed and filtered through a 0.45 μm pore size filter (Millipore, Bedford, USA). Separations were affected by a gradient as follows: 0 min 13% B in A; 10 min 17% B; 16 min 18.35% B; 20 min 22.65% B; 23 min 29.81% B; 25 min 65% B; followed by a 7 min reequilibration time. The mobile-phase flow rate was 0.8 mL/min, and the injection volume was 20 μL. The chromatographic runs were carried out at 28°C. UV detection was performed at 210 nm.

The purity of peaks was checked by a Diode Array Detector coupled to a Varian ProStar module (Varian, Palo Alto, CA, USA) with ProStar 210 Solvent Delivery and a

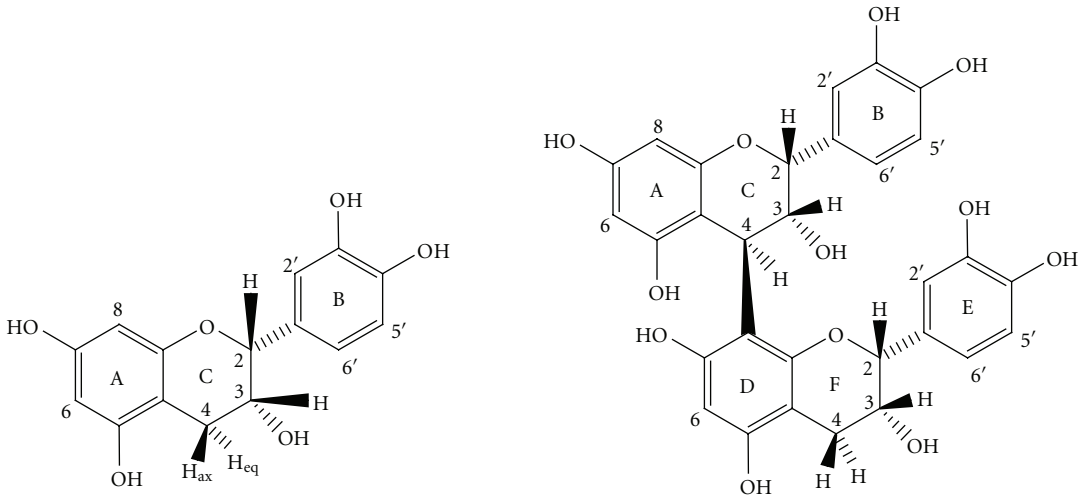

Epicatechin (EP)

Epicatechin-(4β ⟶ 8)-epicatechin (PB2)

Figure 1: Chemical markers of the *G. ulmifolia* dried extracts.

ProStar 335 HPLC-DAD, comparing the UV spectra of each peak with those of authentic reference samples.

An EP reference standard stock solution of 400 μg/mL was prepared in methanol : water (1 : 1). Calibration standard solutions at five levels were prepared by serially diluting the stock solution to concentrations of 10.00, 40.00, 70.00, 100.00, and 120.00 μg/mL. A PB2 stock solution of 250 μg/mL was prepared in methanol : water (1 : 1). Calibration standard solutions at seven levels were prepared by serially diluting the stock solution to concentrations of 20.00, 40.00, 50.00, 70.00, 90.00, 120.00, and 150.00 μg/mL. The samples were filtered through a 0.5 μm membrane (Millipore, Bedford, USA) prior to injection. Each analysis was repeated five times, and the calibration curves were fitted by linear regression [20].

2.6. Thermogravimetry (TG). A simultaneous thermal analysis (STA) system (NETZSCH, model STA 409 PG/4/G Luxx, USA) was used for recording the TG curves of the CE and CEA. About 10 mg of sample was weighed accurately using an STA balance. The weighed sample was heated in a closed aluminum pan at a programmed rate of 10°C/min in a temperature range from 30 to 500°C under a nitrogen flow of 50 mL/min. An empty aluminum pan was used as a reference.

2.7. Total Tannins. The percentage of total tannins in CE and CEA at t_0 and day 21 was evaluated using the Folin-Ciocalteau reagent and following a method from the British Pharmacopoeia [24]. Samples of 100 mg and 166 mg of CE and CEA, respectively, were employed. Each analysis was repeated three times.

2.8. Statistical Analysis. Experimental data were analyzed by one-way ANOVA, and the statistical significance of means was determined by the LSD and Tukey's HSD tests. The Dunnett test was employed to compare contents on different days of the analyses. Differences were considered significant at $P < 0.05$.

3. Results and Discussion

Two dried extracts of *G. ulmifolia*, prepared by different techniques (with or without CSD), were evaluated for the stability of their main components (markers): PB2 and EP.

The development of analytical conditions for the analyses herbal drugs and pharmaceutical formulations containing these extracts must necessarily go through a specific validation. In previous work, a rapid and robust LC assay for separation and quantitative analysis of PB2 and EP in extract of *G. ulmifolia* was developed. The method was validated by regulation RE 899/2003 of the National Health Surveillance Agency, Brazil, and the ICH guidelines [20].

Considering that the stability assay was developed with the aim to get an initial response about the chemical stability of the extracts for research and development purposes, the used protocol allowed the extracts to be evaluated under accelerated conditions [25].

Quantification of these markers in the samples in the test of stability was carried out using external standards (PB2 and EP). In the evaluation of linearity, based on $1/x$-weighted linear regression analysis, the responses for both standards in related concentration ranges were linear. The calibration equations were $Y = 818.21x - 2177.9$ ($n = 7$, $R = 0.9990$) for PB2 and $Y = 885.51x + 953.56$ ($n = 5$, $R = 0.9994$) for EP. The RSDs of the slopes were ≤5% for both analytes ($n = 5$).

No degradation in the CE and CEA samples under stress conditions was observed. No changes in the chromatographic profile occurred during the period of analysis (Figure 2).

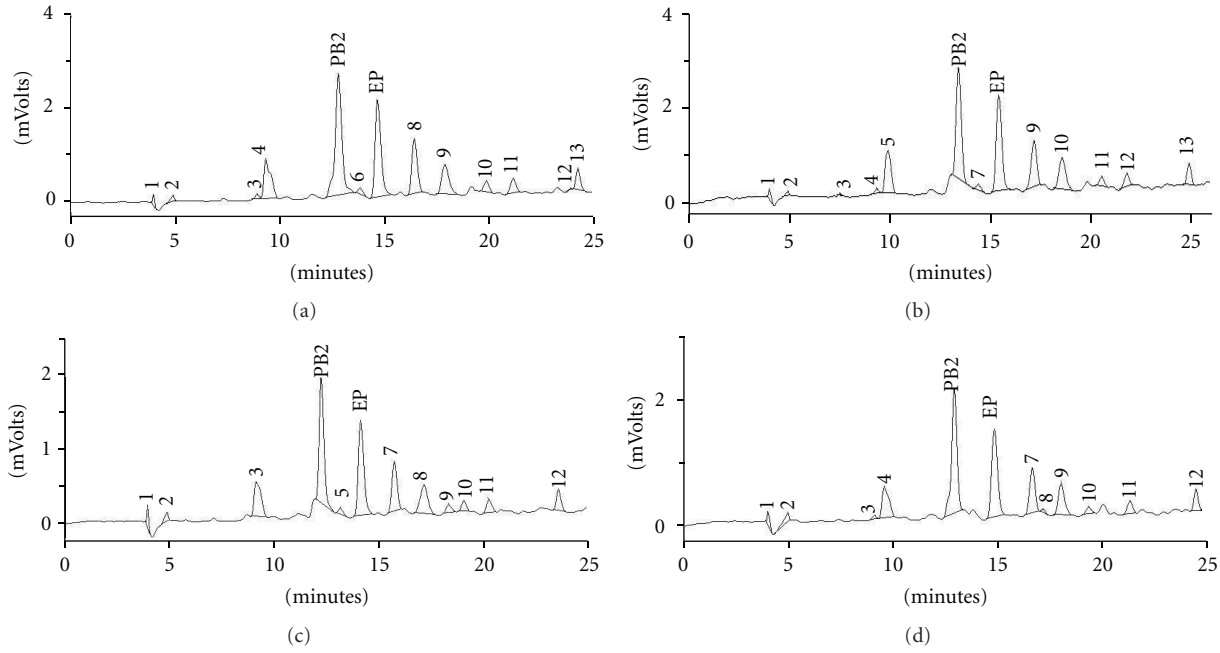

Figure 2: Typical HPLC chromatograms of stress test samples of the crude extract (CE) and the crude extract + colloidal silicon dioxide (CEA) of *Guazuma ulmifolia*. (a) CE at time zero; (b) CE at day 21; (c) CEA at time zero; (d) CEA at day 21.

The peak purity test confirmed that the PB2 and EP peaks remained homogeneous and pure throughout the stress test (data analyzed under DAD). The UV spectra of the compounds (PB2 and EP) did not change between the beginning and end of elution of their individual values, confirming the absence of degradation products.

The chemical stability assay of the CE and CEA dried-extract formulations was determined according to the concentration of PB2 and EP at a storage temperature of 45°C and 75% humidity for 21 days. The final concentration was expressed as μg/mL of PB2 and EP in the dried extract (Table 1).

Figure 3 shows the mean values of the PB2 and EP in the CE and CEA samples for each day of storage analyzed.

The PB2 content remained constant after 21 days of storage, in both the CE and CEA. The EP in the CEA showed a significant change ($P < 0.05$) in concentration from t_0 to day 21. However, no significant change in the concentration of EP was observed in the CE stored under the same conditions.

Figure 4 shows the influence of the presence of the excipient in the dried extract. Apparently, the physical and chemical properties of the CSD can significantly accelerate the increase of EP in the CEA after 21 days. In relation to the concentration of PB2, there was no significant difference between the CE and CEA during the 21 days of analysis.

Proanthocyanidins are commonly composed of monomers of catechin and/or epicatechin with linkages of 4⟶6 and/or 4⟶8. Besides these, other monomers are common: gallocatechin, epigallocatechin, robinetinidin, and fisetinidin [26]. Proanthocyanidins differ structurally according to the number of hydroxyl groups present at aromatic rings

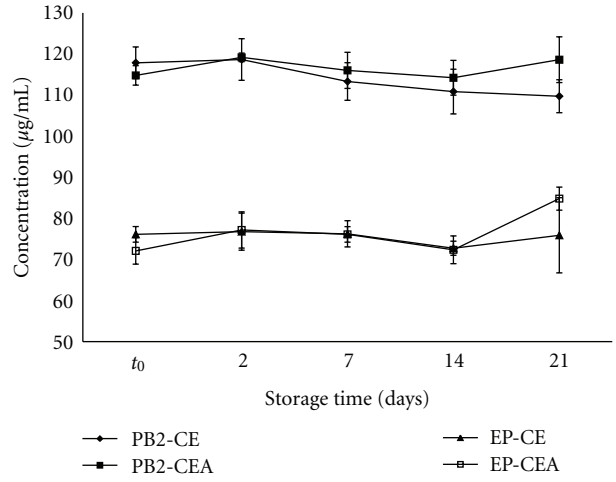

Figure 3: The stability of the crude extract (CE) and the crude extract + colloidal silicon dioxide (CEA) of *Guazuma ulmifolia* at 45°C, 75% relative humidity and 21 days.

and the stereochemistry of the asymmetric carbons of the heterocyclic nucleus. The presence of *O*-methylation, *O*-glycosylation, and *O*-galloylation increase the structural complexity [27].

PB2 is a dimeric proanthocyanidin with chemical linkage of the type 4β ⟶8. Fletcher et al. [28] showed by NMR studies of the procyanidin peracetate that linkages 4⟶6 and 4⟶8 are found in two energetically protected conformations. Therefore, the linkage between epicatechin monomers forming the PB2 may be physically more stable.

Table 1: Stability of the constituents procyanidin B2 (PB2) and epicatechin (EP) of the dried extract of *Guazuma ulmifolia*. Mean ± SD (RSD %).

Days of storage	CE (mg/mg)		CEA (mg/mg)	
	PB2	EP	PB2	EP
Time zero	0.0236 ± 4.5 (3.8)	0.0152 ± 1.4 (1.9)	0.0230 ± 2.7 (2.3)	0.0144 ± 2.3 (3.2)
2	0.0237 ± 6.0 (5.1)	0.0154 ± 3.5 (4.5)	0.0238 ± 1.2 (1.0)	0.0154 ± 3.4 (4.4)
7	0.0226 ± 5.2 (4.6)	0.0152 ± 2.4 (3.2)	0.0232 ± 5.1 (4.4)	0.0152 ± 1.4 (1.9)
14	0.0221 ± 10.5 (9.4)	0.0147 ± 1.2 (1.7)	0.0228 ± 4.8 (4.2)	0.0145 ± 2.4 (3.4)
21	0.0220 ± 9.9 (9.0)	0.0152 ± 6.9 (9.1)	0.0237 ± 7.8 (6.6)	0.0170 ± 2.4 (2.8)

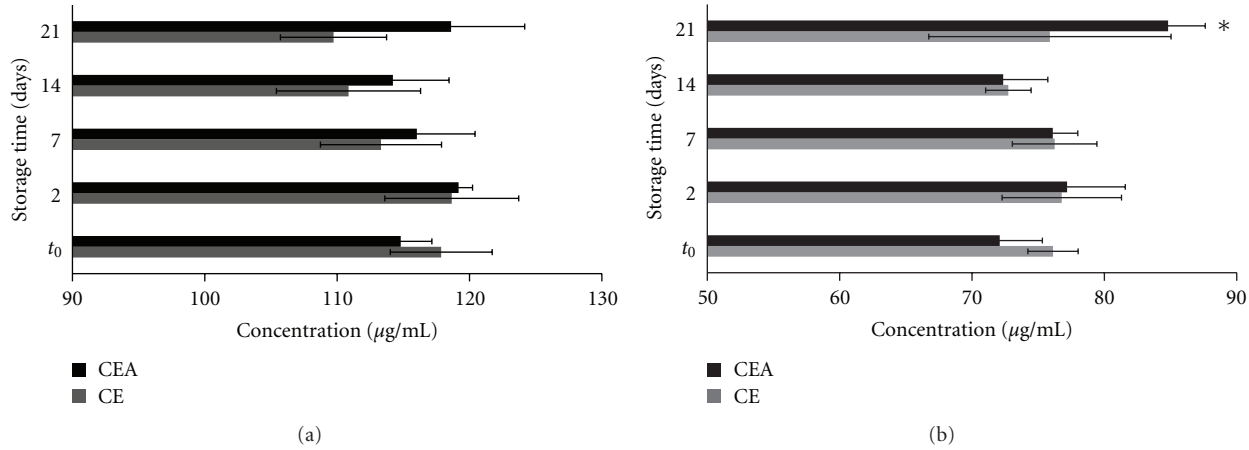

Figure 4: Influence of colloidal silicon dioxide on the dried-extract (CE and CEA) of *Guazuma ulmifolia.* (a) procyanidin B2 (PB2) and (b) epicatechin (EP).

The significant change in concentration of EP in the CEA probably occurred by physical interaction of oligomers and/or polymers of condensed tannins in the extract and CSD. This excipient has a large surface area and a high polarity of silanol groups present on its surface, which leads to adsorption of water and formation of hydrogen bonds [29], facilitated by its hygroscopic property [30]. Therefore, CSD is commonly used as a desiccant agent to protect hygroscopic chemicals and drugs from atmospheric moisture [29]. Thus, this excipient is an excellent candidate adjuvant for the stabilization of plant extracts.

Extracts rich in phenolic substances are congruent with this assumption because they are rich in hydroxyls, capable of hydrogen bond interactions. Döner et al. [31] evaluated the bonding between polyvinylpolypyrrolidone (PVP) and different classes of flavonoids. The bonding increases with the number of hydroxyl groups present in the flavonoid nucleus. Compounds that contain 7- and 4′-hydroxyl groups bond most effectively; the same principle can be extrapolated to the CEA. The increase in the concentration of EP in the CEA (Figure 4(b)) may result from an interaction by hydrogen bonding between oligomers and/or polymers of the condensed tannins and the silanol hydroxyl group of CSD.

Gore and Banker [29] observed that silica has the ability to form a monolayer adsorption of water vapor, suggesting that polar water molecules are adsorbed at specific sites on the silica surface. Oligomeric flavonols and polymers of condensed tannins may show the same pattern of connection to the CSD. Bonding of these substances with CSD would weaken the bonds within the compound, releasing monomeric substances. This would explain the statistical difference found at day 21.

However, the analyses of the total tannin content of CE and CEA at time t_0 and day 21 after the stress tests showed no significant differences. The results for CE were 26.1% ± 0.5 (RSD% 2.0) and 26.6% ± 0.8 (RSD% 3.0), and for CEA were 25.0% ± 1.2 (RSD% 4.9) and 25.4% ± 0.7 (RSD% 2.8) at times t_0 and day 21, respectively.

These results suggest that the physical interactions occurred in the extract CEA produced no alterations in the content of proanthocyanidin. However, they show that the quality control of extracts containing high content of phenolic compounds must be accomplished using dimeric compounds, which are more physically stable.

Figure 5 and Table 2 show the TG data in the temperature range from 25 to 500°C for the CE and CEA. TG curves of CE and CEA presented a characteristic profile of elimination of water surface between 35 and 100°C, thermal stability between 100 and 185°C, following thermal decomposition. The thermal decomposition of CEA occurs in two stages, (Δm_2 = 4.80% and DTG_{peak} = 213°C and Δm_3 = 19.79%

Table 2: Thermogravimetry parameters of the crude extract (CE) and the crude extract + colloidal silicon dioxide (CEA) of *Guazuma ulmifolia*.

Sample	Mass loss (%)	Days of storage				
		t_0	2	7	14	21
CE	1	3.68	4.44	4.51	4.85	4.90
	2	9.70	8.44	8.98	8.38	8.27
	3	32.46	33.06	32.29	31.79	30.75
	Total mass loss (%)	45.87	46.22	46.81	45.45	44.85
CEA	1	2.31	3.54	3.11	2.07	2.36
	2	4.80	4.15	5.13	4.85	4.97
	3	19.79	19.39	20.89	18.98	19.21
	Total mass loss (%)	27.33	27.60	29.47	26.03	26.93

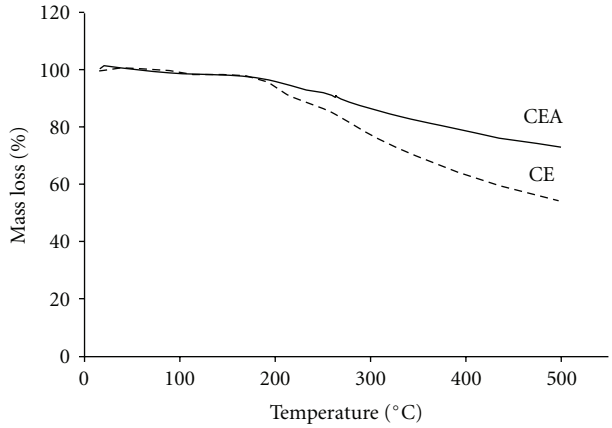

Figure 5: Thermogravimetry curves for the (dashed line) crude extract (CE) and (staked line) crude extract + colloidal silicon dioxide (CEA) of *Guazuma ulmifolia* at time zero.

and DTG_{peak} = 340°C). A similar thermal decomposition was observed for CEA. However, TG curves of CE presented mass losses greater than those of CEA (Δm_2 = 9.70% and DTG_{peak} = 218°C and Δm_3 = 32.46% and DTG_{peak} = 336°C).

The TG analysis indicated no trend in the behavior of CE and CEA, that is, during the days of analysis, the total mass underwent no significant increase or decrease.

The analysis of these data leads us to suppose that CSD conferred some stability, because the CEA lost significantly less total mass. It can be assumed that the CEA was protected from heat to some extent by the CSD, influencing the process of degradation, with smaller percentages of loss of mass from the fusion of chemicals. Thus, we can conclude that the CSD limited the access of water to the extract and/or prevented its degradation [32, 33].

Over the 21 days of the study, there was no significant difference between the two extracts, but considering the TG data and the high temperatures involved, the data suggest that over the long term the CSD would be a good protector for the plant extracts of *G. ulmifolia*. However, further studies should be performed to confirm these results.

As a conclusion, PB2 is an appropriate compound to use as a chemical marker in quality control of the dried extract of *G. ulmifolia*. The stress test showed that the content of total tannins was unchanged. Therefore, in this 21-day screening study, proanthocyanidins in the dried extract of the *G. ulmifolia* showed good compatibility with CSD under stress conditions.

Conflict of Interests

The authors declare that there is no conflict of interests.

Acknowledgments

The authors thank the Brazilian funding agencies CNPq (Conselho Nacional de Desenvolvimento Científico e Tecnológico), Fundacão Araucária, INCT_if, and CAPES (Coordenação de Aperfeiçoamento de Pessoal de Nível Superior). They express gratitude to Professor Dr. Antonio Medina Neto and Professor Dr. Jurandir Hillmann Rohling for technical support with TG, to Dr. Janet W. Reid for revising the English text, and to Professor Dr. Adolf Nahrstedt for contributions.

References

[1] World Health Organization, "International Stability Testing: guidelines for stability testing of pharmaceutical products containing well established drug substances in conventional dosage forms," WHO Technical Report Series 863, 1996, Annex 5.

[2] G. Chawla and A. K. Bansal, "Molecular mobility and physical stability of amorphous irbesartan," *Scientia Pharmaceutica*, vol. 77, no. 3, pp. 695–709, 2009.

[3] A. A. S. Araújo, S. Storpirtis, L. P. Mercuri, F. M. S. Carvalho, M. Santos Filho, and J. R. Matos, "Thermal analysis of the antiretroviral zidovudine (AZT) and evaluation of the compatibility with excipients used in solid dosage forms," *International Journal of Pharmaceutics*, vol. 260, no. 2, pp. 303–314, 2003.

[4] Z. R. Dedania, R. R. Dedania, N. R. Shetha, J. B. Patel, and B. Patel, "Stability indicating HPLC determination of Risperidone in bulk drug and pharmaceutical formulations,"

International Journal of Analytical Chemistry, vol. 2011, Article ID 124917, 6 pages, 2011.

[5] A. K. Shah, B. A. Avery, and C. M. Wyandt, "Content analysis and stability evaluation of selected commercial preparations of St. John's wort," *Drug Development and Industrial Pharmacy*, vol. 31, no. 9, pp. 907–916, 2005.

[6] P. Jin, S. Madieh, and L. L. Augsburger, "The solution and solid state stability and excipient compatibility of parthenolide in feverfew," *AAPS PharmSciTech*, vol. 8, no. 4, article 105, 2007.

[7] Y. Liu and P. A. Murphy, "Alkamide stability in *Echinacea purpurea* extracts with and without phenolic acids in dry films and in solution," *Journal of Agricultural and Food Chemistry*, vol. 55, no. 1, pp. 120–126, 2007.

[8] S. Gafner and C. Bergeron, "The challenges of chemical stability testing of herbal extracts in finished products using state-of-the-art analytical methodologies," *Current Pharmaceutical Analysis*, vol. 1, pp. 203–215, 2005.

[9] M. Hör, M. Heinrich, and H. Rimpler, "Proanthocyanidin polymers with antisecretory activity and proanthocyanidin oligomers from *Guazuma ulmifolia* bark," *Phytochemistry*, vol. 42, no. 1, pp. 109–119, 1996.

[10] J. C. B. Rocha, F. Pedrochi, L. Hernandes, J. C. P. de Mello, and M. L. Baesso, "Ex vivo evaluation of the percutaneous penetration of proanthocyanidin extracts from *Guazuma ulmifolia* using photoacoustic spectroscopy," *Analytica Chimica Acta*, vol. 587, no. 1, pp. 132–136, 2007.

[11] F. J. Alarcon-Aguilara, R. Roman-Ramos, S. Perez-Gutierrez, A. Aguilar-Contreras, C. C. Contreras-Weber, and J. L. Flores-Saenz, "Study of the anti-hyperglycemic effect of plants used as antidiabetics," *Journal of Ethnopharmacology*, vol. 61, no. 2, pp. 101–110, 1998.

[12] A. J. Alonso-Castro and L. A. Salazar-Olivo, "The anti-diabetic properties of *Guazuma ulmifolia* Lam are mediated by the stimulation of glucose uptake in normal and diabetic adipocytes without inducing adipogenesis," *Journal of Ethnopharmacology*, vol. 118, no. 2, pp. 252–256, 2008.

[13] C. Caballero-George, P. M. Vanderheyden, T. De Bruyne et al., "In vitro inhibition of [3H]-angiotensin II binding on the human AT1 receptor by proanthocyanidins from *Guazuma ulmifolia* bark," *Planta Medica*, vol. 68, no. 12, pp. 1066–1071, 2002.

[14] G. A. Magos, J. C. Mateos, E. Páez et al., "Hypotensive and vasorelaxant effects of the procyanidin fraction from *Guazuma ulmifolia* bark in normotensive and hypertensive rats," *Journal of Ethnopharmacology*, vol. 117, no. 1, pp. 58–68, 2008.

[15] M. Hör, H. Rimpler, and M. Heinrich, "Inhibition of intestinal chloride secretion by proanthocyanidins from *Guazuma ulmifolia*," *Planta Medica*, vol. 61, no. 3, pp. 208–212, 1995.

[16] B. Berenguer, C. Trabadela, S. Sánchez-Fidalgo et al., "The aerial parts of *Guazuma ulmifolia* Lam. protect against NSAID-induced gastric lesions," *Journal of Ethnopharmacology*, vol. 114, no. 2, pp. 153–160, 2007.

[17] A. Camporese, M. J. Balick, R. Arvigo et al., "Screening of anti-bacterial activity of medicinal plants from Belize (Central America)," *Journal of Ethnopharmacology*, vol. 87, no. 1, pp. 103–107, 2003.

[18] M. C. Navarro, M. P. Montilla, M. M. Cabo et al., "Antibacterial, antiprotozoal and antioxidant activity of five plants used in izabal for infectious diseases," *Phytotherapy Research*, vol. 17, no. 4, pp. 325–329, 2003.

[19] A. M. M. Felipe, V. P. Rincão, F. J. Benati et al., "Antiviral effect of *Guazuma ulmifolia* and Stryphnodendron adstringens on poliovirus and bovine herpesvirus," *Biological and Pharmaceutical Bulletin*, vol. 29, no. 6, pp. 1092–1095, 2006.

[20] G. C. Lopes, M. L. Bruschi, and J. C. P. de Mello, "RP-LC-UV determination of proanthocyanidins in *Guazuma ulmifolia*," *Chromatographia*, vol. 69, supplement 2, pp. S175–S181, 2009.

[21] A. Castañeda-Ovando, M. D. L. Pacheco-Hernandez, M. E. Páez-Hernández, J. A. Rodríguez, and C. A. Galán-Vidal, "Chemical studies of anthocyanins: a review," *Food Chemistry*, vol. 113, no. 4, pp. 859–871, 2009.

[22] K. C. B. De Souza, P. R. Petrovick, V. L. Bassani, and G. González Ortega, "The adjuvants Aerosil 200 and Gelita-Sol-P influence on the technological characteristics of spray-dried powders from *Passiflora edulis* var. flavicarpa," *Drug Development and Industrial Pharmacy*, vol. 26, no. 3, pp. 331–336, 2000.

[23] M. V. R. Velasco, C. R.M. Maciel, F. D. Sarruf et al., "Desenvolvimento e Teste Preliminar da Estabilidade de formulaç ões cosméticas acrescidas de extrato comercial de *Trichilia catigua* Adr. Juss (e) *Ptychopetalum olacoides* Bentham," *Revista de Ciencias Farmaceuticas Basica e Aplicada*, vol. 29, no. 2, pp. 179–194, 2008.

[24] British Pharmacopoeia Commission, *British Pharmacopoeia*, The Stationary Office, 2008.

[25] H. C. Ansel, N. G. Popovich, and L. V. Allen Jr., *Farmacotécnica. Formas Farmacêuticas e Sistemas de Liberação de Fármacos*, Editorial Premier, 6th edition, 2000.

[26] G. C. Lopes, F. A. V. Machado, C. E. M. Toledo, C. M. Sakuragui, and J. C. P. de Mello, "Chemotaxonomic significance of 5-deoxyproanthocyanidins in *Stryphnodendron* species," *Biochemical Systematics and Ecology*, vol. 36, no. 12, pp. 925–931, 2008.

[27] T. De Bruyne, L. Pieters, H. Deelstra, and A. Vlietinck, "Condensed vegetable tannins: biodiversity in structure and biological activities," *Biochemical Systematics and Ecology*, vol. 27, no. 4, pp. 445–459, 1999.

[28] A. C. Fletcher, L. J. Porter, E. Haslam, and R. K. Gupta, "Plant proanthocyanidins. Part 3. Conformational and configurational studies of natural procyanidins," *Journal of the Chemical Society, Perkin Transactions 1*, no. 14, pp. 1628–1637, 1977.

[29] A. Y. Gore and G. S. Banker, "Surface chemistry of colloidal silica and a possible application to stabilize aspirin in solid matrixes," *Journal of Pharmaceutical Sciences*, vol. 68, no. 2, pp. 197–202, 1979.

[30] A. H. Kibbe, *Handbook of Pharmaceutical Excipients*, London, UK, 3rd edition, 2000.

[31] L. W. Döner, G. Bécard, and P. L. Irwin, "Binding of flavonoids by polyvinylpolypyrrolidone," *Journal of Agricultural and Food Chemistry*, vol. 41, no. 5, pp. 753–757, 1993.

[32] T. F. Moura, D. Gaudy, M. Jacob, A. Terol, B. Pauvert, and A. Chauvet, "Vitamin C spray drying: study of the thermal constraint," *Drug Development and Industrial Pharmacy*, vol. 22, no. 5, pp. 393–400, 1996.

[33] E. A. F. Vasconcelos, M. G. F. Medeiros, F. N. Raffi, and T. F. A. L. Moura, "Influência da temperatura de secagem e da concentração de Aerosil®200 nas características dos extratos secos por aspersão da *Schinus terebinthifolius* Raddi (Anacardiaceae) ," *Revista Brasileira de Farmacognosia*, vol. 15, pp. 243–249, 2005.

Hindawi Publishing Corporation
International Journal of Analytical Chemistry
Volume 2012, Article ID 431954, 5 pages
doi:10.1155/2012/431954

Research Article

Apolar Compounds in Seaweeds from Fernando de Noronha Archipelago (Northeastern Coast of Brazil)

Leandro De Santis Ferreira,[1] Izabel Cristina Casanova Turatti,[1] Norberto Peporine Lopes,[1] Thais Guaratini,[2] Pio Colepicolo,[3] Eurico Cabral Oliveira Filho,[4] and Ricardo Clapis Garla[5]

[1] *Departamentos de Física e Química, Faculdade de Ciências Farmacêuticas de Ribeirão Preto, Universidade de São Paulo, 14040-903 Ribeirão Preto, SP, Brazil*
[2] *Lychnoflora Pesquisa e Desenvolvimento em Produtos Naturais LTDA, Incubadora SUPERA, Campus da USP, 14040-900 Ribeirão Preto, SP, Brazil*
[3] *Instituto de Química, Universidade de São Paulo, 05513-970 São Paulo, SP, Brazil*
[4] *Instituto de Biociências, Universidade de São Paulo, P.O. Box 11461, 05508-090 São Paulo, SP, Brazil*
[5] *Departamento de Oceanografia e Limnologia, Centro de Biociências, Universidade Federal do Rio Grande do Norte, 59072-970 Natal, RN, Brazil*

Correspondence should be addressed to Ricardo Clapis Garla, rgarla@hotmail.com

Received 31 August 2011; Revised 11 November 2011; Accepted 16 November 2011

Academic Editor: Ricardo Vessecchi

Hyphenated techniques of gas chromatography coupled to mass spectrometer were used to determine fatty acids in eleven species of seaweeds from Fernando de Noronha archipelago. The main compounds detected in all studied species were the alcohol phytol and the fatty acids 14 : 0; 15 : 0; 16 : 0; 18 : 0; 18 : 1 n^9; 18 : 2 $\Delta^{9,12}$; 20 : 4; 20 : 5. These fatty acids are commonly found in seaweeds present in warm regions. Thus, we found no specificity in the presence of a particular set of fatty acids and the studied species indicating that they are not useful as taxonomic indicators. However, they could be used in a comparative study with algae found in polluted area because many of the studied seaweeds are widespread and Fernando de Noronha has low human influence.

1. Introduction

Seaweeds are key ecological factors in shallow marine areas forming the base of the trophic web and structuring ecosystems especially on consolidated substrata. They are known by the production of many bioactive compounds. Hence, the pharmaceutical and the cosmetics industries have a special interest in algae as sources of specific molecules [1–4]. Also, several works have investigated their value in human and animal nutrition [5–8]. Among the algae-derived compounds, polyunsaturated fatty acids are especially important as they act as antioxidant agents involved in many physiological processes [9, 10].

The studies to determine the fatty acids profiles started some years before and many of them focused on the use of these compounds as biomarkers for chemotaxonomy, though their concentration may be susceptible to environmental interference [11–14]. Some of the main important factors that influence the algae fatty acid concentration are the temperature, [15, 16], types of habitat [15, 17], and presence of metals and pollutants [12, 13, 18]. Although less common, other approaches using fatty acids have explored the effects of industrial effluents and environmental variables on the amount and quality of fatty acids produced [19, 20] and their role in food assimilation by herbivorous invertebrates [21].

Fernando de Noronha archipelago is an isolated group of islands formed by relatively recent volcanic processes. The islands are located approximately 350 km off the northeastern Brazilian coast and are part of Pernambuco State [22]. The archipelago was established as a marine protected area since 1988, and its marine flora is composed of 128 taxa, including

Table 1: Classification for the eleven species of seaweeds from Fernando de Noronha archipelago in northeastern Brazil analyzed in this study.

Divisions and species
Chlorophyta
Caulerpa verticillata J. Agardh, 1847
Rhodophyta
Asparagopsis taxiformis (Delile) Trevisan de Saint-Léon, 1845
Dictyurus occidentalis J. Agardh, 1847
Dichotomaria marginata (J. Ellis & Solander) Lamark, 1816
Dichotomaria obtusata (J. Ellis & Solander) Lamarck, 1816
Galaxaura rugosa (J. Ellis & Solander) J. V. Lamouroux, 1816
Ochrophyta
Dictyota cervicornis Kützing, 1859
Dictyopteris justii J. V. Lamouroux, 1809
Dictyopteris plagiogramma (Montagne) Vickers, 1905
Padina gymnospora (Kützing) Sonder, 1871
Sargassum sp.

Table 2: Saturated fatty acids present in the eleven seaweeds studied.

Fatty Acids	At	Gr	Db	Dm	Do	Cv	Dc	Dj	S	Pg	Dp
12 : 0	−	−	−	−	−	+	+	+	−	−	−
14 : 0	+	+	+	+	+	+	+	+	+	+	+
15 : 0	+	+	+	+	+	+	+	+	+	+	+
16 : 0	+	+	+	+	+	+	+	+	+	+	+
17 : 0	+	+	−	+	+	+	+	+	+	+	+
18 : 0	+	+	+	+	+	+	+	+	+	+	+
20 : 0	+	+	+	+	+	−	+	+	+	+	+
22 : 0	+	+	+	+	−	−	−	+	+	+	+
24 : 0	+	+	+	+	−	+	−	+	+	−	−

+ presence; − absence. At : *Asparagopsis taxiformis*; Gr : *Galaxaura rugosa*; Db : *Dichotomaria obtusata*; Dm : *Dichotomaria marginata*; Do : *Dictyurus occidentalis*; Cv : *Caulerpa verticillata*; Dc : *Dictyota cervicornis*; Dj : *Dictyopteris justii*; S : *Sargassum* sp.; Pg : *Padina gymnospora*; Dp : *Dictyopteris plagiogramma*.

44 species of Chlorophyta, 62 of Rhodophyta, and 22 of Phaeophyta [23]. The most abundant benthic algae groups found in the archipelago are represented by the families Dictyotaceae and Sargassaceae. Other seaweeds also commonly found are the green algae *Caulerpa verticillata* and red algae *Galaxaura* spp. [23, 24]. As part of a broader research project aimed to study chemical compounds of seaweeds from Fernando de Noronha, herein is provided baseline information on the fatty acids produced by eleven species commonly found in the archipelago.

2. Experimental

2.1. Field Collection. A list of the studied species is presented in Table 1. Samples were collected between February and March 2006 at two sites of the main island, Caieiras Beach (3°50′18.8″S, 32°23′57.3″W) and Sueste Bay (3°52′1.2″S, 32°25′19.7″W). Research permit from the Brazilian Environmental Agency (IBAMA) to collect algae was registered under number 050/2006. Seaweeds were randomly collected by hand by uprooting the whole plant, which were placed in labeled plastic bags, frozen, and sent to the laboratory. The algae were identified, cleaned from epiphytes, animals, and sediment, washed with distilled water, and in an oven at 40°C dried for seven days.

2.2. Preparation of Samples. Ten milliliters (10 mL) of dichloromethane (J. T. Baker, Phillipsburg, NJ, USA) were added to 1 g (dried weight) of each species of algae and submitted to ultrasonic bath for 30 minutes. This procedure was repeated three times and the total extract was concentrated on nitrogen gas. Subsequently, 2.0 mL of 1.0 M sodium methoxide were added to the extract and shaken occasionally during five minutes at 65°C. After cooling the extract, 1.0 mL of water and three samples of 1.0 mL of chloroform (J. T. Baker, Phillipsburg, NJ, USA) was added to each sample, shaken for one minute, and centrifuged at 3000 rpm, or 1612.8 g, to extract methyl esters of the fatty acids. The chloroform phase (3.0 mL), was removed and nitrogen gas was used to evaporate the solvent. Samples were suspended in 1.0 mL ethyl acetate (J. T. Baker, Phillipsburg, NJ, USA), and sodium sulphate anhydrous (Sigma Inc., St. Louis, MO, USA) was added to remove water. This methodology was adapted from Eder et al. [25, 26].

2.3. GC-MS Analysis. Samples were analyzed through GC-MS (gas chromatography coupled to mass spectrometer detector) in a Shimadzu QP2010 with ionization source of 70 eV and fragmentation by electronic ionization (EI). The volume of 1.0 μL for each sample was injected at 220°C in a DBWAX column (30 m × 0.25 mm × 0.25 μm). The analysis occurred with 1-minute sample time in the splitless mode, a column flow of 1.3 mL min^{-1}, a linear velocity of 41.4 cm s^{-1}, and scan between *m/z* 40 and *m/z* 500. Oven's temperature started with 50°C, increasing to 20°C min^{-1} until 200°C, kept in this temperature for 5 minutes, then increased to 5°C min^{-1} until 230°C and kept in this temperature for 30 minutes. For identification of compounds, the peaks were compared with some standards and always consulting the libraries WILEY version no. 7 and NIST version nos. 12 and 62.

3. Results and Discussion

The GC-MS analysis had excellent resolution, and the characteristics of the detected unsaturated and saturated fatty acids are given in Tables 2 and 3. The eleven species have myristic acid (14 : 0), pentadecanoic acid (15 : 0), palmitic acid (16 : 0), stearic acid (18 : 0), oleic acid (18 : 1, n^9), linoleic acid (18 : 2 $\Delta^{9,12}$), arachidonic acid (20 : 4), and eicosapentaenoic acid (20 : 5). The major compounds were hexadecanoic acid methyl ester and phytol, which were detected in all samples analyzed. Other apolar compounds,

Table 3: Unsaturated fatty acids founded in the eleven seaweeds studied.

Fatty Acids	At	Gr	Db	Dm	Do	Cv	Dc	Dj	S	Pg	Dp
14 : 1 n^{5}	−	−	−	−	−	+	−	−	−	−	−
16 : 1 n^{7}	+	+	+	−	+	+	+	+	+	−	−
16 : 1 n^{9}	+	+	−	−	+	+	+	+	+	+	−
16 : 1 n^{9} ETHYL	−	−	−	−	+	−	−	−	−	−	−
16 : 1 $n^{11 \text{ or } 13}$	+	−	−	−	+	+	+	+	+	+	−
16 : 2 $\Delta^{7,10 \text{ or } 9,12}$	+	−	−	−	−	+	−	−	−	−	−
16 : 3 $\Delta^{4,7,10}$	−	−	−	−	−	−	−	+	+	+	+
18 : 1 n^{9}	+	+	+	+	+	+	+	+	+	+	+
18 : 1 $n^{10 \text{ or } 11 \text{ or } 12}$	+	+	+	+	+	+	+	+	+	−	+
18 : 1 $n^{13 \text{ or } 14 \text{ or } 16}$	+	−	−	−	+	+	+	+	−	+	−
18 : 2 $\Delta^{8,11}$	−	−	−	−	−	−	−	+	−	−	−
18 : 2 $\Delta^{9,12}$(E,E) or (Z,Z)	+	+	+	+	+	+	+	+	+	+	+
18 : 3 $\Delta^{6,9,12}$	+	−	−	−	+	+	−	+	+	+	−
18 : 3 $\Delta^{9,12,15}$	+	+	+	−	+	+	+	+	+	+	−
20 : 1 $n^{9 \text{ or } 11}$	−	+	−	−	−	−	−	−	+	+	−
20 : 2 $\Delta^{11,14}$	+	+	−	−	−	+	−	+	+	+	−
20 : 3 $\Delta^{7,10,13 \text{ or } 8,11,14}$	+	−	−	−	+	+	+	+	+	+	−
20 : 4	+	+	+	+	+	+	+	+	+	+	+
20 : 5	+	+	+	+	+	+	+	+	+	+	+
22 : 1 n^{13}	+	−	−	−	−	−	−	−	+	−	−

+ presence; − absence. At: *Asparagopsis taxiformis*; Gr: *Galaxaura rugosa*; Db: *Dichotomaria obtusata*; Dm: *Dichotomaria marginata*; Do: *Dictyurus occidentalis*; Cv: *Caulerpa verticillata*; Dc: *Dictyota cervicornis*; Dj: *Dictyopteris justii*; S: *Sargassum sp.*; Pg: *Padina gymnospora*; Dp: *Dictyopteris plagiogramma*.

Table 4: Other apolar compounds found in seaweed species from Fernando de Noronha.

Compound	At	Gr	Db	Dm	Do	Cv	Dc	Dj	S	Pg	Dp
1-Tetradecanol	−	−	−	+	−	−	−	−	−	−	−
1-Hexadecanol	+	+	+	+	−	−	−	−	+	−	+
1-Hexadecanol-2-methyl	−	−	+	−	−	−	−	−	−	−	−
1-Pentadecanol	−	−	−	+	−	−	−	−	−	−	−
1-Octadecanol	+	+	+	+	−	−	−	−	+	−	+
Phytol	+	+	+	+	+	+	+	+	+	+	+
Hexadecane, 1-iodo	+	−	−	−	−	−	−	−	−	−	−
Benzeneacetamide, N-aminocarbonyl	+	−	−	−	−	−	−	−	−	−	−
3-Buten-2-one, 4-(4-hydroxy-2,2,6-trimethyl-7-oxabicyclo[4.1.0]hept-1-yl)	−	+	+	+	−	−	−	−	+	−	+
Tetrapentacontan,1,54-dibromo	−	−	−	−	−	−	−	−	+	−	−
3-Octyl oxiraneoctanoic acid methyl ester	−	−	−	−	−	−	−	+	−	−	−
1-Docosanol	+	−	−	−	−	−	−	−	−	−	−
Hexadecanamide	+	−	−	−	−	−	−	−	−	−	−
Loliolide	+	+	+	+	−	−	−	−	+	−	+
Isololiolide	+	+	+	+	−	−	−	−	+	−	+

+ presence; − absence. At: *Asparagopsis taxiformis*; Gr: *Galaxaura rugosa*; Db: *Dichotomaria obtusata*; Dm: *Dichotomaria marginata*; Do: *Dictyurus occidentalis*; Cv: *Caulerpa verticillata*; Dc: *Dictyota cervicornis*; Dj: *Dictyopteris justii*; S: *Sargassum* sp.; Pg: *Padina gymnospora*; Dp: *Dictyopteris plagiogramma*.

mainly alcohols, were also identified and are provided in Table 4.

The only seaweed in which 20 : 0 fatty acid was absent was the green algae, *C. verticillata*, and the acid 17 : 0 was absent in only one red algae. There were problems in isomer identification while conducting tentative taxonomic analysis, especially in double and triple bonds of C16 and C18 fatty acids, due to great similarity in retention time and in the molecular fragmentation in mass spectrum.

All compounds detected are common in macroalgae [14]. Few differences were observed in the production of fatty acids by brown, green, and red algae. Also, as only one species of green seaweed was analyzed, this prevents further taxonomic comparisons with brown and red algae. In spite of the fact that GC-MS is a highly efficient and sensitive method of analysis, it was unable to precisely determine which of the polyunsaturated fatty acids with 16 or 18 atoms of carbon was present in each species. Other apolar compounds detected had a more restrict distribution among species, and although most of them were detected in only one species, it was not possible to use them as chemotaxonomy markers, that is, phytol or loliolide. Moreover, the fatty acids referred to as chemotaxonomic agents in previous investigations [14, 17] did not allow discerning brown, green, and red algae in the present study.

Fernando de Noronha is an area subjected to low levels of pollution because it is a marine protected area where anthropic activities are controlled. Hence, it would be interesting to compare the fatty acid profiles obtained in this study with the ones from coastal areas of the main land near of the archipelago region that has different degrees of pollution. For example, *Sargassum* spp. fatty acid profiles or other algae species, which are widely distributed and resistant to environmental changes [20], might be compared to the profiles of specimens collected in areas subjected to agrotoxics, solvents, and metals, as already done by Tewari et al. [19] with mercury. In addition, the baseline information obtained may also be applicable to a long-term ongoing research focusing on the sea urchins, which are important grazers in the archipelago [27], in order to determine possible relationships between the algae species consumed and their assimilation efficiency by those invertebrates.

4. Conclusion

The methodology used allowed determining the fatty acid profile of eleven seaweed species from Fernando de Noronha archipelago. As no specificity was found in the presence of a particular set of fatty acids, these compounds could not be used as taxonomic indicators in this case.

Conflict of Interests

The authors declare that do not have any conflict of interests.

Acknowledgment

The authors thank FAPESP, CAPES, and CNPq for financial support and the Brazilian Environmental Agency (IBAMA) and the Administration of Fernando de Noronha (ADEFN) for providing research permits.

References

[1] R. Martí, M. J. Uriz, and X. Turon, "Seasonal and spatial variation of species toxicity in Mediterranean seaweed communities: correlation to biotic and abiotic factors," *Marine Ecology Progress Series*, vol. 282, pp. 73–85, 2004.

[2] E. Schefuß, G. J. M. Versteegh, J. H. F. Jansen, and J. S. Sinninghe Damsté, "Lipid biomarkers as major source and preservation indicators in SE Atlantic surface sediments," *Deep-Sea Research I*, vol. 51, no. 9, pp. 1199–1228, 2004.

[3] F. Song, X. Fan, X. Xu, J. Zhao, Y. Yang, and J. Shi, "Cadinane sesquiterpenes from the brown Alga Dictyopteris divaricata," *Journal of Natural Products*, vol. 67, no. 10, pp. 1644–1649, 2004.

[4] Q. Xian, H. Chen, H. Liu, H. Zou, and D. Yin, "Isolation and identification of antialgal compounds from the leaves of *Vallisneria spiralis* L. by activity-guided fractionation," *Environmental Science and Pollution Research*, vol. 13, no. 4, pp. 233–237, 2006.

[5] M. P. Viera, J. L. Gómez Pinchetti, G. Courtois de Vicose et al., "Suitability of three red macroalgae as a feed for the abalone *Haliotis tuberculata* coccinea Reeve," *Aquaculture*, vol. 248, no. 1–4, pp. 75–82, 2005.

[6] E. Marinho-Soriano, P. C. Fonseca, M. A. A. Carneiro, and W. S. C. Moreira, "Seasonal variation in the chemical composition of two tropical seaweeds," *Bioresource Technology*, vol. 97, no. 18, pp. 2402–2406, 2006.

[7] L. M. P. Valente, A. Gouveia, P. Rema, J. Matos, E. F. Gomes, and I. S. Pinto, "Evaluation of three seaweeds Gracilaria bursa-pastoris, Ulva rigida and Gracilaria cornea as dietary ingredients in European sea bass (*Dicentrarchus labrax*) *juveniles*," *Aquaculture*, vol. 252, no. 1, pp. 85–91, 2006.

[8] C. Denis, M. Morançais, M. Li et al., "Study of the chemical composition of edible red macroalgae *Grateloupia turuturu* from Brittany (France)," *Food Chemistry*, vol. 119, no. 3, pp. 913–917, 2010.

[9] K. Bouarab, F. Adas, E. Gaquerel, B. Kloareg, J. P. Salaün, and P. Potin, "The innate immunity of a marine red alga involves oxylipins from both the eicosanoid and octadecanoid pathways," *Plant Physiology*, vol. 135, no. 3, pp. 1838–1848, 2004.

[10] Z. B. Aoun, R. B. Said, and F. Farhat, "Anti-inflammatory, antioxidant and antimicrobial activities of aqueous and organic extracts from Dictyopteris membranacea," *Botanica Marina*, vol. 53, no. 3, pp. 259–264, 2010.

[11] K. Uchida and K. Mogi, "Cellular fatty acid spectra of Pediococcus species in relation to their taxonomy," *Journal of General and Applied Microbiology*, vol. 18, no. 2, pp. 109–129, 1972.

[12] J. W. Moore and S. Ramamoorthy, *Heavy Metals in Natural Waters*, Spriger, Berlin, Germany, 1984.

[13] M. Kainz and A. Mazumder, "Effect of algal and bacterial diet on methyl mercury concentrations in zooplankton," *Environmental Science and Technology*, vol. 39, no. 6, pp. 1666–1672, 2005.

[14] S. V. Khotimchenko, V. E. Vaskovsky, and T. V. Titlyanova, "Fatty acids of marine algae from the pacific coast of North California," *Botanica Marina*, vol. 45, no. 1, pp. 17–22, 2002.

[15] V. E. Vaskovsky, S. V. Khotimchenko, B. Xia, and L. Hefang, "Polar lipids and fatty acids of some marine macrophytes from

the yellow sea," *Phytochemistry*, vol. 42, no. 5, pp. 1347–1356, 1996.

[16] L. Iveša, M. Blažina, and M. Najdek, "Seasonal variations in fatty acid composition of *Caulerpa taxifolia* (M. Vahl.) C. Ag. in the northern Adriatic Sea (Malinska, Croatia)," *Botanica Marina*, vol. 47, no. 3, pp. 209–214, 2004.

[17] S. V. Khotimchenko, "Fatty acids of species in the genus *Codium*," *Botanica Marina*, vol. 46, no. 5, pp. 456–460, 2003.

[18] R. Barreiro, L. Picado, and C. Real, "Biomonitoring heavy metals in estuaries: a field comparison of two brown algae species inhabiting upper estuarine reaches," *Environmental Monitoring and Assessment*, vol. 75, no. 2, pp. 121–134, 2002.

[19] A. Tewari, S. Thampan, and H. V. Joshi, "Effect of chlor-alkali industry effluent on the growth and biochemical composition of two marine macroalgae," *Marine Pollution Bulletin*, vol. 21, no. 1, pp. 33–38, 1990.

[20] H. R. Harvey and M. C. Kennicutt II, "Selective alteration of *Sargassum* lipids in anoxic sediments of the Orca Basin," *Organic Geochemistry*, vol. 18, no. 2, pp. 181–187, 1992.

[21] T. E. Cox and S. N. Murray, "Feeding preferences and the relationships between food choice and assimilation efficiency in the herbivorous marine snail *Lithopoma undosum* (Turbinidae)," *Marine Biology*, vol. 148, no. 6, pp. 1295–1306, 2006.

[22] K. M. Knesel, Z. S. Souza, P. M. Vasconcelos, B. E. Cohen, and F. V. Silveira, "Young volcanism in the Borborema Province, NE Brazil, shows no evidence for a trace of the Fernando de Noronha plume on the continent," *Earth and Planetary Science Letters*, vol. 302, pp. 38–50, 2011.

[23] G. Pedrini, Y. Ugadim, M. R. A. Braga, and S. M. B. Pereira, "Algas Marinhas bentônicas do Arquipélago de Fernando de Noronha, Brasil," *Boletim de Botânica da USP*, vol. 13, pp. 93–101, 1992.

[24] V. R. Eston, A. E. Migotto, E. C. Oliveira Filho, S. A. Rodrigues, and J. C. Freitas, "Vertical distribution of benthic marine organisms on rocky coasts of the Fernando de Noronha Archipelago (Brazil)," *Boletim do Instituto Oceanográfico de São Paulo*, vol. 34, pp. 37–53, 1986.

[25] K. Eder, "Gas chromatographic analysis of fatty acid methyl esters," *Journal of Chromatography B*, vol. 671, no. 1-2, pp. 113–131, 1995.

[26] K. Eder, A. M. Reichlmayr-Lais, and M. Kirchgessner, "Studies on the methanolysis of small amounts of purified phospholipids for gas chromatographic analysis of fatty acid methyl esters," *Journal of Chromatography A*, vol. 607, no. 1, pp. 55–67, 1992.

[27] J. S. Eklöf, M. de la Torre-Castro, M. Gullström et al., "Sea urchin overgrazing of seagrasses: a review of current knowledge on causes, consequences, and management," *Estuarine, Coastal and Shelf Science*, vol. 79, pp. 569–580, 2008.